Analysis of NF-κB function in B lymphopoiesis and lymphoid organogenesis

zur Erlangung des akademischen Grades
Doctor rerum naturalium (Dr. rer. nat.)

vorgelegt dem Rat der
Biologisch-Pharmazeutischen Fakultät der
Friedrich-Schiller-Universität Jena

von

Feng Guo

geboren am 27.09.1973
in Wuxi, China

Gutachter:

1. Prof. Dr. Falk Weih
2. Prof. Dr. Peter Zipfel
3. P.D. Harald König

Tag des Rigorosums: 10.08.2005

Tag der öffentlichen Verteidigung: 16.09.2005

Table of Contents

ABBREVIATIONS

Ab (s)	antibody (dies)
Ag	antigen
aly	alympoplasia
BM	bone marrow
bp	base pair
BAFF	B-cell activating factor
BCR	B-cell receptor
BSA	bovine serum albumin
cDNA	complementary DNA
Ci	curie
CLP	common lymphoid progenitor
CMP	common myeloid progenitor
cpm	counts per minute
Cre	cyclization recombination
DC	dendritic cell
ddH_2O	double distilled water
DMEM	Dulbecco's Modified Eagle Medium
DMSO	dimethylsulfoxide
DNA	deoxyribonucleic acid
DN	double-negative
DP	double-positive
DTT	dithiothreitol
E	embryonic day
EDTA	ethylenediamine-N, N-tetraacetate
EF	embryonic fibroblasts
EGTA	ethylenguanidine- N, N-tetraacetate
ES	embryonic stem cells
et al.	Lat. *et alii* and others
FasL	Fas ligand

FCS	fetal calf serum
Floxed	loxP-flanked
FO	follicular
Fr.	Fraction
g	gram
gld	generalized lymphoproliferative disorder
G-CSF	granulocyte-CSF
GM-CSF	granulocyte Macrophage-CSF
h	hour (s)
HEPES	N-[2-Hydroxyethyl]piperazine-N'-[2-ethanesulphonic acid]
HR	homologous recombination
Ig	Immunoglobulin
IMDM	Iscove's Modified Dulbecco's Media
IL	interleukin
IκB	inhibitor of NF-κB
IKK	IκB kinase
kDa	kilodalton
KO	knockout
LIGHT	homologous to lymphotoxins, exhibits inducible expression, and competes with HSV glycoprotein D for HVEM, a receptor expressed by T lymphocytes
LN	lymph node
loxP	locus of X-over of P1
LPS	lipopolysaccharide
Lys	lysine
LT	lymphotoxin
LTβR	lymphotoxin β receptor
LZ	leucine zipper
MAPKKK	mitogen activated protein kinase kinase kinase
MEF	mouse embryonic fibroblast
M	molar

m	milli (10^3)
mAb	monoclonal Ab
M-CSF	macrophage-CSF
mg	milligram
MHC	major Histocompatibility Complex
min	minute (s)
ml	milliliter
mM	millimolar
mRNA	messenger RNA
m	micro (10^6)
mg	microgram
ml	microliter
mM	micromolar
MZ	marginal zone
n	nano (10^9)
N	number
NEMO	NF-κB essential modulator (IKKγ)
neo	neomycin
NF-κB	nuclear factor kappa B
ng	nanogram
NIK	NF-κB inducing kinase
NK	natural killer
NKT	natural killer T
NLS	nuclear localization signal
OD	optical density
O/N	overnight
PAGE	polyacrylmide gel electrophoresis
PBL	peripheral blood
PBS	phosphate buffered saline
PCR	polymerase chain reaction
PFA	paraformaldehyde

pfu	plaque forming units
PP	peyer's patch
PVDF	polyvinylidenedifluoride
RHD	Rel-homology domain
RNA	ribonucleic acid
RT	room temperature
rpm	rotation per minute
RPMI	Roswell Park Memorial Institute Medium
RT-PCR	reverse transcriptase PCR
SD	standard deviation
SDS	sodium-lauryl-sulphate
Ser	serine
SP	spleen
TBE	Tris-boric acid-EDTA
TCR	T cell receptor
TEMED	N, N, N', N' tetramethylene-diamine
Th	thymus
tk	thymidine kinase
TLR	Toll-like receptor
TNF	tumor necrosis factor
TNFR	TNF receptor
TRAF	TNFR-associated factors
TRAIL	TNF related apoptosis inducing ligand
U	unit (s)
µl	microliter
UV	ultra-violet light
V	volt
v/v	volume per volume
WCE	whole cell extract
w/v	weight per volume
wt	wild-type

Zussammenfassung

Die Familie der Transkriptionsfaktoren Rel/Nuclear factor kappa B (Rel/NF-κB) besteht in Säugern aus fünf Mitgliedern: Rel A (p65), RelB, c-Rel, NF-κB1(p105/p50) und NF-κB2 (p100/p52). Das vom *nfκb2* kodierte Protein p100 wird als ein Precursermolekül synthetisiert. Durch den proteolytischen Abbau der hemmenden C-terminalen Domäne des p100 Precursors kommt es zur Bildung des reifen Proteins p52, welches die Fähigkeit besitzt, an DNA zu binden. Durch den induzierten Abbau von p100 über den kürzlich beschriebenen alternativen NF-κB Aktivierungsweg kommt es zu einer Translokation des p52/RelB-Heterodimers in den Zellkern. Aufgrund dessen fungiert das p100 als ein spezifischer und leistungsfähiger Inhibitor von RelB.

Mäuse, denen spezielle NF-κB-Mitglieder fehlen, zeigen vorwiegend Defekte in der B-Zell-Aktivierung, weniger in der B-Zell-Entwicklung. In der vorliegenden Arbeit soll die Funktion von p100 und RelB im Zusammenhang mit der B-Zell-Entwicklung untersucht werden. Hierzu werden $p100^{-/-}$-Mäuse als Modelsystem herangezogen. In den $p100^{-/-}$-Mäusen, die p52 aber nicht p100 produzieren, wurde eine defekte B-Zell-Entwicklung am Beginn der B-Zell-Linien-Entstehung zusammen mit einer fehlerhaften Bildung von B-Zellen in der marginalen Zone der Milz beobachtet. p100 wird innerhalb der Vorläufer von B-Zell-Linien für die korrekte Entwicklung von reifen B-Zellen benötigt. Wenn das p100 als Inhibitor des RelB entfernt wird, dann binden in verschiedenen lymphatischen Geweben RelB-Heterodimere konstitutiv an κB-Motive. Die in $p100^{-/-}$-Mäusen beobachtete erhöhte DNA-Bindungsaktivität der RelB Hetrerodimere kann auf Wildtypniveau zurückgebracht werden, wenn ein Allel des RelB Gens in diesen Mäusen inaktiviert wird ($p100^{-/-}relB^{-/+}$). Dies geht mit einer Erholung der gestörten B-Zell-Entwicklung einher. Der Rückgang der B-Zell-Entwicklung in $p100^{-/-}$ Mäusen kann auf die herabgesetzte Produktion von B-Linien spezifischer Transkriptionsfaktoren (EBF und Pax5) zurückgeführt werden, welche ebenso bei $p100^{-/-}relB^{-/+}$ Mäusen wieder angeschaltet werden. Darüber hinaus bestimmt die Funktion des RelB das Schicksal der B-Lymphozyten gegenüber den myeloiden Zellen durch eine Induktion der C/EBPα-Expression. Diese Ergebnisse zeigen die spezifische Rolle des alternativen NF-κB-

Aktivierungssingnalweges (NF-κB2/p100 und RelB) in Bezug auf die B-Zell-Entwicklung. Die Aktivität von RelB reguliert die Entwicklung von $B220^{+}CD19^{+}$ B-Zellen (Fr. B) im Knochenmark und die Bildung von MZ B-Zellen in der Milz. Die gezielte Regulation des p100-Prozessings in den B-Zell-Precursorn ist ein wichtiger Vorgang in der Entwicklung der B-Zellen und dient der Unterscheidung der B-Zell-Linie von der myeoloiden Linie. Die Aktivierung von NF-κB durch den Lymphotoxin β Rezeptor ist ein kritischer Vorgang in der Entwicklung sekundärer lymphatischer Organe. Über die LTβR-Bindung werden sowohl der klassische (p50/RelA) als auch der alternative (p52/RelB) Signalweg induziert. Um den Einfluss beider Wege auf den NF-κB-Signalweg downstream des LTβR-Signallings vor allem in Bezug auf die lymphoide Organogenese *in vivo* zu analysieren, wurden Mausmodelle Maus etabliert, in welchen spezifisch der *relB* bzw. der *relA* Signalweg auf LTβR exprimierenden Zellen inaktiviert wurde. Um dies zu erreichen mussten zunächst 3 Mauslinien generiert werden, die ein „gefloxtes“ *relB* ($relB^{flox/flox}$) oder *relA* ($relA^{flox/flox}$) bzw. eine Cre-Rekombinase-Aktivität in LTβR-exprimierenden Zellen besitzen. Die Herstellung von $relB^{flox/flox}$-Mäusen ist hilfreich, um die spezifische Funktion von RelB in B-Zellen zu untersuchen, ohne dabei die seine Funktion in anderen Zelllinien zu beeinträchtigen. In der vorliegenden Arbeit ist die Herstellung der $relB^{flox/flox}$-Mäuse im Stadium der Keimzell-Übertragung. Es wurden insgesamt vier *ltbr-cre*^{tg} Gründer-Linien wurden durch pronucleäre Injektionen von *cre*-DNA unter der Regulation eines *ltbr* Promotors hergestellt. In drei Linien entsprach die Expression der *cre*-mRNA derjenigen der endogenen *ltbr*-mRNA. Aus diesen wurden zwei Gründer Linien ausgewählt, um eine Reportermauslinie (R26R) zur weiteren Charakterisierung herzustellen. Des Weiteren wurde ein *ltbr-cre*-knock-in-targeting-Vektor pTVFlox-LTβR-Cre konstruiert, der als eine alternative Methode zur konventionellen transgenen Anwendungen wie der pronucleären Injektion verwendet werden soll.

Summary

In mammals, the Rel/NF-κB family of transcription factors consists of five members RelA (p65), RelB, c-Rel, NF-κB1 (p105/p50), and NF-κB2 (p100/p52). p100, encoded by the *nfκb2* gene, is synthesized as a precursor molecule. The removal of the C-terminal inhibitory domain of p100 by proteolytic processing generates mature DNA-binding protein p52. Degradation of p100 via the recently discovered alternative NF-κB activation pathway results in nuclear translocation of p52/RelB heterodimers.

Mice lacking individual NF-κB members manifest defects mainly in B-cell activation rather than in B-cell development. The major goal of first project is to understand whether NF-κB2/p100 and RelB function in B-cell development by using $p100^{-/-}$ mice as a model system. Not only an arrested mainstream B-cell development at the onset of B-lineage commitment, but also an impaired marginal zone B-cell generation, was found in $p100^{-/-}$ mice (still producing p52 but not p100) in a cell-intrinsic manner. RelB complex bound constitutively to κB motifs in various lymphoid tissues when p100, the inhibitor of RelB, was deleted. The elevated RelB DNA-binding activity was restored to wild-type levels when one allele of the *relB* gene was deleted in $p100^{-/-}$ mice ($p100^{-/-}relB^{-/+}$ mice), correlated with the rescued B-cell development. The impaired B-cell development in $p100^{-/-}$ mice was likely due to the reduced expression of B-lineage transcription factors EBF and Pax5, which was also rescued in $p100^{-/-}relB^{-/+}$ mice. Moreover, the increased RelB function determined the fate of B lymphocytes versus myeloid cells, likely due to the contribution of enhanced C/EBPα expression in $p100^{-/-}$ B-cell precursors. Thus, the findings here unravel a specific role of alternative NF-κB activation pathway (NF-κB2/p100 and RelB) with respect to B-lymphocyte development. RelB activity regulates the emergence of $B220^{+}CD19^{+}$ B cells (Fr. B) in bone marrow and the generation of MZ B cells in spleen. The tightly controlled p100 processing in B-lineage precursors is an important event in B-cell development and B-lymphoid/myeloid-lineage decision.

The activation of NF-κB through lymphotoxin β receptor (LTβR) is critical for secondary lymphoid organogenesis. LTβR signaling induces both classical (p50/RelA) and

alternative (p52/RelB) complexes. To *in vivo* dissect the individual contribution of each NF-κB activation pathway downstream of LTβR signaling with a specific focus on the secondary lymphoid organogenesis, one approach is to generate mouse models, in which *relB* or *relA* can be selectively inactivated in LTβR-expressing cells. Towards this goal, three mouse strains need to be established, including mice harboring floxed *relB* (*relB*$^{flox/flox}$) or *relA* alleles (*relA*$^{flox/flox}$, generated) and mouse strain with Cre recombinase activity in LTβR-expressing cells. The generation of *relB*$^{flox/flox}$ mice is expected to be helpful to characterize specific function of RelB in B cells without losing its function in other lineages. In this study, the generation of *relB*$^{flox/flox}$ mice is in the stage of germline transmission. Four *ltbr-cre*^{tg} founder lines were generated by pronucleus injection of *cre* cDNA under the control of the *ltbr* gene promoter. In three founder lines, the tissue expression pattern of *cre* mRNA was consistent with that of endogenous *ltbr* mRNA. Two lines were selected to breed with a reporter mouse line (R26R) for further characterization. The targeting vector pTVFlox-LTβR-Cre, leading to the generation of *ltbr-cre* knock-in mice as an alternative method to the conventional transgenic approach by pronucleus injection, was also constructed.

1 INTRODUCTION

Rel/nuclear factor (NF)-κB is a dimeric transcription factor comprised of 50 kDa and 65 kDa subunits. It was originally identified as a constitutive nuclear B-cell-specific protein that binds to κB regulatory motifs within the intronic enhancer of the immunoglobulin *Cκ* light chain gene. As its binding activity was closely associated with expression of the *Cκ* gene, it was showed to be involved in B-cell maturation. It is now clear that this DNA-binding activity is the result of multiple Rel/NF-κB related dimers and that these transcription factors are present in all cells [1].

1.1 NF-κB signaling pathway

The Rel/NF-κB family of transcription factors plays a pivotal role in diverse biological processes including innate and adaptive immune responses, inflammation, cell growth and differentiation, apoptosis and survival, cancer, and lymphoid organogenesis.

1.1.1 Rel/NF-κB family of transcription factors

The Rel/NF-κB proteins belong to two classes in vertebrates: one consisting of RelA (p65), RelB, and c-Rel, proteins that are synthesized in their mature forms. These proteins share a highly conserved N-terminal 300 amino acids long Rel-homology domain (RHD). The RHD contains a nuclear localization sequence (NLS) and is involved in dimerization, sequence-specific DNA binding, and interaction with the inhibitory IκB proteins. The second class consists of NF-κB1 (p105/p50) and NF-κB2 (p100/p52), which are synthesized as precursor molecules (p105 and p100) with N-terminal RHD and C-terminal ankyrin repeats (**Figure 1.1 A**). Ubiquitin-dependent proteolysis removes the C-terminal domain, resulting in the production of mature DNA-binding proteins (p50 and

p52). p50 and p52 lack transactivation domain (TAD) that is present in the C-terminal of RelA, RelB, and c-Rel. The NF-κB proteins form numerous homo- and heterodimers [2, 3]. RelB is unique in that it does not homodimerize, and further, is unable to heterodimerize with c-Rel or p65. It forms heterodimers with p100, p52, and p50 [4, 5]. NF-κB dimers bind to the consensus sequences GGGRNNYYCC, where R is purine, Y is pyrimidine, and N is any base.

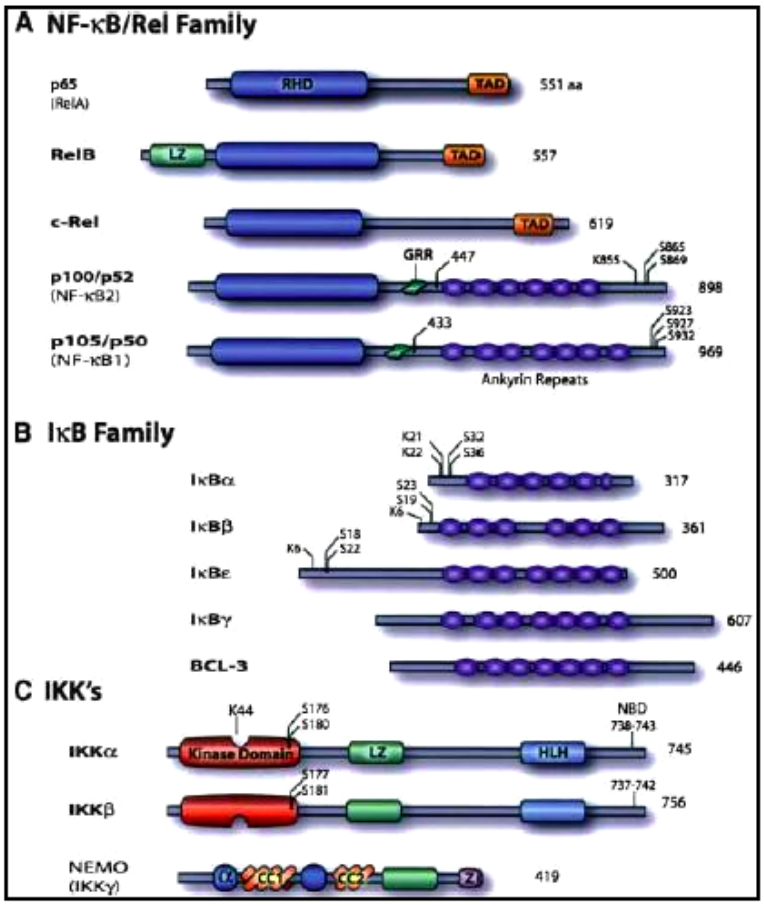

Figure 1.1: **Schematic representation of Rel/NF-κB, IκB, and IKK families.** Members of the Rel/NF-κB, IκB, and IKK families are shown. The number of amino acids in each protein is indicated in the right. Presumed sites of cleavage for p100 (amino acid 447) and p105 (amino acid 433) are shown. Phosphorylation (S) and ubiquitination (K) sites on p100, p105, and IκB proteins are indicated. RHD: Rel homology domain; TAD: transactivation domain; LZ: leucine zipper domain on IKK and RelB; GRR: glycine-rich region; HLH: helix–loop–helix domain; Z: zinc finger domain; CC1/2: coiled-coil domains; NBD: NEMO-binding domain; α: α-helical domain. (Adapted from [6])

1.1.2 IκB family members

In most cell types, NF-κB dimers are retained in the cytoplasm by IκB. The IκB family, which includes IκBα, IκBβ, IκBε, IκBγ, and Bcl-3 in mammalian cells, is characterized by the presence of multiple ankyrin repeats that mediate binding to the RHD of NF-κB proteins (**Figure 1.1 B**). The ankyrin repeats are also present in the C-terminal halves of NF-κB2/p100 and NF-κB1/p105 precursors, which function like IκB molecules. Binding to IκB prevents the NF-κB complex from translocation to the nucleus, thereby maintaining NF-κB in an inactive state. Although there is a possible functional redundancy among the IκB proteins, their different affinity to each NF-κB dimer, the number in the ankyrin repeats, and the expression pattern determine the specificity in the regulation of NF-κB activity by individual IκB protein. For instance, IκBα, IκBβ, and IκBε are shown to preferentially bind to RelA or c-Rel. In contrast, Bcl-3 binds to p50 or p52 homodimers and NF-κB2/p100 binds to RelB.

1.1.3 IκB kinase (IKK) complex

Degradation of IκB proteins is a tightly regulated process that is initiated upon phosphorylation by activated IκB kinase (IKK). IKK is a complex composed of three subunits: IKKα or IKK1 (85 kDa), IKKβ or IKK2 (87 kDa), and IKKγ or NEMO/IKKAP (48 kDa) [7]. IKKα and IKKβ are highly homologous proteins with 52% sequence identity. They contain N-terminal kinase domains as well as leucine zipper (LZ) and helix-loop-helix (HLH) motifs (**Figure 1.1 C**). They can form homo- or heterodimers by virtue of the LZ motifs and the dimerization is essential for the kinase activity. The third subunit IKKγ is the regulatory subunit [8]. IKKγ lacks a kinase domain and exists as a dimer or trimer. Gel filtration analysis indicates that the IKK complex is a large complex, 700–900 kDa in size, suggesting the presence of additional components. Recently, Cdc37 and Hsp90 have been suggested to serve as additional components of the IKK complex [9]. A large number of protein kinases including different protein kinase C (PKC) isozymes and the mitogen-activated protein kinase kinase kinase (MAPKKK) family

members such as NF-κB-inducing kinase (NIK), AKT/PKB, MEKK1, MEKK2, and MEKK3 are found to be inducible activators of the IKK complex [10, 11].

1.1.4 NF-κB activation pathway

Two major signaling pathways lead to the translocation of NF-κB dimers from the cytoplasm to the nucleus. Potent activators, such as tumor necrosis factor (TNF), interleukin-1 (IL-1), and lipopolysaccharide (LPS) activate the IKK complex. In the classical NF-κB signaling pathway (**Figure 1.2**, right part), the activated IKK complex (predominantly in an IKKβ and IKKγ dependent manner) catalyzes the phosphorylation of IκB protein (at sites equivalent to Ser32 and Ser36 of IκBα), polyubiquitination (at sites equivalent to Lys21 and Lys22 of IκBα), and subsequent rapid degradation by the 26S proteasome. The released NF-κB dimers (mainly p50/RelA heterodimers) translocate to the nucleus, bind DNA, and activate the transcription of κB target genes.

Recently, an alternative pathway for NF-κB activation that is dependent on NIK and IKKα has been identified (**Figure 1.2**, left part). This pathway is independent of IKKβ and IKKγ [12-15]. The substrate of NIK-IKKα in this pathway is NF-κB2/p100, which can be phosphorylated at two C-terminal serine residues. Phosphorylation of these sites is essential for p100 processing to p52, which further undergoes polyubiquitination and proteasomal degradation. However, instead of complete p100 degradation, as seen in IκB proteins, phosphorylation-dependent ubiquitination of p100 merely results in the degradation of its inhibitory C-terminal half of p100. Once the C-terminal half is degraded, the N-terminal portion of p100, p52 containing the RHD, is released. As the RHD of p100 is most commonly associated with RelB, activation of the alternative pathway predominantly results in nuclear translocation of p52/RelB heterodimers. Thus, p100 functions as a specific and potent inhibitor of RelB. This alternative pathway can also be induced by activation of lymphotoxin β receptor (LTβR), B-cell activating factor belonging to the TNF family receptor (BAFF-R), CD40, and LPS but not TNFR1/TNFR2 [16-19].

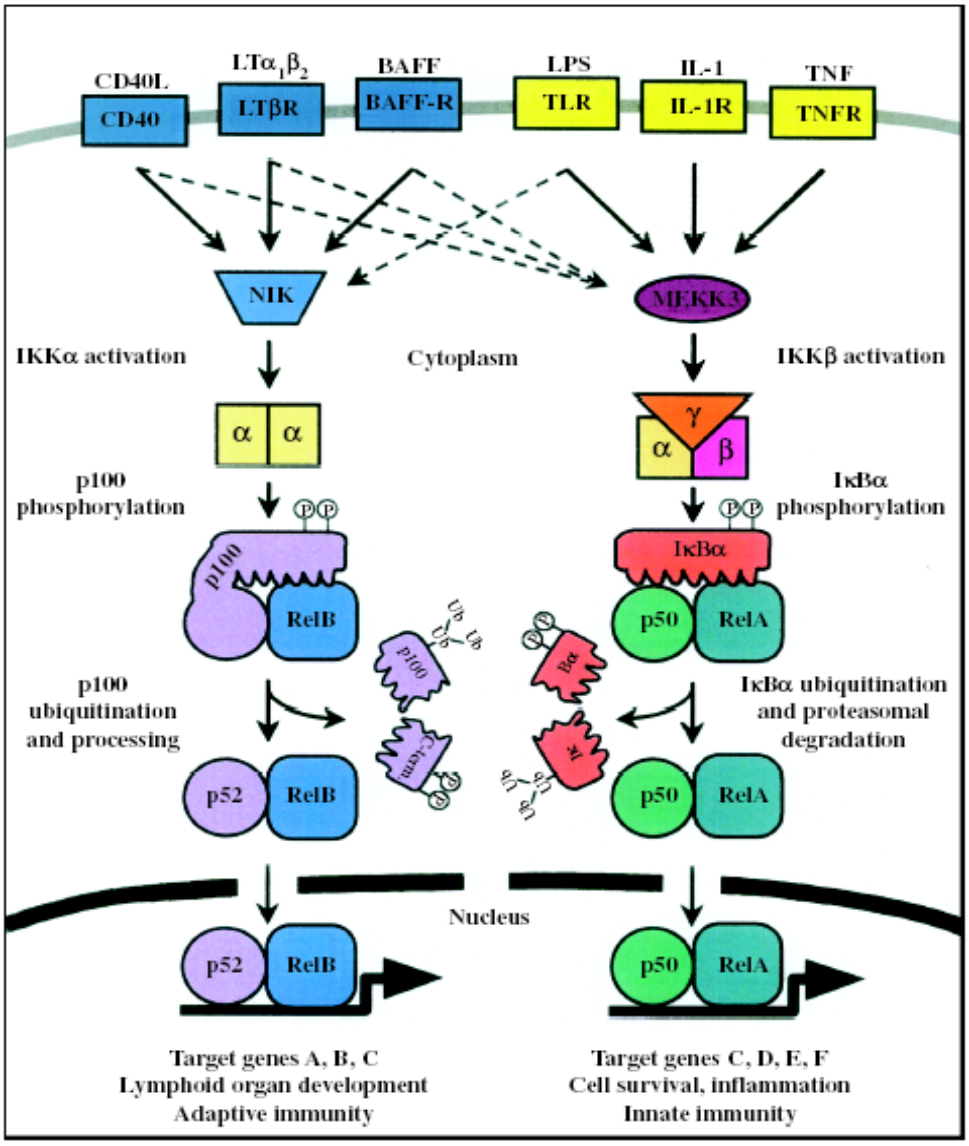

Figure 1.2: Activation of NF-κB by the alternative (left) and the classical (right) pathways. Signalings through TNFR, IL-1R, and TLR activate the classical NF-κB pathway involving predominantly the β and γ subunits of the IKK complex. Nuclear translocation and DNA-binding of p50/RelA heterodimers are accomplished through IκBα phosphorylation and ubiquitin-dependent proteasomal degradation. Membrane-bound $LT\alpha_1\beta_2$ heterodimers, CD40L, and BAFF, on the other hand, activate via NIK and IKKα. Phosphorylation of p100 results in the processing of the precursor of the p52 subunit and nuclear accumulation of p52/RelB heterodimers. There is significant cross talk, since signaling through the LTβR also results in the induction of RelA complexes and LPS can also trigger the processing of p100 to p52. It is likely that the two pathways activate distinct or only partially overlapping sets of genes. (Adapted from [13])

1.1.5 Distinct and redundant functions of NF-κB proteins

Rel/NF-κB family members have distinct as well as redundant functions, which are indicated by the phenotypes observed in mice lack for individual NF-κB proteins. The pathological changes and cell lineages affected in different NF-κB mutant mice are listed in **Table 1-1** [20].

NF-κB deficient mice	Phenotypes
nfκb1$^{-/-}$	Develop normally and exhibit no histopathological changes [21]; exhibit multiple defects in the function of immune system; susceptible to *Listeria monocytogenes* and *Streptococcus pneumoniae*, respond normally to *Haemophilus influenza* and *Escherichia coli*, and more resistant to murine encephalomyocarditis (EMC) virus due to the increased production of β-interferon [21]
nfκb2$^{-/-}$	Develop normally; absence of marginal zone in spleen; disorganized B- and T-cell areas in spleen and lymph nodes; lack of Peyer's patches; fail to mount a T-cell dependent antibody response [22, 23]
relA$^{-/-}$	Embryonic lethality between days E15 and E16 postcoitum due to fetal hepatocyte apoptosis; *relA*$^{-/-}$ fibroblasts and macrophages also exhibit increased sensitivity to apoptosis induced by TNFα [24]
relB$^{-/-}$	Multi-organ inflammation; atrophy of thymic medulla; splenomegaly; disorganized B- and T-cell areas in spleen; myeloid hyperplasia in spleen and bone marrow; absence of lymph nodes and Peyer's patches [25-27]
c-rel$^{-/-}$	Develop normally; defects in B-cell proliferation and isotype switching [28, 29]; *c-rel*$^{-/-}$ T cells fail to proliferate in response to mitogens which can be overcome by exogenous IL-2; activated T cells also express reduced amounts of IL-3 and GM-CSF [29, 30]

Table 1-1: Pathological changes in mice deficient in individual Rel/NF-κB proteins.

Lack of both *nfκb1* and *nfκb2* in mice results in osteopetrosis, B-cell developmental defects, thymic and lymph node atrophy, disorganized spleen structure, and myeloid hyperplasia [31]. *tnfr*$^{-/-}$*relA*$^{-/-}$ mice can survive embryonic lethality. They lack lymph nodes as well as Peyer's patches and reveal defective spleen architecture [32]. *relA*$^{-/-}$*c-rel*$^{-/-}$ mice die between days E15 and E16 postcoitum as a result of fetal hepatocytes apoptosis [33]. *nfκb1*$^{-/-}$*relA*$^{-/-}$ mice, like *relA*$^{-/-}$*c-rel*$^{-/-}$ mice, display an earlier onset of embryonic death (around E13) due to fetal liver apoptosis [34]. *nfκb1*$^{-/-}$*relB*$^{-/-}$ mice reveal increased severity that is observed in *relB*$^{-/-}$ mice [13, 35].

1.1.5.1 Mice lack of C-terminal inhibitory domain of p100

NF-κB2 is synthesized as precursor molecule p100. The removal of C-terminal inhibitory domain of p100 precursor by proteolytic processing generates active p52. To better understand the physiological roles of NF-κB2, particularly the p100 precursor *in vivo*, *p100*$^{-/-}$ mice have been generated by Rodrigo's lab [36]. In these mice, targeted disruption of the C-terminal portion of the *nfκb2* gene is generated by introducing a stop signal at codon 451 in combination with a SV40 poly (A) and the *neo* cassette, which results in the expression of 450 amino acids long p52 molecule, rather than the full-length p100 precursor (**Figure 1.3**).

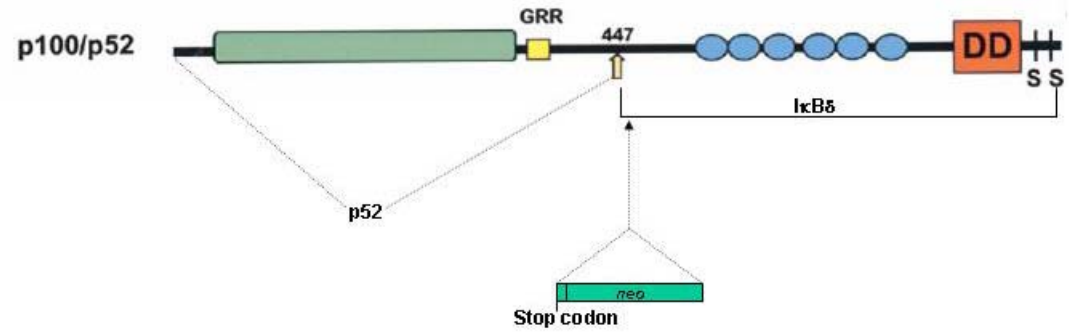

Figure 1.3: Schematic representation of the targeting strategy of C-terminal ankyrin repeats domain in the *nfκb2* gene. In *p100*$^{-/-}$ mice, the targeted disruption of the C-terminal portion of the *nfκb2* gene is generated by introducing a stop signal at codon 451 followed by SV40 poly (A) and the *neo* cassette.

p100$^{-/-}$ mice appear normal at birth but develop multiple pathologies postnatal. These pathologies include gastric hyperplasia, spleen and thymic atrophy, enlarged lymph nodes, and myeloid hyperplasia. *p100*$^{-/-}$ mice survive no longer than 21 days after birth mainly due to the marked gastric hyperplasia. A significant increase of κB DNA-binding activity, mainly comprising RelB complexes, is found in different lymphoid and non-lymphoid tissues of *p100*$^{-/-}$ mice. The expression of Rel/NF-κB-regulated genes such as TNFα, ICAM1, and VCAM-1 is upregulated in *p100*$^{-/-}$ mice.

1.2 B-lymphocyte development

B cells are an important component of adaptive immunity. The main function of B-cell is to produce and secrete soluble antibodies that recognize foreign antigens (bacterial, fungal, etc.). These Y-shaped antibodies, of which there are five classes (IgM, IgD, IgG, IgA, and IgE), are composed of two heavy chains and two light chains.

B cells develop in bone marrow, liver (in the fetus), and a specialized organ termed the bursa of Fabricius in birds. B-cell takes its name from 'bursa'. B-cell development is a tightly controlled process. Generation of immature B cells in bone marrow is referred to as central (or primary) B-cell development. Bone marrow B-lineage precursors proliferate and progress through a highly regulated maturation process that culminates in the production of immature, surface immunoglobulin (Ig)-expressing B lymphocytes. These newly formed, immature B-lymphocytes then migrate into spleen, where they differentiate into mature, naïve B cells in a process referred to as peripheral (or secondary) B-cell development (**Figure 1.4**).

The number of B-lineage cells in bone marrow is far greater than the number of mature B cells that are generated in spleen [37, 38]. The marked cell loss, occurring during the process of generating bone marrow B-lineage, is due to a series of selection events. First, Ig heavy-chain gene rearrangements are productive in only approximately one third of pro-B cells. Furthermore, an even smaller fraction of these cells progress to complete functional light-chain gene rearrangements [39]. Those cells with nonproductive Ig gene rearrangements undergo apoptosis and are eliminated from bone marrow, possibly by a macrophage mediated mechanism [40]. Finally, selection events are also operative in cells that have differentiated to the surface IgM^+ stage. Some of these surface IgM^+ cells are eliminated, because they are potentially self-reactive [41, 42]. As a result, while approximately 2×10^7 IgM^+ immature bone marrow B lymphocytes are produced daily in mouse, only 5-10% of these cells survive and exit bone marrow as transitional B cells [43-45].

Immature splenic B cells are referred to as 'transitional' cells because they are 'in transit' from bone marrow and they comprise a distinct short-lived 'developmental transition' from immature into mature B cells. Transitional B cells comprise approximately 10-15% of all splenic cells. There are at least two major subsets of transitional B cells, transitional type 1 (T1) and type 2 (T2) (**Figure 1.4**) [46]. As for the mature B cells in spleen, there are three main types: follicular mature (FO), marginal zone (MZ), and B 1 cells [47]. B1 B cells, which are enriched in peritoneal and pleural cavities, are self-renewing cells [48].

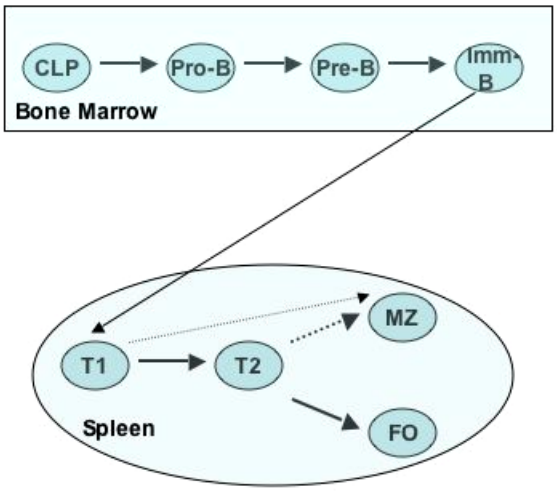

Figure 1.4: An overview of B-cell development in bone marrow and spleen. In bone marrow, common lymphoid progenitors (CLPs) commit to B-cell lineage through pro-B and pre-B stages. Immature B cells, which have rearranged their immunoglobulin genes, subsequently migrate to spleen and differentiate to mature FO and MZ B cells. T1: transitional type 1, T2: transitional type 2.

1.2.1 Transcriptional control of early B-cell development

The development of B-lineage cells from multipotent progenitors requires the coordinated activity of many transcription factors. These proteins have been shown to function in a transcriptional hierarchy, and in a combinatorial manner, to regulate the expression of genes that comprise the B-lineage differentiation program. PU.1, E2A, early B cell factor (EBF), and B-cell-specific activator protein (BSAP)/Pax5 are critical for the proper development of early B-lymphoid cells.

1.2.1.1 Early B-cell development process

The hematopoietic system continuously regenerates all blood cells throughout life. One of the earliest steps is the commitment of pluripotent progenitors to either common lymphoid progenitors (CLPs) or common myeloid progenitors (CMPs). The IL-7 receptor $(IL\text{-}7R)^+$ CLPs give rise to all lymphocytes (B, T, DC, and NK cells) whereas the $IL\text{-}7R^-$ CMPs are able to generate all myeloid cell types (erythrocytes, megakaryocytes, granulocytes, and macrophages) [49].

Subsequent expression of the pan B-cell marker B220 on CLPs coincides with the differentiation to pre-pro-B cells. Cells at pre-pro-B stage, also termed as Fraction (Fr.) A1/A2 according to the nomenclature of Hardy, are $B220^+CD43^+CD19^-IgM^-$ [50]. The early pro-B (termed as Fr. B) cells represent committed B-lineage cells that have undergone rearrangement of D_H-J_H segments at immunoglobulin heavy chain locus (**Figure 1.5**) [51]. Productive V_H-DJ_H recombination at late pro-B stage (Fr. C) results in the expression of Igμ proteins as part of pre-B cell receptor (pre-BCR) on the cell surface. The transition from pre-pro B stage (Fr. A) to early pro-B stage (Fr. B) is characterized by the expression of CD19 [52, 53]. The acquisition of CD19 expression actually represents an important step in murine B-lineage differentiation and corresponds to the ability of pro-B cells to proliferate in response to IL-7 without other stromal cell derived factors [50, 51]. The pre-BCR acts as an important checkpoint to control the transition from pro-B to pre-B stage. At the pre-B stage, the heavy chain is associated with a surrogate light chain, *λ5* and *VpreB*, as well as the signal transducing molecules *mb1*/*Igα* (CD79*α*) and *B29*/*Igβ* (CD79β). Signaling through pre-BCR promotes allelic exclusion at the *IgH* locus, stimulates proliferate cell expansion, and induces differentiation to small pre-B cells, which start to recombine immunoglobulin light-chain genes. Successful light-chain gene rearrangement leads to the emergence of immature IgM^+ B cells that emigrate from bone marrow to the periphery [54, 55].

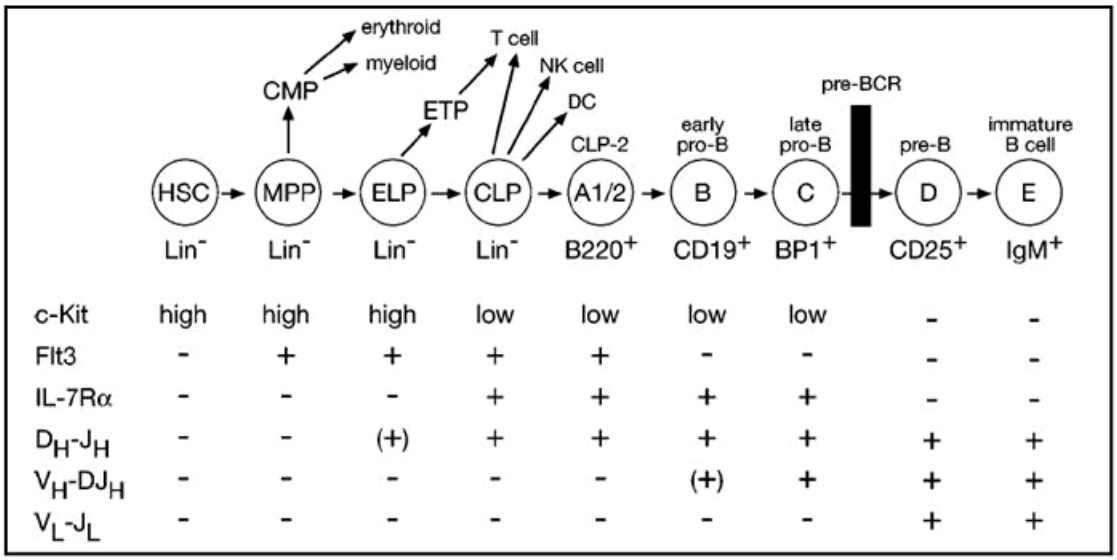

Figure 1.5: Schematic diagram of B-cell development in bone barrow. The expression of signaling receptors, the rearrangement status of immunoglobulin genes, and the initiation of expression of characteristic cell surface proteins are indicated for successive progenitor cell stages in mouse B lymphopoiesis. Lin^-, negative for the expression of lineage-specific markers. (Adapted from [56])

1.2.1.2 PU.1

PU.1 (Spi-1) is a member of the Ets transcription factor family that is expressed exclusively in hematopoietic cells [57]. PU.1 plays an essential role in the development of both lymphoid and myeloid lineages [57, 58]. PU.1 expression is highest in macrophages but can also be detected in neutrophils, B, and early T lymphocytes. *PU.1*$^{-/-}$ mice die around birth and fail to generate myeloid as well as lymphoid cells, but do contain normal erythrocytes and megakaryocytes [58, 59]. The *PU.1*$^{-/-}$ progenitor cells propagate *in vitro* in the presence of the multilineage cytokines IL-3, IL-6, and SCF, but fail to respond to M-CSF, G-CSF, GM-CSF, and IL-7 owing to the absence or the reduced expression of the corresponding receptors [60]. Retroviral reconstitution experiments have implicated a role of PU.1 in the myeloid versus lymphoid lineage decision, as low PU.1 expression induces B-cell development in *PU.1*$^{-/-}$ progenitors, whereas high PU.1 level suppresses the B-cell fate and promotes instead macrophage differentiation [61, 62]. PU.1 has been implicated in the regulation of expression of IL-

7Rα, which is required for proper lymphoid development, and M-CSF, which is required for proper macrophage development.

1.2.1.3 E2A

The *E2A* gene encodes two proteins E12 and E47, which are members of the basic helix–loop–helix (bHLH) family of transcription factor [63]. E2A proteins belong to a subgroup of bHLH proteins, referred to as E-proteins that also includes HEB and E2-2 [64]. These E-proteins bind to a common 'E-box' motif, 5'-CANNTG-3', and form homo- and heterodimers with other bHLH proteins. E12 and E47 are expressed in many cell types in a heterodimeric form but form a unique homodimeric complex only in B-lineage cells [65, 66]. Most $E2A^{-/-}$ mice die before or shortly after birth [67, 68]. B-cell development in $E2A^{-/-}$ mice is arrested at the earliest stage in the absence of D_H-J_H rearrangements (pre-pro-B stage). The few $B220^+CD43^+$ cells in $E2A^{-/-}$ bone marrow express *IL-7R*, *Igβ/B29,* and *Igμ* transcripts, whereas *Rag1*, *mb-1*, *λ5*, *CD19*, and *Pax5* expression could not be detected [68, 69]. Interestingly, transgenic expression of either E12 or E47 is sufficient to promote the development of B-lineage cells, indicating functional redundancy between these two proteins with respect to their roles in B-cell development [65].

1.2.1.4 EBF

EBF belongs to the transcriptional regulatory protein family O/E proteins, which are expressed in olfactory neurons, adipocytes, and B lymphocytes. EBF binds the palindromic sequences 5'-ATTCCCNNGGGAAT-3' through an N-terminal cysteine-rich DNA-binding domain containing a zinc coordination motif [55, 70, 71]. EBF is expressed at all stages of B-lineage differentiation with the exception of terminally differentiated plasma cells [72, 73]. Interestingly, the lack of EBF arrests B-cell development at the same stage as observed in $E2A^{-/-}$ mice [74]. The few $B220^+CD43^+$ cells present in $EBF^{-/-}$ bone marrow express *IL-7R* as well as *Igμ* transcripts, but fail to transcribe *Rag1*, *Rag2*, *mb-1*, *Igβ/B29*, *λ5*, *VpreB*, *CD19*, and *Pax5* genes [74].

The similar defects in B-cell development of E2A and EBF mutant mice strongly suggests that these two transcription factors act in concert to control the earliest phase of B lymphopoiesis. EBF is a likely the target of E2A [68, 74, 75]. Compound heterozygous $E2A^{+/-}EBF^{+/-}$ mice provide direct genetic evidence for this cooperation, because B-cell development is arrested at a slightly later stage (early pro-B stage) than that caused by deletion of either gene [76]. Forced expression of E2A and EBF in hematopoietic precursors reveals that they do cooperatively activate many B-cell-specific genes [77, 78]. Hence, an important function of E2A and EBF is to activate the B-lymphoid gene expression program at the onset of B-cell development [76]. However, the mere activation of B-cell-specific gene expression program and V_H-J_H recombination by E2A and EBF is not sufficient to commit B-cell progenitors to B-lymphoid lineage in the absence of Pax5 [79].

1.2.1.5 Pax5

B-cell-specific activator protein (BSAP) is encoded by the *Pax5* gene and is expressed in all B-lineage cells with the exception of plasma cells. In $Pax5^{-/-}$ mice B-cell development is arrested at the early pro-B-cell stage, resulting in the lack of $CD19^+$ cells in bone marrow. B-lineage progenitors are able to rearrange D_H-J_H but no detectable V_H-DJ_H rearrangements [79-81]. $Pax5^{-/-}$ pro-B cells express E2A and EBF at normal levels, indicating that E2A and EBF are upstream of Pax5 in the genetic hierarchy of B-cell development. In addition, most B-lineage-associated genes are expressed normally with the exception of *CD19*, *N-myc*, *mb-1*, and *LEF-1*, which have been shown to be Pax5 target genes [82].

$Pax5^{-/-}$ pro-B cells, which can be cultured *ex vivo* in the presence of IL-7 and stromal cells, still retain a broad lympho-myeloid potential characteristic of uncommitted progenitors [83, 84]. Upon IL-7 withdrawal and appropriate cytokine stimulation, $Pax5^{-/-}$ pro-B cells are able to differentiate *in vitro* into functional T cells, NK cells, dendritic cells, macrophages, osteoclasts, and granulocytes (**Figure 1.6**) [83]. This multilineage potential of $Pax5^{-/-}$ pro-B cells is, however, suppressed by retroviral restoration of Pax5

expression, which rescues the development to the mature B-cell stage [82]. Following injection into *Rag2*$^{-/-}$ mice, *Pax5*$^{-/-}$ pro-B cells are able to home to bone marrow, where they undergo self-renewal and develop into functional cells of all major hematopoietic lineages including T cells and erythrocytes [84, 85].

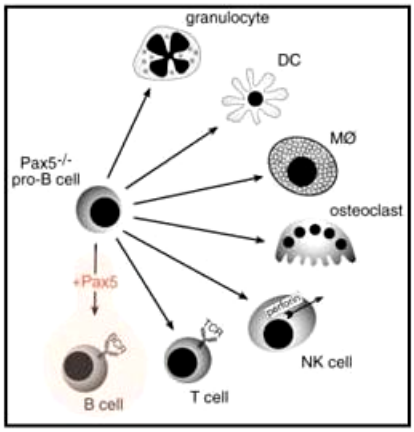

Figure 1.6: B-lineage commitment by Pax5. *Pax5*$^{-/-}$ pro-B cells are early progenitor cells, which can differentiate along the indicated hematopoietic lineages with the exception of B-cell pathway. (Adapted from [56])

Interestingly, the ectopic expression of C/EBPα and GATA transcription factors strongly promotes myeloid differentiation of *Pax5*$^{-/-}$ pro-B cells *in vitro* [86]. C/EBPα is a member of CCAAT/enhancer-binding protein family, which contains a conserved leucine-zipper dimerization motif adjacent to a basic DNA-binding domain [87]. Within the hematopoietic system, C/EBPα is exclusively expressed in early myeloid progenitors. It is upregulated during granulocyte development and downregulated along the monocytic pathway [88, 89]. The loss of C/EBPα in mice results in the complete absence of mature granulocytes due to the arrest at an early myeloblast stage [90]. Recently, it was shown that the enforced expression of C/EBPα or C/EBPβ in differentiated B cells leads to a rapid and efficient reprogramming into macrophages. C/EBPs induce these process by inhibiting Pax5, leading to the downregulation of its target gene CD19, and synergizing with endogenous PU.1, resulting in the upregulation of its target Mac-1 [91]. C/EBPβ may also play a role in B-cell differentiation since ablation of this factor, which is expressed predominantly in mature B cells [92], leads to a decreased number of B cells in bone marrow.

At lineage commitment, Pax5 fulfills a dual role by repressing the 'lineage-inappropriate' genes and simultaneously activating the B-cell-specific genes, which leads to the consolidation of B-lymphoid gene expression program [83]. The *M-CSFR* and *BLNK* genes are illustrative examples of both classes of genes. The expression of *M-CSFR* enables *Pax5*$^{-/-}$ pro-B cells to differentiate into monocytes under the influence of M-CSF, whereas its repression by Pax5 renders B-cell precursors unresponsive to this myeloid cytokine. On the other hand, the *BLNK* gene is entirely dependent on Pax5 function for its expression in committed B-lymphocytes (**Figure 1.7**) [81, 93].

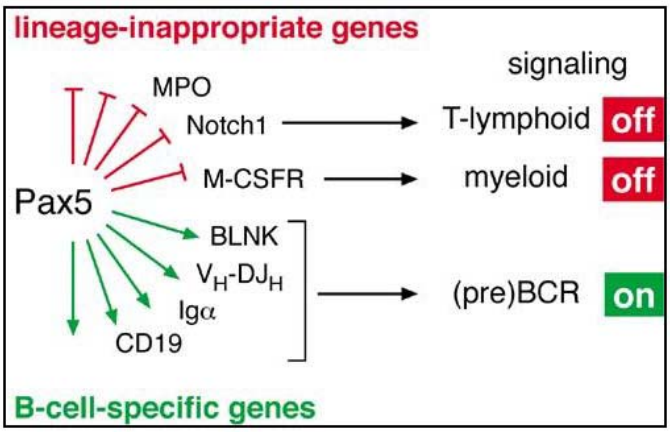

Figure 1.7: Dual role of transcription factor Pax-5 in B-cell development. Pax-5 inactivates myeloid signaling by repressing the *M-CSFR* gene. It also represses myeloperoxidase (*MPO*) expression. At the same time, Pax-5 activates (pre)-BCR signaling by promoting V_H-DJ_H rearrangements and by inducing the expression of *BLNK, CD19*, and *mb-1*. (Adapted from [56])

1.2.2 Spleen marginal zone and marginal zone B cells

The splenic marginal zone (MZ) is the major route of entry of antigens, antigen presenting cells, and lymphocytes into the white pulp [13]. It is located at the outer limit of the white pulp (WP), bordered innermost by the MZ sinus and outermost by the red pulp (RP). The marginal sinus surrounds B-cell follicles and T-cell areas (periarteriolar lymphoid sheath; PALS) (**Figure 1.8**) [48, 94]. The MZ is characterized by the presence of two distinct macrophage populations MZ macrophages (MZM) and metallophilic marginal macrophages (MMM), separating red and white pulp in spleen. These

specialized macrophages can be discriminated by ER-TR9 and MOMA-1 mAbs, respectively. The mucosal addressin cellular adhesion molecule-1 (MAdCAM-1) is expressed on stromal sinus-lining cells in the MZ.

The main compartment of MZ-resident lymphocytes comprises 'naïve' MZ B cells, which have a distinctive phenotype and function compared to mainstream B cells. MZ B cells only represent about 5% of splenic B cells. MZ B cells is characterized by high surface expression of CD21/CD35 and negative/low expression of CD23, whereas follicular B cells are CD21/CD35^{in}CD23^{in} [13]. The β2, LFA-1, and α4β1 integrin are expressed at higher levels on MZ B cells compared to follicular B cells [95]. It has been shown that the 'naïve' MZ B-cell compartment originates from recirculating precursors from rat lymph [96]. The MZ and MZ B-cell compartment are not fully formed until 3-4 weeks after birth in rodents and 1-2 years in humans. The precise cellular and molecular basis for the delay in MZ B cell maturation remains unclear, but this delay may have a clinical correlation in the inability of infants under the age of two to mount effective immune responses to selected polysaccharide antigens [48].

MZ B cells are a crucial component of early immune responses to blood-borne pathogens [94]. Along with B1 B cells, they have been described as cells that are endowed with "natural memory" and that provide a bridge between innate and adaptive immune responses. These two types of B cells are believed to be the source of most natural antibodies. MZ B cells also play an important role in the immune response to T-independent type 2 (TI-2) antigens. Pyk-2-deficient mice lack MZ B cells. These mice have a striking defect in TI-2 responses to artificial multivalent antigens [97]. Mice that lack NF-κB1 have a defect in MZ B-cell development, and these mice are defective in their ability to defense a number of gram-negative bacteria [98].

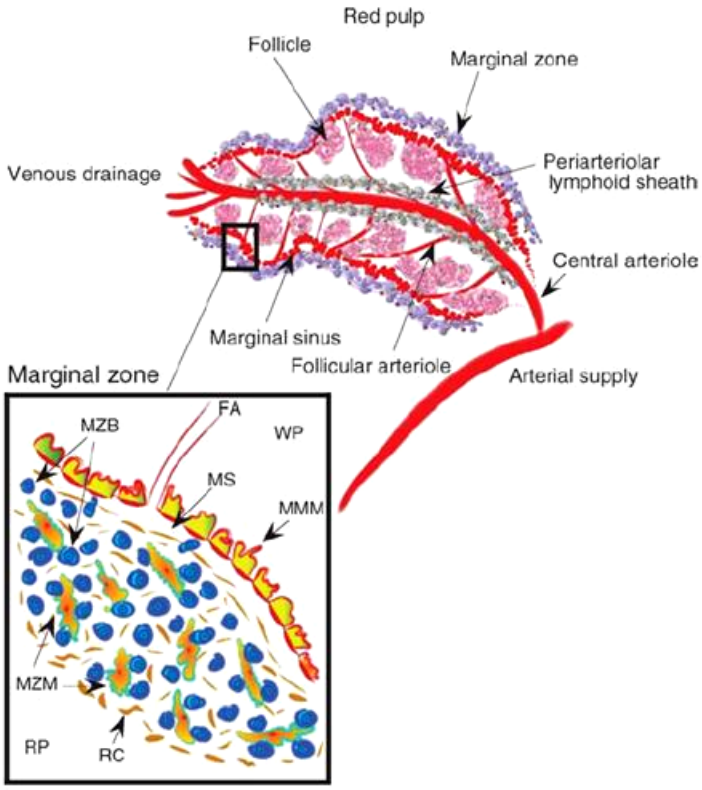

Figure 1.8: Microstructure of spleen and spleen marginal zone. Central arterioles are surrounded concentrically by PALS and B-cell follicles. These arterioles branch into follicular arterioles, which feed into the marginal sinus. The marginal zone lies between the sinus and the red pulp of spleen. Inset shows the marginal zone in cross-section. MZ B cells play pivotal roles in cooperation with MZ macrophages and dendritic cells in filtering mechanism of spleen to clear blood-borne antigens. FA: follicular arteriole; RC: reticular cell. (Adapted from [99])

1.2.2.1 Molecular signals that affect marginal zone B cells

The origin of MZ B cells is not well defined. The current model for the cellular pathway in generating of MZ B cells is shown in **Figure 1.4**. The detailed molecular nature of signaling that is required for MZ B-cell generation and maintenance, as well as the intercellular signals between resident MZ cells is not clear. Many recent studies using mutant mouse models underscore clearly the direct or indirect involvement of several signaling pathways. They are summarized in **Table 1-2**.

Mouse system*	Observations
Clonal signals	
81x, MD2, MD4, M54, 3H9, 3-32, M167 transgenics	Larger proportion of MZ and reduced follicular B cells; BCR/co-signal-dependent selection of specific B-cell clones in MZ
L5$^{-/-}$, *Il7*$^{-/-}$, *Il7rα*$^{-/-}$, *Rag*$^{-/-}$ conditional	Larger proportion of MZ and B1 B cells and reduced follicular B cells
CD79a$^{-/-}$ tail	XID-like phenotype for B-cell development and TI immune responses
CD79a$^{-/-}$ ITAM	Decreased B1 and MZ B cells; low TD and normal TI responses; increased Ca response
CD79a$^{-/-}$ ITAM/*Cd79b*$^{-/-}$ tail	Complete BM block at the pro-B-cell stage
CD19$^{-/-}$	Lack of MZ B cells; defects in TD and TI responses
CD21$^{-/-}$	Slight increase in MZ B cells and decrease in follicular B cells; decreased B-cell co-signalling
CD22$^{-/-}$, *Shp1*$^{-/-}$	Hyperactive B cells; altered selection; increased B1 cells; autoimmune traits
CD45$^{-/-}$	Reduced positive B-cell selection
CD72$^{-/-}$	Increased B1 cells; hyperactive B cells
CD5$^{-/-}$	Altered B-cell signalling and selection
Btk$^{-/-}$(XID), *Pi3k*$^{-/-}$, *Pkcβ*$^{-/-}$	Altered selection into MZ and B1 B cells; altered TI immune responses
Aiolos$^{-/-}$	Decreased MZ and B1 B cells; hyperactive B cells
Lifespan and survival	
Baff$^{-/-}$, *Baffr*$^{-/-}$ (A/WySnJ)	Lack of B cells beyond NF/TR stage
Baff-transgenic	Increase in TR and MZ B cells, in particular; B-cell autoimmune manifestation
Bcma$^{-/-}$	Normal
Taci$^{-/-}$	Increased B cells; decreased TI responses
Ltα$^{-/-}$, *Ltβ*$^{-/-}$, *Ltr*$^{-/-}$	Disorganized B/T areas; reduced MZ B cells; PP and LN missing
Tnf$^{-/-}$, *Tnfrl*$^{-/-}$	Normal MZ B cells; B-cell ringing; GC defects
Retention, movement and migration	
Pyk2$^{-/-}$	Lack of MZ B cells; normal B1 cells; hyporesponsivity to chemokines
Lsc$^{-/-}$	Low MZ B cells; normal B1 cells; greater MZ migration after serum activation
Dock2$^{-/-}$	Low MZ and B1 B cells; reduced chemokine migration
Vav1$^{-/-}$, *Vav2*$^{-/-}$, *Vav1/Vav2*$^{-/-}$	Defects in B-cell maturation, B1 cells and immune responses
Transcription factors	
Nfκb1$^{-/-}$, *RelB*$^{-/-}$, *RelA/cRel*$^{-/-}$	Low MZ B cells; defects in the LT/chemokine loop
RelA$^{-/-}$, *cRel*$^{-/-}$	Normal MZ B cells

Table 1-2: Knockout and transgenic mice with alterations in MZ B cells. Mouse models have been classified into the following groups: signals that involve the BCR, pathways that involve in the lifespan and survival of MZ B cells, and signals that participate in MZ B-cell retention and migration. (Adapted from [48])

1.2.3 Rel/NF-κB function in B-cell maturation and activation

The expression and intranuclear level of Rel/NF-κB subunits change substantially during B-cell maturation, indicating that these proteins play a critical role in B lymphopoiesis. c-Rel is expressed at all stages of B-cell development, but is expressed at the highest level and is constitutively nuclear in mature B cells [100]. RelB is expressed during the later stages of B-cell maturation and can bind to regulatory sites within the Ig heavy chain locus. Terminally differentiated plasma cells and LPS-differentiated B cells express all five isoforms (p52, RelB, c-Rel, p50, and RelA). The nuclear κB DNA-binding activity in mature B-lymphocytes consists mainly p50/c-Rel heterodimers, which is different from

pre-B cells that have largely inducible p50/p65 heterodimers [101] . Despite changes in the abundance and the subunit composition of NF-κB transcription factors throughout B-cell development [102, 103], mice lacking individual NF-κB protein have defects mainly in B-cell activation rather than development (**Table 1-3**).

Rel/NF-κB deficiency mice	B-lineage phenotypes
nfκb1$^{-/-}$	Loss of marginal zone B cells and peritoneal B1 B cells [98]; mature quiescent B cells turn over rapidly when activated by LPS and CD40; splenic B cells proliferate poorly due to a cell-cycle block in G1 and enhanced mitogen-induced apoptosis [104]; *nfκb1*$^{-/-}$ B cells fail to mount a normal humoral response when challenged with various antigens [21]
nfκb2$^{-/-}$	Abnormally low numbers of follicular B cells; proliferation is moderately reduced in response to LPS, anti-IgD-dextran, and CD40; undergo normal class-switch recombination, but generate inadequate humoral responses to various T-cell-dependent antigens [22, 23]
relA$^{-/-}$	Mice injected with p65-deficient fetal liver cells show a decrease in the populations of pro-B cells, pre-B cells, immature B cells, and recirculating mature B cells [105]; MZ B cells are partially reduced [98]
relB$^{-/-}$	Crippled in proliferate response, undergo normal IgM secretion and class switching [106], defective MZ B-cell development [107]
c-rel$^{-/-}$	Impaired B-cell proliferation in response to range of individual mitogens due to a cell-cycle block in G1 and elevated activation-induced apoptosis [104, 108, 109]; MZ B cells are partially reduced [98]

Table 1-3: B-lineage cells affected in individual Rel/NF-κB mutant mice.

Functional redundancy among these proteins, however, prevents the emergence of clear phenotypes. Indeed, the deficiency in different combination NF-κB proteins leads to distinct B-cell developmental defects (**Figure 1.9**). In *nfκb1*$^{-/-}$*nfκb2*$^{-/-}$ double knockout mice, B-cell development is blocked at the T1 stage in spleen due to the defects in BAFF signaling [31]. It has been shown that BAFF-R can activate the alternative NF-κB pathway by inducing p100 processing into active p52 complexes [110]. The combined loss of NF-κB1 and RelA results in the absence of B220^{+} cells in bone marrow. Interestingly, this defect does not appear to be cell-intrinsic since it can be rescued by co-

transplanting *nfκb1*$^{-/-}$*relA*$^{-/-}$ together with wild-type bone marrow into recipient mice [34]. In bone marrow of mice reconstituted with *c-rel*$^{-/-}$*relA*$^{-/-}$ fetal liver cells, immature B-cell numbers are relatively normal. However, the frequency of splenic B cells is reduced ~10-fold due to 5–10-fold decreased Bcl-2 expression. This reduction is mainly due to the absence of the mature, long-lived B cells although immature and transitional B cells are also fewer in numbers [33, 111].

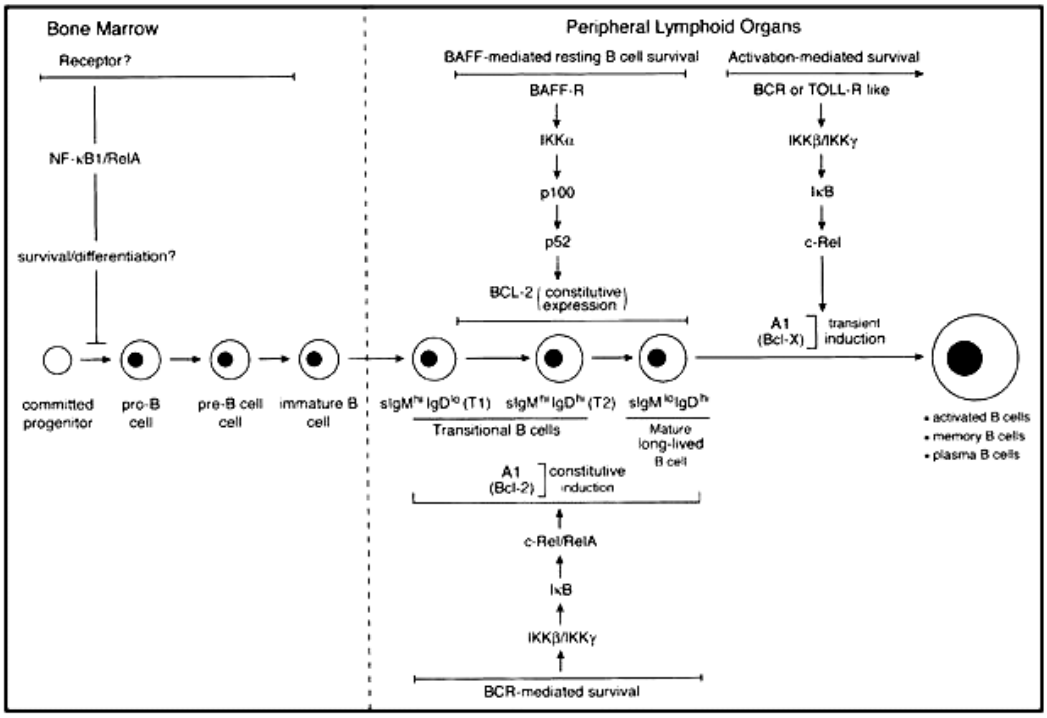

Figure 1.9: Function of Rel/NF-κB members in B-cell development and activation. Rel/NF-κB transcription factors prevent B-cell apoptosis during maturation and activation by transcriptionally regulating distinct sets of Bcl-2-like pro-survival genes at different developmental checkpoints in response to various extracellular signals. (Adapted from [112])

1.3 Secondary lymphoid organogenesis

Primary lymphoid organs, in mammalian bone marrow and thymus, provide environments that support the development and the initial maturation of antigen-specific lymphocytes and other hematopoietic cells. The secondary lymphoid organs are spleen, lymph node (LN), and organized lymphoid tissues associated with mucosal surfaces including Peyer's patches (PP), tonsils, gut-associated lymphoid tissues (GALT), and nasal-associated lymphoid tissues (NALT). They provide sites where encounters between rare antigen-specific lymphocytes and their cognate antigens can occur efficiently.

1.3.1 Signals in secondary lymphoid organ development

The development of secondary lymphoid organs is a complex process that depends on the correct expression of several molecules within a defined timeframe during ontogeny. The anatomic features of secondary lymphoid organs are well defined; however, the signals that lead to the establishment and maintenance of this organized structure are only beginning to be understood.

1.3.1.1 The role of lymphotoxin (LT) in lymphoid organ formation

The first signaling pathway shown to be essential for development and organization of lymphoid tissue involves signaling through lymphotoxin β receptor (LTβR). The LTβR is a member of tumor necrosis factor (TNF) receptor family. LTβR triggering can be mediated by membrane-bound $LT\alpha_1\beta_2$ heterotrimers (mLT) and LIGHT. However, in the absence of LIGHT, nearly all LNs and PPs develop, indicating that $LT\alpha_1\beta_2$ signaling through LTβR has a dominant role in lymphoid organogenesis although LIGHT contributes to the formation of mesenteric lymph nodes.

The importance of LTβR signaling pathway for the formation of secondary lymphoid organs, such as LN and PP as well as the lymphoid compartment in spleen, has been

clearly demonstrated by injections of soluble LTβR-immunoglobulin fusion proteins during embryogenesis and by analysis of mutant mice, in which LTβR signaling does not take place [113]. Injections of soluble LTβR-immunoglobulin fusion proteins during embryogenesis inhibit the lymphoid organ formation at E12.5, blocking the development of all LNs and PPs, whereas injections at E15.5 allow the formation of brachial and axillary lymph nodes [114]. The complete absence of LN and PP in *lt*$\alpha^{-/-}$, *lt*$\beta^{-/-}$, and *lt*$\beta r^{-/-}$ mice further supports the crucial role of LTβR signaling in the formation of secondary lymphoid organs.

1.3.1.2 NF-κB signaling in secondary lymphoid organ development

LTβR is predominantly expressed on stromal cells in various lymphoid tissues. Upon binding of membrane-bound $LT\alpha_1\beta_2$ heterotrimers, both classical and the alternative NF-κB activation pathway are engaged. The importance of the alternative signaling pathway and the activation of p52/RelB heterodimers in lymphoid organogenesis is illustrated by the lack of LN, PP, and disorganized spleen microarchitecture in *nik*$^{-/-}$ and *aly*/*aly* (a point mutation in the gene that encodes NIK) mice [115-117]. In addition, similar abnormalities in secondary lymphoid organ formation have been reported in *ikk*$\alpha^{-/-}$ or *ikk*α^{AA} (NIK phosphorylation sites replaced by alanines), *nfκb2*$^{-/-}$, and *relB*$^{-/-}$ mice, although LN development in *relB*$^{-/-}$ mice seems normal until birth [113, 118, 119]. Germinal centers (GCs) are severely impaired in *aly*/*aly, nfκb2*$^{-/-}$, and *relB*$^{-/-}$ mice [107], whereas *nfκb1*$^{-/-}$ mice have a much milder defect. In addition, these mice completely lack follicular dentritic cell (FDC) networks within B-cell follicles, whereas spleens from *nfκb1*$^{-/-}$ mice develop FDC networks although they are less developed compared to wild-type controls. Formation of splenic MZ and MZ B cells are also severely impaired in different NF-κB-deficient mice. RelB contributes to MZ organization and expression of certain chemokines, such as BLC and SLC, by being part of p52/RelB complexes in stromal cells downstream of LTβR, and RelB is required for MZ B-cell development in a cell autonomous manner. In addition, RelB is essential for the development of MMM. *nfκb2*$^{-/-}$ mice lack MMM and have normal or only slightly reduced numbers of MZM in a cell-intrinsic manner. NF-*κ*B1/p50 is required in a cell autonomous manner for the

generation of MZ B cells [98]. The loss of either RelA or c-Rel leads to a less severe but detectable reduction in MZ B-cell numbers (**Table 1-4**).

Mouse mutant	*nfkb1*$^{-/-}$	*nfkb2*$^{-/-}$	*relB*$^{-/-}$	*c-rel*$^{-/-}$	*bcl-3*$^{-/-}$	*relA*$^{-/-}$*tnfr1*$^{-/-}$	*tnfr1*$^{-/-}$	*ltbr*$^{-/-}$	*aly/aly*	*ikka*^{AA}
B-cell follicles										
B/T cell segregation	+	+/–*	–	+*	+*	–	+*	–	–	N/R
Germinal centers	+	–	–	–	–†	–	–†	–†	–	–
FDC networks	+	–	–	N/R	–	–	–	–	–	N/R
Marginal zone										
MZM	+	+	–	N/R	–	N/R	+‡	N/R	–	N/R
MMM	+	–	–§	+	+/–‡	–	+‡	–	–	N/R
MZ B cells	–	N/R	–	–/+	N/R	–/+	+	–	–	N/R
Marginal sinus	+	–	–	+	+/–	–	–	N/R	–	N/R
Analysis of BM chimeras										
Stromal defects¶	–	+	+	N/R	N/R	+	+	+	+	N/R
Hematopoietic defects¶	–	–	–	N/R	N/R	–	–	–	+	+**

This table is based on citations in the text. *aly/aly*, spontaneous alymphoplasia mutant with defective NF-κB-inducing kinase (NIK); *ikka*^{AA}, IKK^{AA}-knockin mice; LTα/β and TNF-deficient mice are very similar to mice lacking LTβR. LTβR (*ltbr*$^{-/-}$) and tumor necrosis factor receptor-1 (*tnfr1*$^{-/-}$), respectively, except that the defects reside in hematopoietic cells. *tnfr2*$^{-/-}$ mice show normal spleen microarchitecture; N/R, not reported. FDC, follicular dendritic cell; MMM, metallophilic marginal macrophage; MZ, marginal zone; MZM, marginal zone macrophage.

*Development of B-cell follicles is poor.

†Small numbers of PNA^{+} clusters in both T- and B-cell areas.

‡Reduced numbers, disorganized.

§MMM are present but scattered in the red pulp.

¶Stromal/hematopoietic defects with respect to germinal center and follicular dendritic cell network formation.

**Based on the analysis of *ikka*$^{-/-}$ wildtype chimeras.

Table 1-4: Comparison of spleen phenotypes of mice lacking Rel/NF-κB family members or specific upstream signaling components.

The classical NF-κB pathway that triggered upon LTβR involves the activation of p50/RelA heterodimers. The role of RelA in lymphoid organogenesis is less well understood owing to the embryonic lethality of *relA*$^{-/-}$ mice, which is caused by massive TNF-induced hepatocyte apoptosis around E15. Mice deficient for both RelA and TNFR-1 (p55) rescue the early lethality and they also lack secondary lymphoid organs, such as LN and PP, and an organized splenic microarchitecture [32]. However, the exact contribution of RelA to this phenotype is unclear since the lymphoid organ development is already affected by the loss of the TNFR-1 pathway. Targeted disruption of the *tnfr1* gene blocks signaling from TNF, $LT\alpha_3$, and $LT\alpha_2\beta_1$, but signaling can still occur via $LT\alpha_1\beta_2$ to LTβR. PPs are either absent or reduced in number in *tnfr1*$^{-/-}$ mice, indicating that TNFR signaling plays a role in PP development. It has been reported that the *relB* gene transcription is regulated by NF-κB, particularly by RelA. However, in *relA*$^{-/-}$ fibroblasts, RelB complexes are still induced upon LTβR triggering although at reduced levels [17], indicating that RelA is not absolutely required for the induction of RelB complexes downstream of LTβR. Taken together, RelA and RelB may function distinctly in secondary lymphoid organogenesis rather than RelB simply being a transcriptional

target of RelA.

LTβR signaling also regulates the expression of adhesion molecules and chemokines. These molecules seem to be essential for lymphoid organ development. After LTβR ligation, activation of p52/RelB heterodimers results in the production of lymphoid chemokines CXCL12 (SDF1), CXCL13 (BLC), CCL19 (ELC), and CCL21 (SLC), whereas the upregulation of vascular-cell adhesion molecule 1 (VCAM1) requires the activation of p50/RelA heterodimers [107, 120].

1.3.1.3 The complex phenotypes of *relB*$^{-/-}$ mice

RelB shares many common features with other Rel/NF-κB proteins. However, only RelB contains an N-terminal leuzine zipper motif, which along with the C-terminal non-homologous transactivation domain participates in full transcriptional activation. High levels of RelB expression are restricted to specific region of lymphoid tissues, correlated with constitutive basal NF-κB activity in these tissues. Interestingly, *relB*$^{-/-}$ mice exhibit a complex phenotype [25], including multi-organ inflammatory, severe deficits in adaptive immunity, splenomegaly, and lack of LNs as well as PPs. Loss of cellular immune responses in these mice is consistent with the observed deficit in thymic medullary epithelial cells and the loss of functional dendritic cells [27]. Multi-organ inflammation is exaggerated in mice also lacking p50, indicating that p50 and RelB cooperate in the regulation of genes that limit inflammation [35]. The importance of RelB in lymphoid organogenesis is evident in *relB*$^{-/-}$ mice, particularly in the development of PP and LN [17, 118]. Moreover, *relB*$^{-/-}$ mice unable to form germinal centers (GCs), marginal zone structure, and follicular dendritic cell network upon antigen challenge in spleen. Almost no MZ B cells develop in *relB*$^{-/-}$ mice and this defect is cell-intrinsic [107]. These findings highlight the role of p52/RelB heterodimers (probably in response to LTβR signaling) in the regulation of κB target genes during lymphoid organogenesis and the maintenance of intact structure of these tissues.

1.4 Conditional gene targeting

Gene targeting, defined as the introduction of site-specific modifications into the mouse genome by homologous recombination, is generally used for the production of null or ‘‘knockout’’ animals to study gene function *in vivo*. Homologous recombination of foreign DNA with endogenous genomic sequences is a relatively infrequent event in mammalian cells compared to random integration. The only efficient gene targeting method established presently utilizes pluripotent murine embryonic stem cell (ES) lines. Using these cells, selection of rare, homologous recombination ES clones *in vitro* can be accomplished. Gene-targeted ES cells are then injected into blastocysts. They can contribute to all cell lineages (including germ cells) of the resulting chimeras. The breeding of germline chimeras, which transmit an ES cell derived mutant chromosome to their progeny, allows the generation of animals with the desired genetic alteration [121, 122].

Conditional gene targeting, in contrast, can be defined as a gene modification, which is restricted to certain cell types or different development stages of mouse. The conditional mutation confined to a particular cell lineage would greatly aid in the determination of a gene’s function in that particular cell lineage or tissue. A powerful feature of a conditional gene inactivation strategy using the Cre/loxP recombination system is that the same loxP sites-flanked mouse can be used for gene ablation in a large number of different tissues or at different development stages, by simply mating it with a corresponding Cre-transgenic line that displays the desired tissue or temporal specificity of expression. Thus, the same genetically modified animal can be used to answer a variety of questions relating to the expression and function of the target gene.

1.4.1 Cre-mediated recombination

The Cre protein is the 38 kDa product of the *cre* (cyclization recombination) gene of bacteriophage P1 and is a site-specific DNA recombinase of the Int family. Cre recognizes a 34 bp site on the P1 genome called loxP (locus of X-over of P1) and

efficiently catalyzes reciprocal conservative DNA recombination between pairs of loxP sites (**Figure 1.10**).

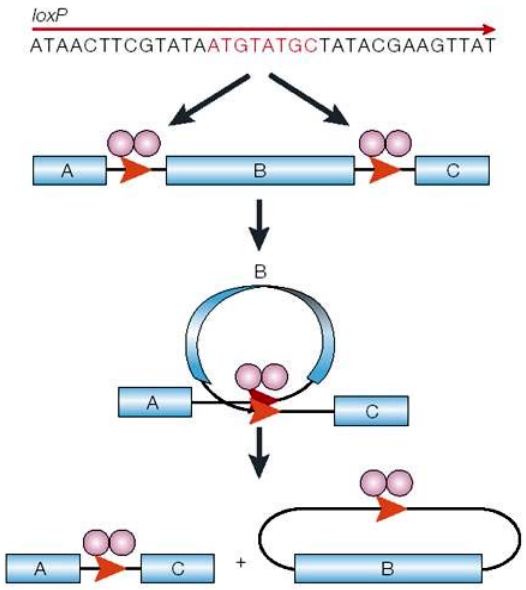

Figure 1.10: Cre-mediated recombination. The 34 bp loxP consists of two 13 bp inverse repeats (black) that flank an 8 bp non-palindromic core sequence (red). This core sequence confers directionality to these sites (red arrows). Dimers of Cre catalyze in *cis* the conservative recombination between two directly repeated loxP sites (red arrowheads), resulting in the formation of a synaptic structure, the excision of region B, and the juxtaposition of regions A and C. If region B is an essential region of a gene, then the recombination event results in gene inactivation. (Adapted from [122])

1.4.2 Strategy for generating conditional gene modification

The use of the Cre/loxP recombination system requires the generation of both a mouse strain harboring a loxP-flanked (floxed) segment of the target gene and a second strain expressing the Cre recombinase under the control of certain promoters. A conditional mutant is then generated by crossing these two strains so that the floxed target gene is mutated in a spatial or temporal manner according to the pattern of Cre expression in the particular strain used (**Figure 1.11**).

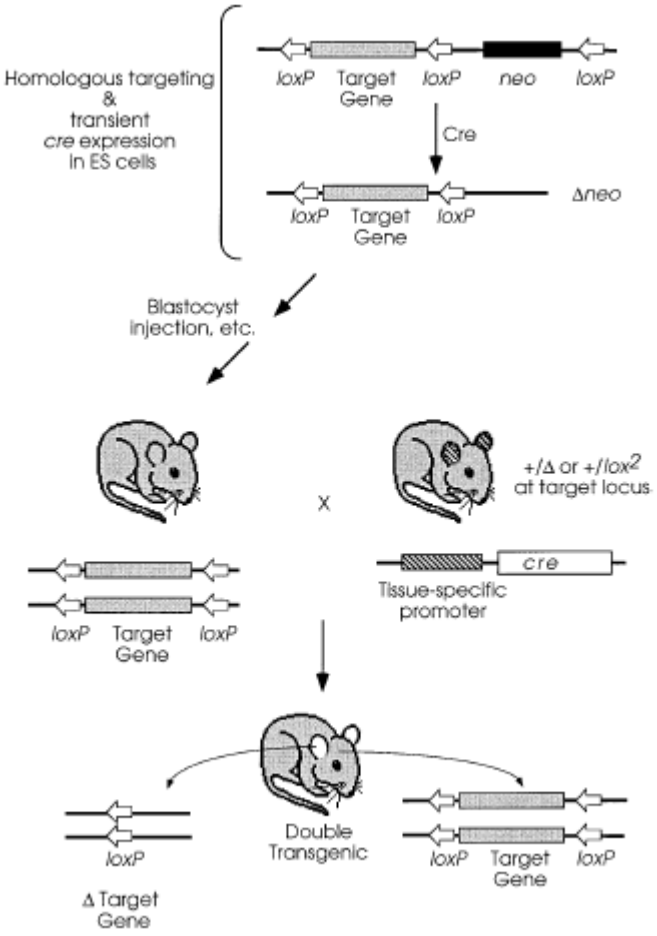

Figure 1.11: Conditional gene ablation by Cre recombinase. The target endogenous gene is modified by homologous targeting in ES cells so that it is flanked by two directly repeated loxP sites. In the situations that require removal of the *neo* gene, a third loxP site is positioned so that the *neo* gene can be excised by transient expression of Cre in ES cells. After identification of clones that retain the loxP-flanked target gene, mice are generated from ES cells by standard procedures. Mating of the loxP-modified mouse with a Cre-transgenic mouse will generate a double-transgenic mouse, in which the loxP-modified gene will be deleted in the tissues in which the Cre transgene is expressed. In the example shown, Cre is expressed in the ears (striped) of the Cre-transgenic line so that deletion of the loxP-modified target gene is confined solely to the ears (white) of the double-transgenic mouse. (Adapted from [121])

1.4.2.1 Recombination events upon transient Cre transfection

The flox-and-delete strategy can be used for conditional gene mutation and is especially useful if lethality is anticipated in conventional mutants. This type of targeting vector contains three loxP sites in the same orientation, two of them flanking the selection marker gene and an isolated loxP within one arm of homology. The floxed selection

marker for the targeting vector usually is the *neo* gene or *neo*/*HSVtk* genes. After identification of the homologous recombinant ES clones, transient Cre expression leads to three different recombination products (**Figure 1.12**). The recombination, which happens between the loxP sites flanking the *neo* gene, leaves one loxP site in the genome which generates, together with the isolated loxP site, the floxed version of the target gene (type I). The second recombination product (type II), the deletion between the isolated loxP site and the inner loxP site flanking the *neo* gene is usually not of practical use and will not be found if ES colonies are screened for G418 sensitivity after Cre expression since such colonies retain the *neo* gene. If the recombination occurs between the outer loxP sites, a large deletion is created which is similar to the conventional gene targeting (type III). After identification of those transformants in which homologous recombination has replaced one copy of the endogenous gene with the mutant variant of the targeting construct, the *neo* gene can be removed by Cre-mediated recombination; leaving behind only the 34-bp loxP site forms the floxed allele together with the isolated loxP site. Unless placed in a coding exon or another critical region of the gene, the loxP site is unlikely by itself to interfere with gene expression.

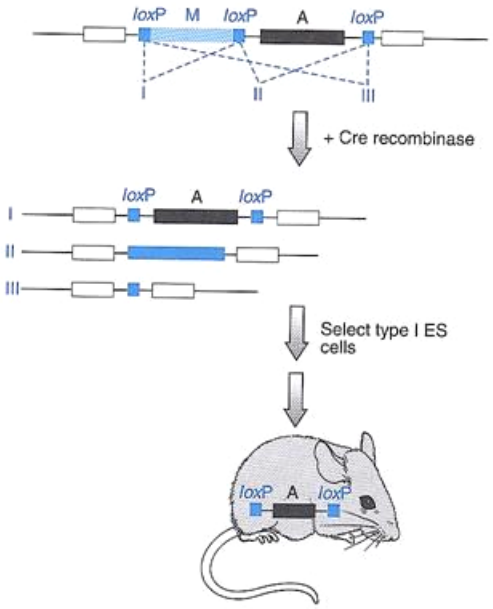

Figure 1.12: Cre-mediated recombination in homologously recombined ES cells. Transfection of a Cre-recombinase encoding plasmid results in different recombination products among the introduced loxP sites. Type I recombinants are used to generate mice in which the target locus is flanked by loxP sites. **M**: marker gene; **A**: a target locus.

1.5 Aims

Deletion of individual members of Rel/NF-κB family does not affect mainstream B-cell development although defective B-cell activation upon stimulation is observed, mainly due to the increase of apoptosis. The deficiency in different combination of NF-κB members indicates a distinct role of NF-κB proteins in B-cell development. In the absence of RelB, development and function of particular B-cell subset are impaired. The aim of the first project is to understand the role of RelB-specific inhibitor NF-κB2/p100 and RelB in B-cell development. Towards this goal, $p100^{-/-}$ mice, lacking the inhibitory p100 precursor but still expressing active p52 subunit of NF-κB2, will be analyzed with an emphasis on the development of mainstream B-cell and other B-cell subsets.

The activation of NF-κB through LTβR is critical for secondary lymphoid organogenesis. LTβR signaling induces both classical (p50/RelA) and alternative (p52/RelB) complexes. The importance of alternative pathway in lymphoid organogenesis is illustrated by the similar phenotypes in mice lacking individual NF-κB members, upstream kinases, and receptors. The contribution of RelA in this process is suggested by the lack of LNs and PPs in $relA^{-/-}tnfr1^{-/-}$ mice. It is still unclear that which NF-κB activity contributes to which part of secondary lymphoid organogenesis. There is also no direct proof that whether RelB and/or RelA does function downstream of LTβR signaling *in vivo*, regulating the development of secondary lymphoid organs. The aim of the second project is to generate tools to dissect the individual contribution of both NF-κB pathways downstream of LTβR signaling *in vivo* with a specific focus on lymphoid organogenesis. To fulfill this, mouse models will be established, in which a specific inactivation of *relB* or *relA* in LTβR-expressing cells could be achieved using gene targeting technology. Phenotypic analysis of $relB^{ltbr\text{-}cre}$ and $relA^{ltbr\text{-}cre}$ mice will unravel the contribution of classical (RelA complexes) and alternative NF-κB pathway (RelB complexes) to LTβR-dependent processes on the organic level. The generation of $relB^{flox/flox}$ mice will be useful to investigate the specific function of RelB in other cell types, when crossed with different Cre-transgenic mice. For example, the role of RelB in B cells could be studied without the influence of losing RelB function in other cell types.

2 MATERIALS AND METHODS

2.1 Materials

2.1.1 Mice

The generation of *p100*$^{-/-}$ [36], *relB*$^{-/-}$, and *nfκb1*$^{-/-}$ [22]mice has been previously reported. *p100*$^{-/-}$ and *relB*$^{-/-}$ mice were mated to generate *p100*$^{-/-}$*relB*$^{+/-}$ and *p100*$^{-/-}$*relB*$^{-/-}$mice. *p100*$^{-/-}$ and *nfκb1*$^{-/-}$ mice were mated to generate *p100*$^{-/-}$*nfκb1*$^{+/-}$ and *p100*$^{-/-}$*nfκb1*$^{+/-}$ mice. All animal were housed and bred under the standard conditions with water and food ad libidum in the pathogen free mouse facility of Forschungszentrum Karlsruhe, Institute of Toxicology and Genetics. For timed pregnancies, mice were mated and the noon of the day vaginal plugs was accepted at 0.5 days post coitus (d.p.c).

2.1.2 Chemicals

All general chemicals were purchased from Carl Roth GmbH & Co (Karlsruhe), Merck (Darmstadt), Sigma Chemie GmbH (Deisenhofen), and Invitrogene GmbH (Karlsruhe) and with highest purity grade.

2.1.3 Radiochemicals

[^{32}α-P]-dCTP (Amersham Life Science)

2.1.4 Primers

All primers were synthesized by MWG-Biotech AG (Ebersberg) and were of HPSF purified grade.

2.1.4.1 Primers for real-time PCR

(Primers with melting temperature (Tm) of 58-60ºC were designed using Primer Express® Software v2.0 from Applied Biosystems)

774-**Pax5**-794:	GACATCTTCACCACCACGGAA
927-**Pax5**-909:	AGGACTGTGGGCCTGGAAC
599-**E2A**-618:	GGACATACAGCGAAGGTGCC
749-**E2A**-731:	GCCTGACTCAAGGTGCCAA
714-**EBF**-734:	CCATGTCCTGGCAGTCTCTGA
865-**EBF**-847:	TCCATCCTTCACTCGGGCT
690-**CD19**-710:	AGAGCACCCGGTCAGAGAGAT
840-**CD19**-821:	GAGCCACACTGCTGACCTTG
1857-**mb1**-1877:	ATTGTTTCCCTCAGACACCCC
2007-**mb1**-1988:	CATGTCCTGGGTCTGGTTGC
1491-**BLNK**-1509:	GGAGGCTGAACTGCTCGGT
1641-**BLNK**-1622:	CGCAACTAGGGTGTACGGCT
5980-**Notch1**-5998:	CCAGATCCTGCTCCGGAAC
6143-**Notch1**-6123:	AAGCCGACTTGCCTAGGTCAT
804-**M-CSF-R**-824:	GCTGGAAATCCCCCTAAACAG
954-**M-CSF-R**-936:	GAAGTTCATGGTGGCCGTG
456-**MPO**-474:	CCCAGGCATAAAAACCCGT
606-**MPO**-586:	TGAATTCTCCACTTCCCCCAG
897-**C/EBPα**-917:	GAGCCGAGATAAAGCCAAACA
1056-**C/EBPα**-1037:	GACCAAGGAGCTCTCAGGCA

370-**PU.1**-390:	CCGCAGCTACAGCAGCTCTAT
420-**PU.1**-400:	GACGTGCATCTGTTCCAGCTC

β-actin Forward:	TGGCGCTTTTGACTCAGGA
β-actin Reverse:	GGGAGGGTGAGGGACTTCC

2.1.4.2 Primers for genotyping *relB*$^{flox/flox}$ mice

10139-**RelB**-10146:	TGAGAGTGGATCTCTGTG
10360-**RelB**-10342:	TCGATGATTTCTGCGCGA

2.1.4.3 Primers for genotyping *ltbr-cre*^{tg} mice

ltbr-exon2-forw (270-**ltbr-**288):	CCCTTATCGCCATAGAAAAC
ltbr-exon3-rev (448-**ltbr**-467):	GTTCCAGTGTTCATTATAGG
cre-rev (3038-**cre**-3056):	GCGCGCCTGAAGATATAGA

2.1.5 Plasmids

2.1.5.1 Plasmid gifts (obtained from)

pLTNT (Dr. H. Schorle), pTVFlox-0 (Dr. P. Zhu), and pGK-Cre (Dr. M. Blum)

2.1.5.2 Plasmid constructs

pRelBXS11.2-LLTNL, pTVFlox-LRelBXS11.2, and pTVFlox-LTβR-cre
Plasmid maps are described in the results part of thesis.

2.1.6 Cell culture – cell lines and cell culture media

Unless otherwise stated, all tissue culture media and PBS used for washing cells were purchased from Invitrogen GmbH together with the supplements such as Penicillin/Streptomycin and Glutamax. Trypsin was purchased from Difco Laboratories

and was diluted to 0.25% in 15 mM sodium citrate and 134 mM potassium chloride, which were kept as stocks at -20ºC.

2.1.6.1 Cell lines

Embryonic stem cells (ES): E14.1, CJ7, and Kunt I
Mouse embryonic fibroblasts (EF): home made
B-cell lines: BaF3, WEHI 231, and 70Z/3

2.1.6.2 ES Media

Reagent	Volume	Catalog Nr.	Store
D-MEM (1×), liquid - with GlutaMAX™ I, Sodium Pyruvate	500 ml	Gibco 31966-047	4°C
GlutaMAX™-I Supplement, 200mM	6 ml	Gibco 35350-038	-20°C
2-Mercaptoethanol (1,000×), liquid	1.2 ml	Gibco 31350-010	4°C
MEM Non Essential Amino Acids Solution (100×), liquid	6 ml	Gibco 11140-035	4°C
Penicillin-Streptomycin Solution	6 ml	Gibco 15140-114	4°C
ESGRO® (LIF) [Murine LIF]	1 ml (1,000 u)	ESG 1107	-20°C
FBS	75 ml	Biochrom AG S0115	-20°C
Sodium Pyruvate MEM 100 mM liquid	6 ml	Gibco 11840-030	4°C

2.1.6.3 EF Media

Reagent	Volume	Catalog Nr.	Store
D-MEM (1×), liquid - with Sodium Pyruvate	500 ml	Gibco 41966-029	4°C
D-MEM (1×), liquid - with GlutaMAX™ I, Sodium Pyruvate	5.5 ml	Gibco 25030-024	-20°C
Penicillin-Streptomycin Solution	5.5 ml	Gibco 15140-114	4°C
FBS	50 ml	PAA A15-649	-20°C

2.1.7 Bacteria strains

DH5α (Gibco), TOP10 (Gibco), and JM110 (deficient for Dam and Dcm, Stratagene)

2.2 Methods

The following routine molecular biology methods were performed according to standard protocols (Sambrook and Russell, 2001):
Mini plasmid preparation, restriction digests of DNA, spectrophotometric quantification of nucleic acids, phenol: chloroform extraction, preparation of electrocompetent bacteria, ligation reactions, blunting reaction with T4 DNA polymerase, dephosphorylation of plasmids with CIP, electroporation of bacteria, precipitation of nucleic acids, and basic PCR reaction

The following routine molecular biology manipulations were performed by using kits or commercially available reagents according to the manual.
Site-directed mutagenesis (Quickchange™ Site-Directed Mutagenesis Kit, Stratagene)
Cloning of long (3-10 kb) PCR products (TOPO® XL PCR Cloning Kit, Invitrogen)
Cloning of PCR products (TOPO TA Cloning®, Invitrogen)
Labeling of DNA by random priming (*redi*prime™ II Kit, Amersham)
Large scale plasmid preparation (Qiagen Plasmid Maxi Kit, Qiagen)
Total RNA extraction (NucleoSpin RNA II kit, Macherey-Nagel Company)
Isolation and purification of DNA from agarose gel (EasyPure DNA purification Kit, Biozyme)

The methods described in detail below are those developed or modified in this thesis.

2.2.1 Preparation of single cell suspensions from lymphoid organs

Different lymphoid organs were collected. Tissues were pushed through a metal sieve into 6 cm petri dishes with FACS buffer using plunger. The cell aggregates, which were collected into petri dishes, were passed through 10 ml syringe with a 21 Gauge needle for 3-5 times. Cells were followed being lysated in ACK lysis buffer at room temperature (RT) for 5 minutes (min). After two times washing with FACS buffer, cells were finally resuspended in 10 ml FACS buffer and passed through cell strainer with 40 μm pore size. An aliquot of 10 μl cells was taken into trypan blue solution for counting trypan blue negative cells using hemocytometer. All the centrifugation steps were performed at 1,500 revolutions per minute (rpm) for 5 min at 4^{o}C.

FACS buffer: PBS with 2% fetal calf serum (FCS), kept at 4^{o}C

ACK lysis buffer: 0.15 mM NH_4Cl, 1 mM $KHCO_3$, and 0.1 mM Na_2EDTA pH 7.2-7.4, adjusted with 1 N HCl, filter-sterilized, and stored at RT

2.2.2 Analysis of cells by flow cytometry

Flow cytometry was performed using a Becton Dickinson FACSstar. All the monoclonal antibodies (mAbs) used for flow cytometric analysis were purchased from BD biosciences. FITC-conjugated mAbs were diluted 1:100, PE-conjugated mAbs 1:200, and Cy-conjugated mAbs or biotin-conjugated mAbs 1:300 before use. Single cell suspensions were washed twice with FACS buffer. The following flourochrome conjugated mAbs were used: anti-B220-Cy/PE/FITC (clone RA3-6B2), anti-CD4/FITC (clone RM4-5), anti-CD8/PE (clone 53-6.7), anti-CD11b/FITC (clone M1/70), anti-CD19/PE (clone 1D3), anti-CD21-FITC (clone 7G6), anti-CD23-PE (clone B3B4), anti-CD43/FITC (clone S7), anti-CD117(c-kit)-Biotin (clone 2B8), anti-CD127(IL-7R)-Biotin (clone B12-1), anti-Gr-1-PE (clone RB6-8C5), anti-IgM-Bio/FITC (clone R6-60.2), anti-IgD-FITC (clone 11-26), anti-Thy1.2-FITC (clone 53-2.1), anti-CD45.1-Biotin (clone A20), and anti-CD45.2-Biotin (clone 104). Biotinylated mAbs were detected with Streptavidin-PerCP (diluted 1:300).

Staining with mAbs was performed in a standard method. In brief, 0.5 $\times 10^6$ cells were stained with different combinations of mAbs in FACS buffer in U-bottom 96-well plate (CellStar, Griener) on ice for 30 min. After that, cells were washed two times with FACS buffer and fixed with 4% formaldehyde in PBS for 10 min at RT. After washing for two times, cells were resuspended in FACS buffer for analysis or for storage at 4°C. Data were analyzed using CELLQuest Pro™ software (BD Bioscience).

Apoptotic cells were detected by Annexin-V-FITC (BD biosciences) according to the manufacturer's specifications. Briefly, 1×10^6 cells were suspended with 100 µl incubation buffers in U-bottom 96-well plate. After washing, cells were stained in Annexin-V staining solution. After incubating for 15 min at RT, cells were washed twice with 200 µl of incubation buffer and finally resuspended in 100 µl incubation buffer for flow cytmetric analysis. Data were analyzed using CELLQuest Pro™ software (BD Bioscience).

Incubation buffer: 10 mM HEPES/NaOH, pH 7.4, 120 mM NaCl, and 5 mM $CaCl_2$

Annexin-V staining solution: 10 ml of Annexin-V-FITC stock and 20 µl of propidium iodide stock (50 µg/ml) were diluted in 1500 µl incubation buffer that is sufficient for 15 samples

2.2.3 Purification of pro-B Cells

Bone marrow (BM) cells were first stained with anti-CD19-PE mAb (Pharmingen, 2-2.5 µl/10×10^6 cells) in FACS buffer (90 µl/10×10^6 cells) on ice for 30 min. After washing with excess FACS buffer, cells were resuspended in MACS buffer (90 µl/10×10^6 cells) and incubated with anti-PE MicroBeads (Miltenyi Biotech, 10 µl/10×10^6 cells) for 15 min at 6-10°C. After washing with excess MACS buffer, cells were resuspended in 1 ml MACS buffer, passed through cell strainer (40 µm pore size) on to the MACS negative selection column (LD; Miltenyi Biotech), and depleted $CD19^+$ B cells as per the manufacturer's specifications. Afterwards the $CD19^-$ B-cell portion was collected and recounted. Cells were then stained with anti-B220-Cy5 mAb (Pharmingen) in FACS buffer on ice for 30 min and incubated with anti-Cy5 MicroBeads (Miltenyi Biotech, 10

µl/10×10^6 cells) for 15 min at 6-10°C. After washing with excess MACS buffer, cells were resuspended in 1 ml MACS buffer and passed through cell strainer (40 µm pore size) on to the MACS positive selection column (MS; Miltenyi Biotech) to obtain the $B220^+$ B cells. An aliquot of cells from each step of purification procedures was used for flow cytometric analysis to check the purity.

MACS Buffer: 0.5% Bovine Serum Albumin (BSA) in PBS without Ca^{2+} and Mg^{2+} and 2 mM EDTA

2.2.4 Extraction and analysis of RNA

2.2.4.1 Total RNA isolation from cells

5×10^6 cells were pelleted in 1.5 ml eppendorf tubes and resuspended in 350 µl lysis buffer RA1, containing 3.5 µl β-mecaptoethanol. The total RNA isolation was performed using 'NucleoSpin RNA II' kits purchased from Macherey-Nagel Company. The procedures were performed following the manufacturer's instructions. Contamination DNA was removed by a DNase I solution. Total RNA was kept frozen at -80ºC.

2.2.4.2 Determination of RNA concentration and agarose gel electrophoresis of RNA samples

RNA concentration was determined spectrophotometrically (Eppendorf spectrophotometer) by taking readings at 260 nm against a blank, ddH_2O. A solution of 50 µg/µl DNA or 40 µg/µl RNA in a 1 cm quartz cuvette will give an absorbance of 1 at 260 nm. The concentrations were calculated according to absorbance values and total volume of RNA solution. Protein contamination during the isolation procedure was assessed by A260/A280 ratio with a value of 1.7 or greater as an indication of a good purity. The quality of RNA samples and genomic DNA contamination were further assessed by agarose gel electrophoresis. Aliquots of RNA samples (minimum 0.5 µg) were diluted in water and 10 × gel loading buffer. 0.8% (w/v) agarose gels containing ethidium bromide to a final concentration 100 µg/ml were prepared in 1 × TAE buffer.

Samples were loaded and observed by illumination with UV light and photographs were taken using an Eagle Eye photocamera system (Stratagene).

10 × gel loading buffer: 0.25% bromophenolblue, 0.25% xylene cyanol FF, and 15% Ficoll in water; kept at RT, final 1 × concentration

1 × TAE buffer: 0.04 M Tris-acetate and 0.01 M EDTA

2.2.4.3 First strand cDNA synthesis of total RNA samples

First strand complementary DNA (cDNA) was synthesized from total RNA by using M-MLV Reverse Transcriptase (Promega) as described by the manufacturer. 1-5 µg total RNA was added in a 1.5 ml sterile RNase-free Eppendorf tube together with 0.5 µg oligo (dT) 12-18 (New England Biolabs). The volume was completed to 14 µl with sterile ddH_2O. The reaction mixture was heated to 70ºC for 10 min to melt secondary structure within the template, and then quickly chilled on ice for 5 min. Following brief centrifugation, 5 µl M-MLV 5 × Reaction buffer, 5 µl 10 mM dNTP mix (Peq Lab) (10 mM each dATP, dGTP, dCTP, and dTTP at neutral pH), and 200 units M-MLV Reverse Transcriptase were added. The samples were incubated at 42ºC for 60 min following heat inactivation at 70ºC for 15 min. Then the cDNA samples were ready for amplification by PCR. The samples were diluted 5-fold (final volume 100 µl) with sterile ddH_2O before they were used as template for amplification.

2.2.4.4 Real-time PCR

5 µM primers mix was prepared by adding 20 µl sense (100 pmol/µl) and 20µl antisense (100 pmol/µl) primers to 360 µl sterile ddH_2O. For each template (cDNA), three independent PCR reactions were performed (triplet) to avoid pipetting errors. Run a housekeeping gene (β-actin) and the genes of interest together. Run NTC (without adding template) as negative control as well. The reaction was set up in 20 µl volume, containing 10 µl 2 × SYBR-Green Mix, 4 µl Primermix, 4 µl template, and 2 µl ddH_2O. Run the PCR with protocol SYBR-40 (50°C 2 min, 1 cycle; 95°C 10 min, 1 cycle; 95 °C 15 s→ 60 °C 30 s → 72 °C 30 s, 40 cycles; 72°C 10 min, 1 cycle). Analyze the real-time PCR

result with the SDS 7000 software. Check if there is any bimodal dissociation curve or abnormal amplification plot. Data were exported and analyzed with Pfaffel methods that provide a means for quantification of a target gene transcript in comparison to a reference gene.

2.2.5 Generation of bone marrow chimeras

Bone marrow cells were isolated from arm bones, tibiae, and femora of 3-week-old wild-type and *p100*$^{-/-}$ mice. Bones were first thoroughly cleaned and rinsed with 70% alcohol and washed extensively in sterile PBS. The ends of the bones were cut off and the bone marrow cells were flushed out with PBS into a petri dish containing 1-2 ml sterile PBS using a 2 ml syringe with a 23 Gauge needle. The cells were then passed through the same syringe for additional 2-3 times and an aliquot of cells was used for counting the number of cells. Up to 4-6 × 10^6 cells were injected intra venous (i.v.) per mouse in different combinations of donor and recipient mice as described in the results section. Before injection, around 6-week old recipient mice were irradiated with 2 × 550 rad with 3 hours interval and rested for 4-6 hours after the second irradiation. After the injection of bone marrow cells, mice were kept under pathogen free conditions and were analyzed after 6 weeks. For the analysis of chimerism, peripheral blood was collected by cardiac puncture at necropsy and immediately transferred into 15 ml falcon tubes containing 10 ml of PBS with 5mM EDTA and centrifuged at 1,500 rpm for 5 min at 4ºC. The pellets were resuspended in 2 ml of ACK lysis buffer and kept at RT for 5 min and then centrifuged. ACK lysis was repeated and the pellets were washed two times with FACS buffer and the leukocytes were resuspended in 100 µl FACS buffer. The cell suspension was transferred to eppendorf tubes and centrifuged at 2,000 rpm for 5 min at 4^{o}C and the pellets were resuspended in PBND buffer containing protinase K and kept on an incubator shaker at 55ºC for 2-3 hours. The lysates obtained were used for analysis by PCR to check the chimerism.

For the generation of mixed bone marrow chimeras, bone marrow cells from wild-type (CD45.1$^+$) and *p100*$^{-/-}$ mice (CD45.2$^+$) mice was isolated and 3 × 10^6 cells from each mouse were mixed and injected i.v. into irradiated either CD45.1$^+$ or CD45.2$^+$ wild-type

recipients. The mice were analyzed after 6 weeks. For the analysis of chimerism of the mixed bone marrow chimeras, lymphocytes were stained with anti-CD45.1 or anti-CD45.2 mAb and were analyzed by flow cytometry.

PBND buffer: PCR buffer with nonionic detergents; 50 mM KCl, 10 mM Tris-HCl pH 8.3, 2.5 mM $MgCl_2$, 0.1 mg/ml gelatin, 0.45% v/v NP-40, 0.45% v/v Tween-20, and 0.1 µg/ml Proteinase K (3 µl from 10 mg/ml stock); this buffer was kept at 4°C without Proteinase K which was added just before use.

2.2.6 Extraction and analysis of proteins

2.2.6.1 Preparation of nuclear and cytoplasmic fractions

Cells were and pelleted in a 1.5ml Eppendorf tube. Supernatant was aspirated and cells were gently resuspended in 400 ml buffer A. The sample was incubated on ice for 15 min, and then 25 µl 10% NP-40 was added, vortexed vigorously for 20 seconds, and centrifuged at 13,000 rpm for 1 min at 4ºC. At this step, the supernatant contains cytoplasmic RNA and proteins and pellet contains nuclei and cell debri. An aliquot of supernatant, 200-300 µl was transferred to a new tube as ***cytoplasmic*** fraction. The nuclear pellet was washed once with 200 µl buffer A gently, buffer was removed and 60 µl of buffer C was added without resuspending. The sample was then placed on an Eppendorf shaker for 15 min at 4ºC to ensure vigorous mixing such that the pellet remains intact and floats around. Following centrifugation at 13,000 rpm for 5 min at 4ºC, 50 µl of ***nuclear*** fraction was recovered and protein concentration was determined. Cytoplasmic and nuclear fractions were stored at -80ºC.

Buffer A: 10 mM HEPES pH 7.9, 10 mM KCl, 0.1 mM EDTA, 0.1 mM EGTA, 1× proteinase inhibitors, and 2.5 mM DTT

Buffer C: 20 mM HEPES pH 7.9, 0.4 M NaCl, 1 mM EDTA, 25% glycerol, 1 × proteinase inhibitors, and 2.5 mM DTT

Proteinase inhibitors: One tablet in 2 ml ddH_2O gives 25 × stocks (Roche)

Both buffers were stored at 4ºC without proteinase inhibitors and DTT.

2.2.6.2 Protein concentration determination

Protein concentration was determined by BioRad microassay procedure following the manufacturer's instructions. Bovine IgG was used as a protein standard. Several dilutions of standard were prepared (1-25 µg/µl). In dry cuvettes, 800 ml diluted standards or appropriate amount of samples (2-3 µl cytoplasmic or nuclear extract) diluted in 800 ml ddH_2O were placed. 200 ml Dye Reagent Concentrate (5 × stock, BioRad) was added and gently mixed. For blanks, 800 ml ddH_2O was used. After 5 min RT incubation, OD595 measurement was performed and a standard curve (concentration in mg/ml versus OD595) was plotted to determine the concentrations of extracted samples.

2.2.7 Electro-mobility Shift Assay (EMSA)

2.2.7.1 Preparation of probes

Following single stranded oligonucleotides were used:

Oct-1 up: 5'-GAT CCT GTC GAA TGC AAA TCA CTA GAA A-3'

Oct-1 lo: 5'-GAT CTT TCT AGT GAT TTG CAT TCG ACT C-3'

Igκ up: 5'-GAT CCA GAG GGG ACT TTC CCA CAG GA-3'

Igκ lo: 5'-GAT CTC CTC TGG GAA AGT CCC CTC TG-3'

2.2.7.1.1 Annealing of oligonucleotides

Following reaction mix was prepared:

2 µl	each single stranded oligo (100 pmol/ml)
200 µl	TE (pH 7.5)
2 µl	NaCl (5 M)

(1 pmol/ml oligo concentration in the final volume of 206 µl)

The reaction was incubated at 80ºC for 15 min and left at RT O/N.

2.2.7.1.2 Radioactive labeling of the annealed oligonucleotides

Following reaction mix was prepared:

10 µl	ddH_2O

2 µl	annealed oligo (2 pmol total)
2 µl	10 × REACT 2 buffer (Invitrogen)
2 µl	dNTPs (0.5 mM each without dCTP)
3 µl	^{32}P-dCTP (10 µCi/µl)
1 µl	Klenow fragment (6.5 U, Invitrogen)

The reaction was in a total volume of 20 µl and was incubated at RT for 20 min.

2.2.7.1.3 Purification of radioactive labeled probes

10 µl of blue dextran solution (0.7% (w/v) in water) was added to the labeling mix. Sephadex G-50 (Sigma) in TE buffer was used to prepare 1 ml column in 1 ml syringe the bottom of which was plugged with glass wool. Labeling mix with blue dextran was added on the column and unincorporated radioactivity was left in the column by eluting 200-400 µl blue solution (DNA complexed with blue dextran) in TE. One µl of this elute was measured using scintillation counter 1211 Minibeta (Wallac). A total of 20,000-50,000 cpm per reaction was used for bandshift assay.

2.2.7.2 EMSA Assay

Following solutions are required:

5 × Binding Buffer (BB):	50 mM Tris-HCl, 250 mM NaCl, 5mM EDTA, and 25% glycerol; kept at RT and before use DTT is added to a final concentration of 25 mM
Buffer C	with 1 × proteinase inhibitors and 2.5 mM DTT
Unspecific competitors:	Sonicated calf thymus DNA (1 µg/µl) for Igκ bandshift or dI: dC homopolymer (1 µg/µl; Sigma) for Oct-1 bandshift

Rabbit anti-Rel/NF-κB polyclonal antisera for EMSA

preimmune serum (PI):	KD 57 or rabbit serum (Sigma):
anti-p50:	KD 57-8: anti-p50
anti-p52:	KD 38-2:
anti-p65 (RelA):	KD 13-3:

anti-RelB: KD 6-8 or RR 2-8:

All working solutions and binding reactions should be prepared on ice, 5 × BB and buffer C were prepared on ice before setting up the binding reactions. Below are the components of a binding reaction:

nuclear extract solution	5 µl (2-4 mg extract)
5 × BB (final 1×)	4 µl
competitor	(0.4 µg (0.4 µl/reaction) calf thymus (1/10) or 2 mg (2 ml/reaction) dI: dC (1/2) for 4 mg nuclear extract)
antiserum	for antibody challenge reactions only
oligo	20,000-50,000 cpm
ddH_2O	complete the volume to 20 µl

Preferentially, premixes were prepared for each oligo shift by adding 5 × BB, competitor and ddH_2O the total amounts of which were determined according to the total number of reactions. Then, the mix was distributed to precooled tubes, followed by addition of appropriate volumes of buffer C and protein extract for each sample. For antibody challenge reactions, 1 µl of appropriate antiserum (see above for antisera used) was added and the reactions were incubated on ice for 10 min. The radioactively labeled probe was then added and the reactions were kept at RT for 20 min. Once complete, 2 µl 10 × gel loading buffer per reaction was added and the reaction mix was loaded onto 5% gel. While the binding reactions were incubated, the wells of the gel were washed and pre-run was performed at 150 V for 10 min using 0.25 × TBE as running buffer. A typical run is at 150 V for 2-3 h at RT. Then the gel was dried at 80ºC for 30 min and exposure was performed using Hyperfilm MP (Amersham).

5% polyacrylamide gels: 8.3 ml acrylamide: bisacrylamide (30%), 2.5 ml 5 × TBE (final 0.25 ×), and 39.2 ml ddH_2O, total volume 50 ml.

2.2.8 Southern Blotting

2.2.8.1 Electrophoresis of DNA through gels

0.8% agarose gel was prepared by dissolving the corresponding amount of agarose in TAE and the solution was cooled to 60ºC in a water bath. Samples (digested with restriction enzymes) were loaded. The electrophoresis was performed at 100 V (5 V/cm) for 2-3 h. The gel was then photographed with a ruler under UV light.

10 × gel loading buffer: 1 mM EDTA pH 8.0, 0.25% (w/v) bromophenol blue, 0.25% (w/v) xylene cyanol, and 50% (v/v) glycerol

2.2.8.2 Transfer of DNA from gel to membrane

The gel was depurinated in 0.25 M HCl for 20 min and denatured in 0.4 N NaOH for 20 min until the gel pH down to < 9.0. Then DNA was transferred to membrane (Hybond-N+, Amersham) with 0.4 N NaOH using a capillary blotting method. After overnight (O/N) transfer, the membrane was rinsed with 2 × SSC. UV light cross linking (UV-crosslinker using Auto-Crosslink program, Stratagene) was then performed for the air-dried membrane to immobilize the DNA.

20 × SSC: 175.3 g NaCl, 27.6 g NaH_2PO_4, and 7.4 g EDTA dissolved in 800 ml water and pH adjusted to 7.4 with NaOH

2.2.8.3 Radioactive labeling of DNA probes

Radioactive labeling of DNA probes was performed with a *redi*prime™ II Kit according to instructions of manufactures. The purification of the radioactive labeled probe is describe in 2.2.7.1.3

2.2.8.4 Hybridization and analysis

The membrane was placed DNA-side up in a hybridization tube and was pre-hybridized in 20 ml of Church buffer at 68ºC with rotation for 2-3 h in a hybridization oven

(Amersham). The probe (purified and labeled) was denatured at 95ºC for 5 min and snap cooled on ice. The hybridization was carried out by addition of appropriate amount of radioactively labeled probe for 12-18 h at 68ºC. The membrane was washed two times for 20 min each at 68ºC in 2 × SSC and 0.5 × SSC containing 0.1% SDS. Finally, the membrane was air dried and exposed to Hyperfilm MP Films (Amersham) at -80ºC for several hours to days. Quantifications were performed with a Fuji film FLA-3000 fluorescent image analyzer.

Church buffer: 1M $NaPO_4$ pH 7.2, 7% SDS, and 1 mM EDTA

2.2.8.5 Stripping DNA probes

To allow reuse of the Southern blots, radioactively labeled DNA probe was stripped by incubating the membranes in a strip buffer (0.1 × SSC, 1% SDS) at 95ºC for 20 min. The process can be repeated in case a strong radioactivity remained. The membranes were them used for reprobing from the prehybridization as usual.

2.2.9 Isolation of genomic DNA from cells

Cells were grown to confluency in the 0.2% gelatin-coated 96-well plates, washed with PBS, and lysated in 50 µl genomic DNA lysis buffer per well. The lysates were incubated at 55ºC with shaking for at least 3 h or overnight. After a brief centrifuge, 100 µl of ice-cold ethanol were added and mixed on a shaker at RT until DNA was visible. Then the DNA was pelleted by centrifugation at 2,000 rpm for 30 min. After wash with 70% ethanol twice, air-dry the DNA. Finally, the DNA was dissolved in H_2O or restriction digestion mixtures.

Lysis buffer: 10 mM Tris Ph 7.5, 10 mM EDTA, 10 mM NaCL, 0.5% sarcosyl (N-lauroylsarcosine; Sigma), and 1 mg/ml proteinase K (add immediately before use)

2.2.10 Preparation DNA for pronucleus injection

1% agarose gel containing ethidium bromide was prepared. Samples (digested with restriction enzymes) were loaded. The electrophoresis was performed at 100 V (5 V/cm) for 2-3 h. The band of interest was cut out and placed into dialysis tubing (flat width 25 mm), which was sealed at one end with a clamp. 350 µl TE was filled into the tubing, the air bubbles were removed, and another end was also sealed. This array was placed into an eletrophoresis chamber filled with TAE in such a manner that the DNA could electrophoretically move from the gel slice into TE inside the tubing. The TE containing the eluted DNA was pipetted out and extracted subsequently with phenol-chloroform. The DNA was then dissolved in injection buffer to a final concentration 2 ng/µl. 10-20 µl DNA was checked on a gel to verify the concentration and purity. The remaining DNA was passed through a 0.22 µM steril filter and aliquoted directly into sterile Eppendorf tubes.

Injection buffer: 10 mM Tris pH 7.5-8.0 and 0.1 mM EDTA

2.2.11 Cell culture

2.2.11.1 Mammalian cells other than ES cells

All cells were maintained at 37ºC in an incubator (Forma Scientific, labortect GmbH) with 5% CO_2 and 95% humidity. Cells were grown on appropriate sized petri dishes and plates (Greiner Labortechnik).

2.2.11.1.1 Primary Pro-B cell

Purified murine pro-B cells were grown on a semi-confluent layer of γ-irradiated (3,000 rad) ST2 cells in IMDM supplemented with 10% fetal calf serum, 2 mM glutamine, 50 µM β-mercaptoethanol, 100 U/ml penicillin, and 100 µg/ml streptomycin. IL-7, IL-3, Flt-3, SCF, M-CSF, and GM-CSF (10 ng/ml each PeproTech EC Ltd.) was added to culture according to different purposes of the experiment.

2.2.11.1.2 B-cell lines

All cells were grown in RPMI 1640 supplemented with 7.5% fetal calf serum, 2 mM glutamine, 10 mM HEPES, 2 mM pyruvate, 50 μM β-mercaptoethanol, and 50 μg/ml gentamycin. The Ba/F3 cells were grown in RPMI 1640 as above supplemented with 10% of IL-3 containing WEHI 231-conditioned media.

2.2.11.2 ES cells

2.2.11.2.1 Preparation of feeder cells for ES-cell culture

E14.5 pregnant mouse (*CD44*$^{+/-}$) was sacrificed and its abdomen was swabbed by 70% ethanol. After opening up abdomen, uterus was removed and placed in a Petri dish with PBS. Then the embryos were removed from uterus an extra-embryonic membranes as well as intestine, liver, heart, lung, and head were cut out. The carcasses were washed in PBS again and transferred to a new dish with 0.25% trypsin solution. After mincing with scalpel blades, the mushy tissues were incubated in a total volume of 15 ml trypsin solution at 37ºC for 30 min. To obtain single feeder cells, a cell strainer was used to filter the minced tissues. The cells were then resuspended in the medium and plated onto 15 cm dishes (about one embryo per dish). The feeder cells can be split for propagation or frozen down at this stage. Mitotically inactivated cells prepared by gamma ray irradiation severed as feeder cells for ES cell culture.

2.2.11.2.2 ES cell culture

ES cells were cultured on the top of confluent feeder cell layer on 0.2% gelatin (G-9391, Sigma) coated dishes (Corning® 100mm TC-Treated Culture Dish, Item #430167). The incubator used for ES cell culture was with the conditions of 5% CO_2 and 90% humidity. Thorough typsinization (to generate single cell suspension) and a daily medium feeding interval were performed to avoid the differentiation of ES cells. A centrifugation speed of 1,000 rpm was used for spin down of ES cells. The freezing medium for ES cells was 80% FCS and 20% DMSO. Other conditions for ES cell culture and storage were basically the same as those for normal mammalian cells shown above.

2.2.11.2.3 Electroporation of ES cells

ES cells were split one day before transfection to allow cells in a logarithmic growth phase. Cells (about 1×10^7) were trypsinized, replated for 15 min, washed with cold E-buffer twice, and resuspended in 0.8 ml E-buffer. After transferring to a pre-cold cuvette (4 mm, peQLab), cells were mixed with 25 μg of linearized targeting vector. Electroporation was performed with a pulse of 400 V and a capacity of 250 μF in a Bio-Rad gene pulser (Bio-Rad). Typically, a time constant was between 3.5-6 ms. The cuvette was allowed to stand on ice for 10 min before seeding cells on the 10 cm dishes. The selection was started by addition of G418 (250 μg/ml, Gibco BRL11811-023) 24 h after electroporation and ganciclovir (2 μM, Sigma G2536) 48 h after electroporation, and maintained for 7-10 days. The resistant ES colonies were then picked under microscope and cultured for freezing and DNA preparation.

E-Buffer: PBS with 5mM HEPES, pH7.05

3 RESULTS

3.1 The role of p100 and RelB in B lymphopoiesis

One of Rel/NF-κB family members, RelB, has been shown to play an important role in mature B-cell activation and MZ B-cell development. However, whether RelB functions in the development of mainstream B cells has not been well defined. NF-κB2/p100 functions as a specific inhibitor of RelB in alternative NF-κB activation pathway. Therefore, mice lacking the potent RelB inhibitor p100 are good model systems (see **Figure 1.3**) for intensively studying the function of p100 and RelB with respect to B-cell development.

3.1.1 Defective B lymphopoiesis in *p100*$^{-/-}$ mice

3.1.1.1 Lack of the inhibitory p100 precursor results in reduced number of B cells in the periphery

The effect of p100 on B-cell development was first studied in spleen, which contains a high proportion of B lymphocytes. Flow cytometric analysis was performed using antibodies that recognize different lineage-specific cell surface markers. The B lymphocytes were identified by the presence of pan-B cell marker B220 (CD45R).

Spleens of 3-week-old *p100*$^{-/-}$ mice were anemic and approximately 2–3-fold smaller than that in wild-type mice. Out of five independent experiments on 3-week-old mice, an approximately 2-fold reduction of the B220^{+} cell population and, correspondingly, a 2-fold increase of Thy-1.2^{+} T cells in spleen were observed by flow cytometry (**Figure 3.1 A**). However, the absolute number of Thy-1.2^{+} T cells remained unchanged due to the reduced number of whole lymphocytes in spleen.

Furthermore, splenic B cells were examined by the surface expression of immunoglobulin molecules. In mutant mice, the reduction of B cells took place mainly in the $B220^{+}IgM^{+}$ B-cell pool with a mean frequency of 21.7 ± 1.4% compared to 39.1 ± 4.7% in wild-type mice. The $B220^{+}IgM^{-}$ B cells showed only a mild reduction from 11.6 ± 0.5% in wild-type mice to 9.9 ± 1.7% (**Figure 3.1 B**). Similar results were observed in lymph nodes (LN) and peripheral blood (PBL) (data not shown). Thus, the lack of p100 in mice results in a diminished number of B lymphocytes in the periphery.

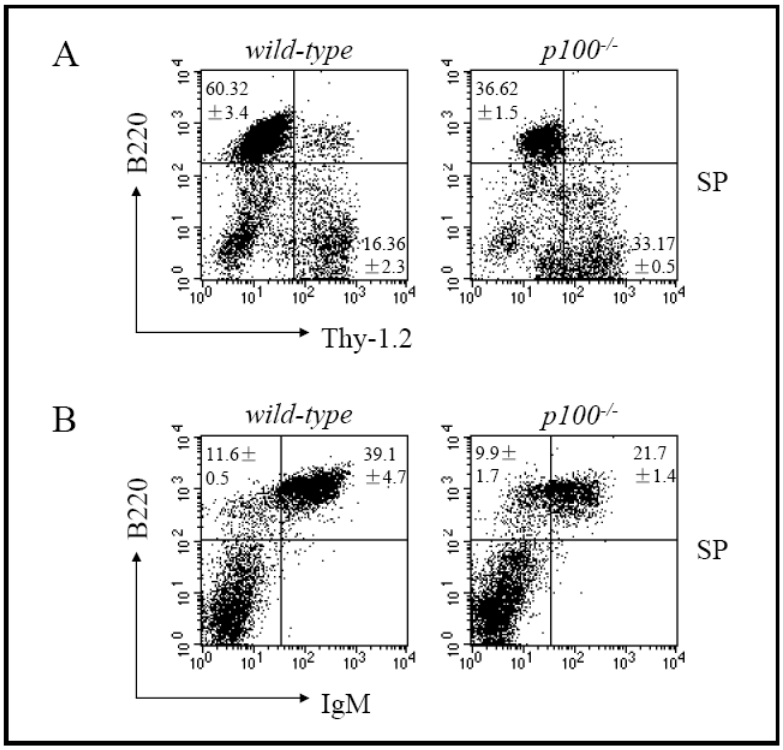

Figure 3.1: Reduction of B lymphocytes in the periphery due to p100-deficiency in mice. (A) Splenocytes were isolated from 3-week-old wild-type (left panels) and mutant mice (right panels) and were analyzed for the expression of B220 and Thy-1.2 by flow cytometry. **(B)** B-cell profiles in spleen (SP) were examined by flow cytometry after staining with anti-B220 and anti-IgM monoclonal antibodies (mAbs). Percentages of relevant populations are indicated. Numbers indicate mean values (%) ± SD from five mice.

3.1.1.2 Lack of p100 results in B-cell developmental arrest at an early stage

Despite the moderate reduction of B lymphocytes in the periphery in 3-week-old *p100*$^{-/-}$ mice, a noted decrease of B lymphocytes in bone marrow was detected by flow cytometry. The percentage of B220^{+} cells was reduced almost 5-fold compared to control littermates (*p100*$^{-/-}$, 10.99 ± 2.0% vs. wild-type, 50.94 ± 2.1%). The reduction of bone marrow B cells was observed in both B220^{+}IgM^{-} and B220^{+}IgM^{+} B-cell populations (**Figure 3.2 A**). B220^{+}IgM^{-} cells in bone marrow are composed of B-lineage precursors. B220^{+} precursors start expressing IgM when they differentiate into the immature B-cell stage (see **Figure 1.5**).

The early phase of B-cell development can be divided into different stages according to the expression of specific cell surface markers (see **Figure 1.5**). The transition from the pre-pro-B stage (Fr. A) to the early pro-B stage (Fr. B) is characterized by the expression of CD19 [52, 53]. Thus, CD19 expression on B lymphocytes in *p100*$^{-/-}$ mice was examined to determine the developmental stage at which the B-cell differentiation was blocked.

As shown by flow cytometric analysis after staining with anti-B220 and anti-CD19 mAbs, the B220^{+}CD19^{+} double-positive cells (Fr. B) were dramatically (~8-fold) reduced in 3-week-old mutant mice with a mean frequency of 6.15 ± 2.1% compared to 46.5 ± 3.1% in wild-type mice. The percentage of the B220^{+}CD19^{-} population (Fr. A), however, was comparable between mutant and wild-type mice (**Figure 3.2 B**). Moreover, the B220^{+}CD19^{-} cells from either mutant or wild-type mice were IL-7R^{+}CD43^{+}c-Kit^{low} (data not shown), characterizing B-cell progenitors at the Fr. A stage.

Thus, the lack of p100 in mice causes a nearly complete developmental block in B lymphopoiesis at the transition stage from pre-pro-B (Fr. A) to early pro-B (Fr. B), which is indicated by the massive reduction of B220^{+}CD19^{+} cells in bone marrow (**Figure 3.2 C**). Therefore, NF-κB2/p100 is indeed involved in the development of mainstream B cells.

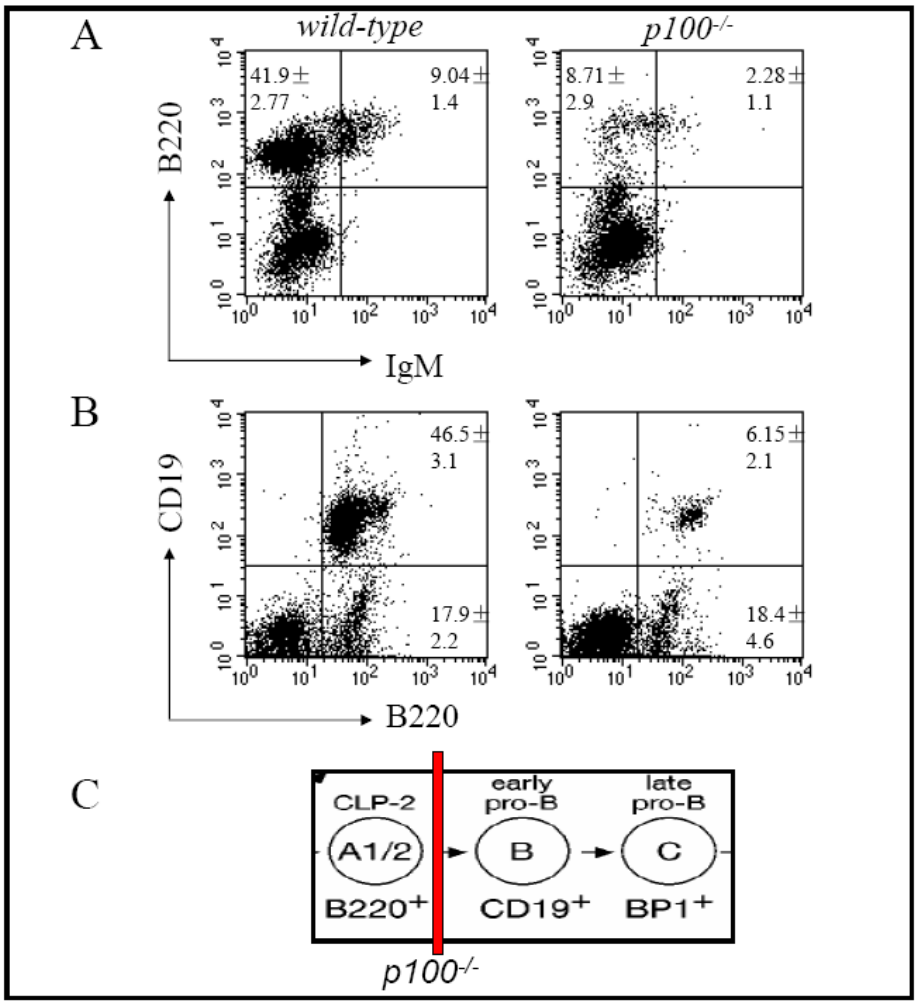

Figure 3.2: B-cell development is arrest at an early stage in mice lacking p100. (A) Flow cytometric analysis of bone marrow (BM) cells from 3-week-old wild-type and *p100*$^{-/-}$ mice. Single cell suspensions were prepared and analyzed for the expression of the indicated cell surface markers B220 and IgM. **(B)** B220 and CD19 expression were analyzed. Lymphocytes were gated for the analysis. Percentages of relevant populations are indicated. **(C)** Schematic representation of the developmental stage at which the B-cell differentiation was arrested in *p100*$^{-/-}$ mice. Vertical bar (in red-color) indicates the development block.

3.1.1.3 B-cell developmental defect in *p100*$^{-/-}$ mice is cell-intrinsic

To examine whether the B-cell developmental arrest is a hematopoietic defect or a defect in the stromal compartment that supports B-cell differentiation, bone marrow reconstitution experiments were performed. After lethal irradiation, wild-type recipients were reconstituted with wild-type (wt→wt) or *p100*$^{-/-}$ bone marrow cells (*p100*$^{-/-}$→wt) to generate bone marrow chimeras. Mice were checked for their chimeric status by PCR genotyping from peripheral blood leukocytes or tail clips for further experiments. Chimeras were analyzed six weeks after the bone marrow transplantation.

In bone marrow, the percentage of B220^{+}CD19^{+} double-positive cells was reduced dramatically in *p100*$^{-/-}$→wt chimeras, 4.65 ± 1.1% vs. 40.35 ± 3.2% in wt→wt chimeras. The percentage of B220^{+}CD19^{-} cells in *p100*$^{-/-}$→wt chimeras was comparable to that in wt→wt chimeras, though (**Figure 3.3 A**). This profile was exactly same as what had been observed in *p100*$^{-/-}$ mice (see **Figure 3.2**) with respect to B-cell development in bone marrow. The reduction of B cells in the periphery, for example in spleen, was also detected in *p100*$^{-/-}$→wt chimeras (**Figure 3.3 B**), which was similar to that in *p100*$^{-/-}$ mice as well.

Thus, the irradiation-resistant stromal microenvironments in wild-type recipients could not support the proper B-cell development when transplanted with bone marrow cells from *p100*$^{-/-}$ mice. These observations suggest that the B-cell development abnormality in mice lacking p100 arises from the hematopoietic compartment rather than the non-hematopoietic (stromal) compartment.

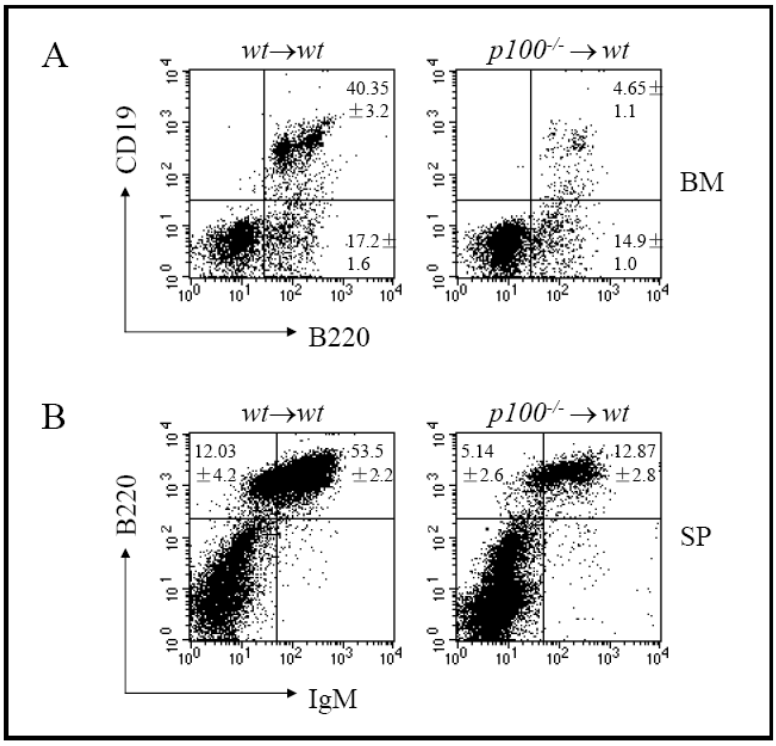

Figure 3.3: Analysis of B-cell development in bone marrow chimeras. Lymphocytes from **(A)** BM and **(B)** SP were isolated from lethally irradiated mice that were transplanted with bone marrow cells as indicated. **(A)** B220 and CD19 expression in BM. **(B)** B220 and IgM expression in SP was analyzed by flow cytometry.

The requirement of p100 in hematopoietic cells for proper B-cell development was clearly demonstrated from the above observations. It is not clear, however, whether p100 is required within B-cell precursors or in accessory cells for their development. To address this point, mixed bone marrow reconstitution experiments were performed using C57BL/6 congenic mice. These mice differ only in the *CD45* locus which was used to distinguish the reconstitution of hematopoietic system from either wild-type ($CD45.1^+$) or *p100*$^{-/-}$ ($CD45.2^+$) bone marrow cells.

Bone marrow cells from $CD45.1^+$ wild-type and $CD45.2^+$ *p100*$^{-/-}$ mice were mixed at equal proportions and injected into the lethally irradiated $CD45.1^+$ wild-type recipients ($CD45.1^+$ wt & $CD45.2^+$ *p100*$^{-/-}$→$CD45.1^+$ wt). All the animals were checked for their chimeric status by PCR analysis as mentioned before. Six weeks after bone marrow transplantation, reconstitution of B, T, and myeloid lineages was analyzed by flow

cytometry. Single cell suspensions were labeled with CD45.1 or CD45.2 in combination with lineage markers B220 and CD19 (B cells), CD4 and CD8 (T cells), or Gr-1 (granulocytes). Results on B lymphocytes are addressed here only.

A normal profile of B220 and CD19 expression (**Figure 3.4 A**, left panel) was found in bone marrow of mixed chimeric mice ($CD45.1^+$ wt & $CD45.2^+$ *p100*$^{-/-}$→$CD45.1^+$ wt). Flow cytometric analysis revealed that about 60% of lymphocytes in mixed chimeric mice were derived from $CD45.1^+$ wild-type bone marrow, whereas $CD45.2^+$ *p100*$^{-/-}$ bone marrow contributed to 40%. Interestingly, bone marrow cells from $CD45.2^+$ *p100*$^{-/-}$ mice were not able to generate $B220^+CD19^+$ cells efficiently (11.6 ± 1.3%), in spite of the co-existence of $CD45.1^+$ wild-type bone marrow cells (**Figure 3.4 A,** low-right panel). The majority of $B220^+CD19^+$ cells (47.0 ± 6.2%) in the mixed chimeric mice were generated by $CD45.1^+$ wild-type bone marrow cells (**Figure 3.4 A,** up-right panel).

On the other hand, $B220^+CD19^-$ precursors generated by $CD45.2^+$ *p100*$^{-/-}$ bone marrow were actually 2-fold increased (22.2 ± 0.3%) compared to those from $CD45.1^+$ wild-type bone marrow (11.5 ± 1.4%). Nevertheless, the increased number of $B220^+CD19^-$ precursors from $CD45.2^+$ *p100*$^{-/-}$ bone marrow did not differentiate properly and generated less $B220^+CD19^+$ cells (11.6 ± 1.3%) than those from $CD45.1^+$ wild-type bone marrow did (47.0 ± 6.2%). The differences among individual subpopulations generated by either $CD45.1^+$ wild-type or $CD45.2^+$ *p100*$^{-/-}$ bone marrow cells became even more evident when these populations ($B220^+CD19^-$, $B220^+CD19^+$, and $B220^-CD19^-$) were plotted on a bar chart (**Figure 3.4 B**).

Thus, *p100*$^{-/-}$ bone marrow cells could not undergo normal B-cell development even with the support of wild-type bone marrow cells. p100 is required within B cells rather than in any other cell types for proper mainstream B-cell maturation. Taken together, these data indicate that the B-cell developmental abnormality in mice lacking p100 is a hematopoietic defect and is intrinsic to B cells.

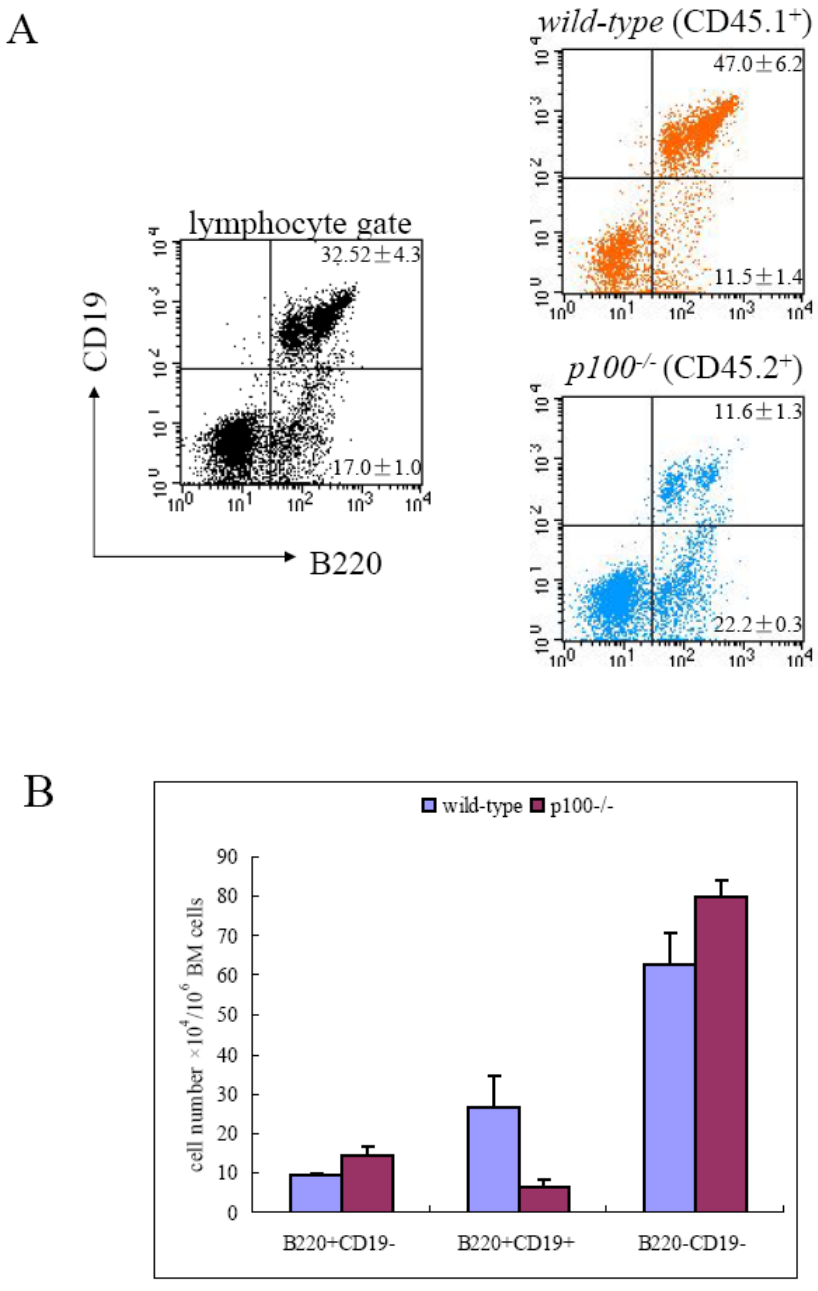

Figure 3.4: Analysis of B-cell development in mixed bone marrow chimeric mice. (A) Bone marrow cells were isolated from lethally irradiated mice that were reconstituted with mixed bone marrow at a 1:1 ratio. Flow cytometric analysis was performed after staining with anti-CD45.1 or anti-CD45.2 together with anti-B220 and anti-CD19 antibodies. Lymphocytes were gated. **(B)** Statistics chart for the absolute numbers of $B220^{+}CD19^{-}$, $B220^{+}CD19^{+}$, and $B220^{-}CD19^{-}$ cells generated from either $CD45.1^{+}$ wild-type or $CD45.2^{+}$ *p100*$^{-/-}$ bone marrow cells.

3.1.2 B-cell developmental defect in *p100*$^{-/-}$ mice is due to enhanced RelB DNA-binding activity

The C-terminal portion of p100 precursor specifically inhibits nuclear translocation of RelB complexes in the alternative NF-κB activation pathway (**Figure 3.5,** left panel**,** see **1.1.4**) [17]. In *p100*$^{-/-}$ mice (targeted disruption only on the C-terminal portion of the *nfκb2* gene, see **Figure 1.3**), p52 molecule can still be synthesized but p100 precursor cannot. A constitutive increase of κB DNA-binding activity (**Figure 3.5,** right panel), mainly comprising p52/RelB complexes, was observed in nuclear extracts from various lymphoid and non-lymphoid tissues of *p100*$^{-/-}$ mice, according to published data [36] and the current work (see **Figure 3.8**, lane 4).

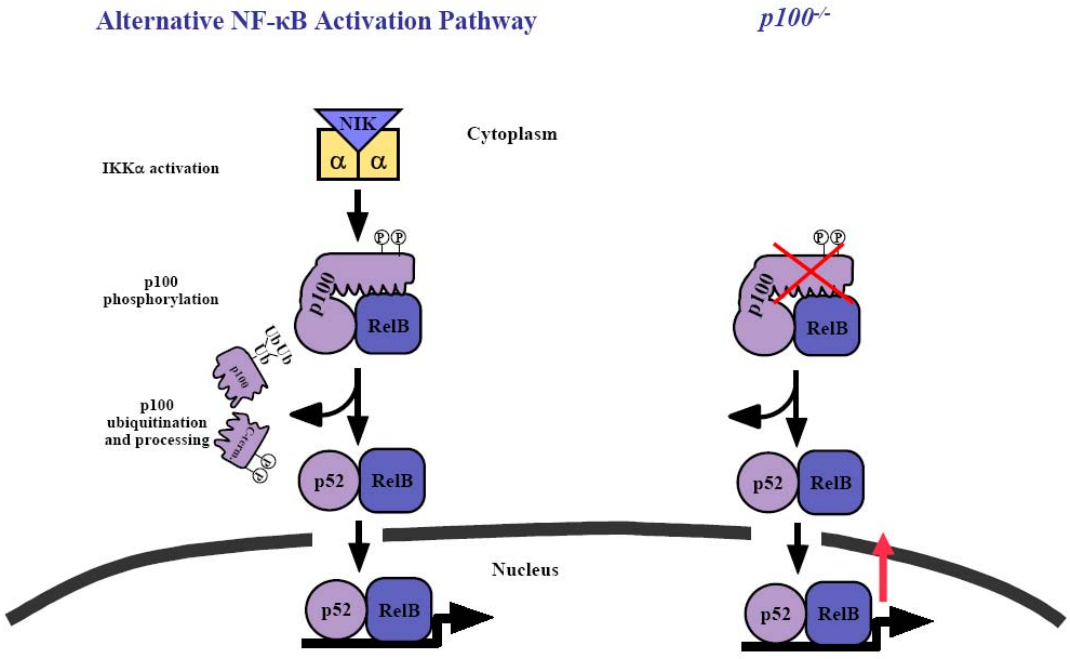

Figure 3.5: Schematic representation of increase κB DNA-binding activity in mice lacking p100. Activation of alternative NF-κB pathway leading to the nuclear translocation of p52/RelB heterodimers is shown in the left panel. The targeted disruption of C-terminal of p100 resulting in the constitutively activation of p52/RelB heterodimers is shown in the right panel. Cross in red indicates the deletion of C-terminal portion of p100.

3.1.2.1 B-cell developmental defect in *p100*$^{-/-}$ mice is rescued by deleting one allele of the *relB* gene

RelB heterodimers bind constitutively to κB motifs in lymphoid tissues of *p100*$^{-/-}$ mice. One possibility is that the defective B-cell development in these animals is due to increased RelB function. To address this point, *relB*$^{-/-}$ mice were bred with *p100*$^{-/-}$ mice (**Figure 3.6 A**). *p100*$^{-/-}$*relB*$^{-/+}$ as well as *p100*$^{-/-}$*relB*$^{-/-}$ mice were examined to investigate the effect of RelB activity on B-cell development.

Unlike *p100*$^{-/-}$ mice, *p100*$^{-/-}$*relB*$^{-/+}$ mice were healthy during the four-month of observation. B-cell development was investigated both in bone marrow and spleen. Flow cytometric analysis of bone marrow cells from 3-week-old *p100*$^{-/-}$*relB*$^{-/+}$ mice revealed an increase in B220^{+}CD19^{+} double-positive B cells with a mean frequency of 57.6 ± 3.2% (**Figure 3.6 B,** middle panel) compared to 4.65 ± 1.1% in *p100*$^{-/-}$ mice (**Figure 3.6 B,** left panel). The percentage of bone marrow B220^{+}CD19^{+} B cells in *p100*$^{-/-}$*relB*$^{-/+}$ mice reached that in wild-type controls, 65.2 ± 1.1% (**Figure 3.6 B,** right panel). The percentages of B220^{+}CD19^{-} cells were comparable among *p100*$^{-/-}$, *p100*$^{-/-}$*relB*$^{-/+}$, and wild-type mice. Similarly, normal profiles of B lymphocytes were observed in the periphery, such as in spleen, when B220 and IgM expressions were analyzed by flow cytometry (**Figure 3.6 C,** middle and right panels).

In conclusion, when one allele of the *relB* gene is inactivated in *p100*$^{-/-}$ mice (*p100*$^{-/-}$*relB*$^{-/+}$), the number of bone marrow B220^{+}CD19^{+} B lymphocytes is completely recovered to that in wild-type mice. The reduction of peripheral B lymphocytes in *p100*$^{-/-}$ mice is rescued in *p100*$^{-/-}$*relB*$^{-/+}$ mice as well. Thus, the developmental arrest of B lymphocytes (B220^{+}CD19^{-} (Fr. A) to B220^{+}CD19^{+} (Fr. B)) in bone marrow and the impaired B lymphopoiesis in periphery in *p100*$^{-/-}$ mice are rescued upon deletion of one *relB* allele. These observations support the assumption that the strength of RelB activity affects mainstream B-cell development.

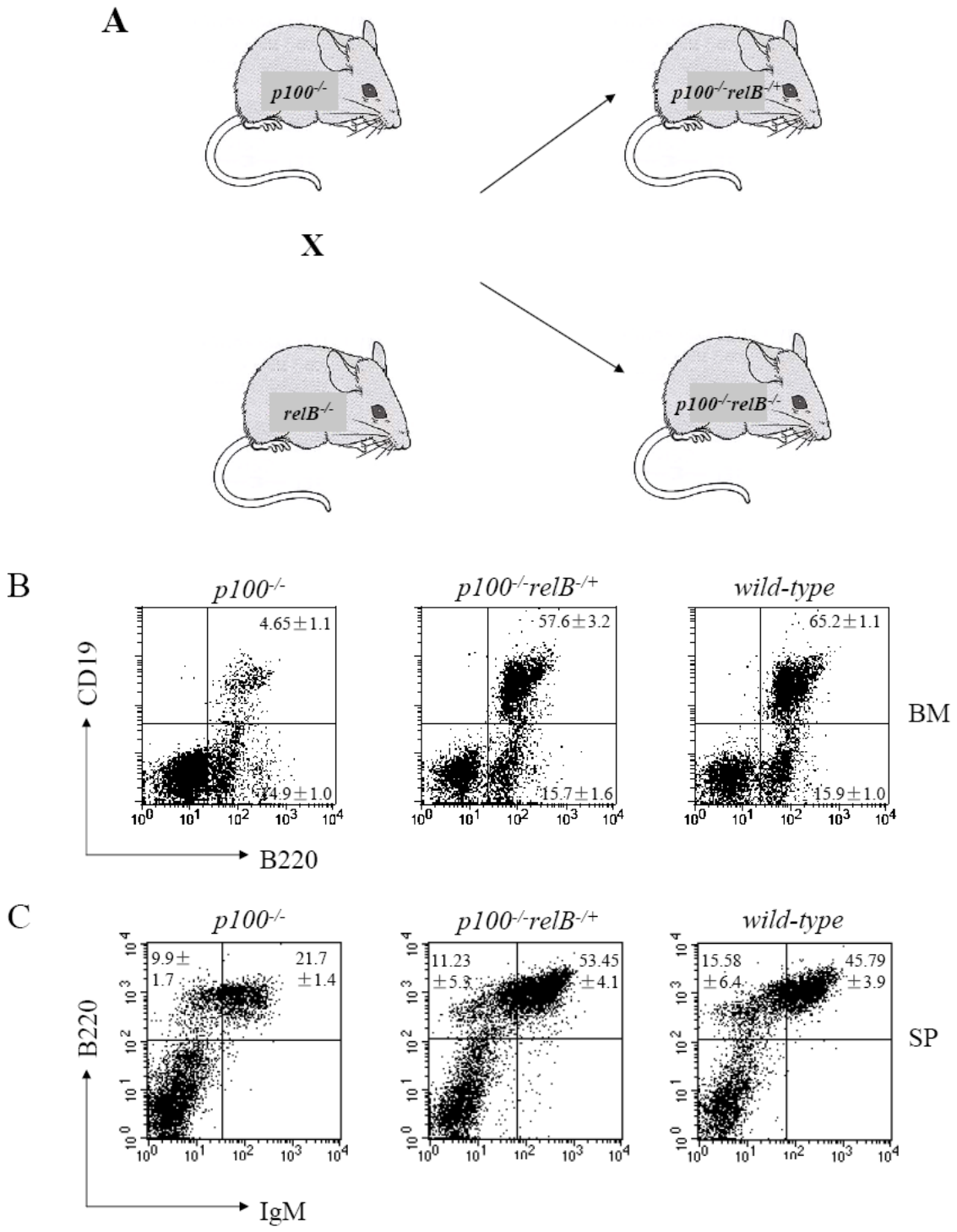

Figure 3.6: B-cell development is rescued in *p100*$^{-/-}$*relB*$^{-/+}$ mice. (A) Schematic representation of the breeding strategy for investigating the effects of RelB activity on B-cell development. B-cell development was examined in **(B)** BM and **(C)** SP by flow cytometric analysis from mutant and wild-type mice as indicated. Lymphocytes were gated. Numbers indicate mean values (%) ± SD from four mice.

3.1.2.2 B-cell developmental defect in *p100*$^{-/-}$ mice can not be rescued by complete deletion of the *relB* gene

When two alleles of the *relB* gene were completely deleted in *p100*$^{-/-}$ mice (*p100*$^{-/-}$*relB*$^{-/-}$), flow cytometric analysis revealed a slight reduction of bone marrow B220^{+}CD19^{+} cells in 3-week-old double mutant mice compared to that in wild-type mice (**Figure 3.7 A,** left and right panels). Moreover, only a total of 8% B220^{+} cells were detected in spleen. Both B220^{+}IgM^{-} and B220^{+}IgM^{+} B-cell populations were markedly reduced in *p100*$^{-/-}$*relB*$^{-/-}$ mice (**Figure 3.7 B**). These phenotypes in B lymphopoiesis either in bone marrow or in spleen were very similar to what had been reported in *relB*$^{-/-}$ mice (**Figure 3.7 A** and **B**, middle panels) due to the increased apoptosis and the abnormal mature B-cell proliferation [106].

Actually, *p100*$^{-/-}$*relB*$^{-/-}$ mice, at around 4-week of age, started manifesting other similar phenotypes to *relB*$^{-/-}$ mice; for example, splenomegaly, and lack of PP as well as LN. Thus, the complete inactivation of the *relB* gene could not rescue the phenotype of *p100*$^{-/-}$ mice; to the contrary, these mice develop the phenotype of *relB*$^{-/-}$ mice.

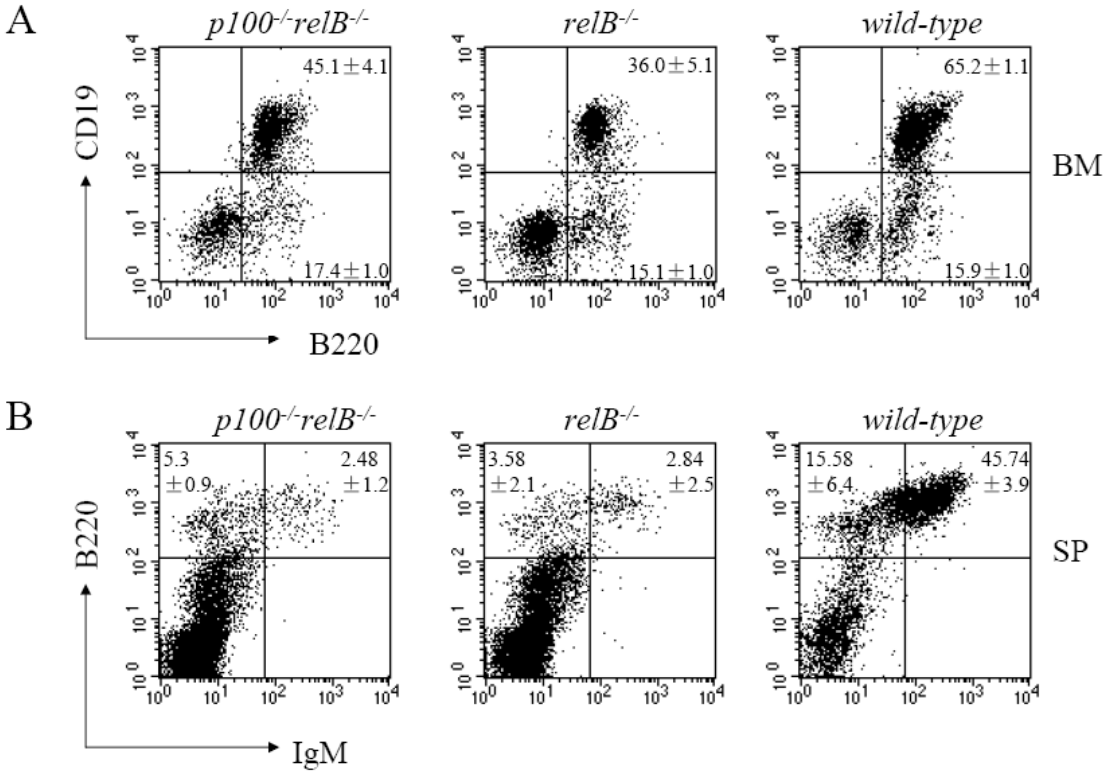

Figure 3.7: Failure to rescue B-cell developmental defect upon complete deletion of the *relB* gene in *p100*$^{-/-}$ mice. (A) BM and **(B)** SP cells were isolated from 3-week-old double mutant (left panels), *relB*$^{-/-}$ (middle panels), and wild-type mice (right panels) for flow cytometric analysis. **(A)** B220 and CD19 expression in BM, **(B)** B220 and IgM expression in SP were examined.

3.1.2.3 RelB activity affects B-cell development

B-cell development is arrested in a cell-intrinsic manner in *p100*$^{-/-}$ mice. Interestingly, normal B-cell development is found in *p100*$^{-/-}$*relB*$^{-/+}$ mice. In order to understand the molecular mechanisms in the above observations, the κB DNA-binding activity in nuclear extracts of mutant and wild-type mice was examined by the electrophoretic mobility shift assay (EMSA). Due to technical difficulties to perform EMSA successfully in sorted B220^{+}CD19^{-} B cells, this experiment was done with thymocyte nuclear extracts.

In wild-type mice, RelB DNA-binding activity was identified by anti-RelB antibody challenge, which was significantly enhanced in *p100*$^{-/-}$ mice (**Figure 3.8**; compare supershifted bands in lane 2 and 4). When one allele of the *relB* gene was deleted in *p100*$^{-/-}$ mice, the elevated RelB DNA-binding activity was restored to more or less same levels as that in wild-type control (compare supershifted bands in lane 2, 4, and 6). As expected, when two alleles of the *relB* gene were deleted, the RelB DNA activity could not be detected at all (lane 8).

In conclusion, *p100*$^{-/-}$ mice lacking RelB inhibitor exhibit constitutively increased RelB DNA-binding activity corresponding to B-cell developmental defect. *p100*$^{-/-}$*relB*$^{-/+}$ mice, lacking one allele of the *relB* gene in *p100*$^{-/-}$ mice, exhibit rescued RelB DNA-binding activity (wild-type levels), correlated with the rescue in the B-cell developmental defect. These observations strongly indicate that the strength of RelB activity plays a crucial role in B lymphopoiesis. High levels of RelB activity (*p100*$^{-/-}$) interfere with the B-cell development at the early stage; normal (medium) levels of RelB activity (*p100*$^{-/-}$*relB*$^{-/+}$) favor this process; absence of RelB activity (*p100*$^{-/-}$*relB*$^{-/-}$) affects mainly B-cell activation and survival rather than mainstream B-cell development.

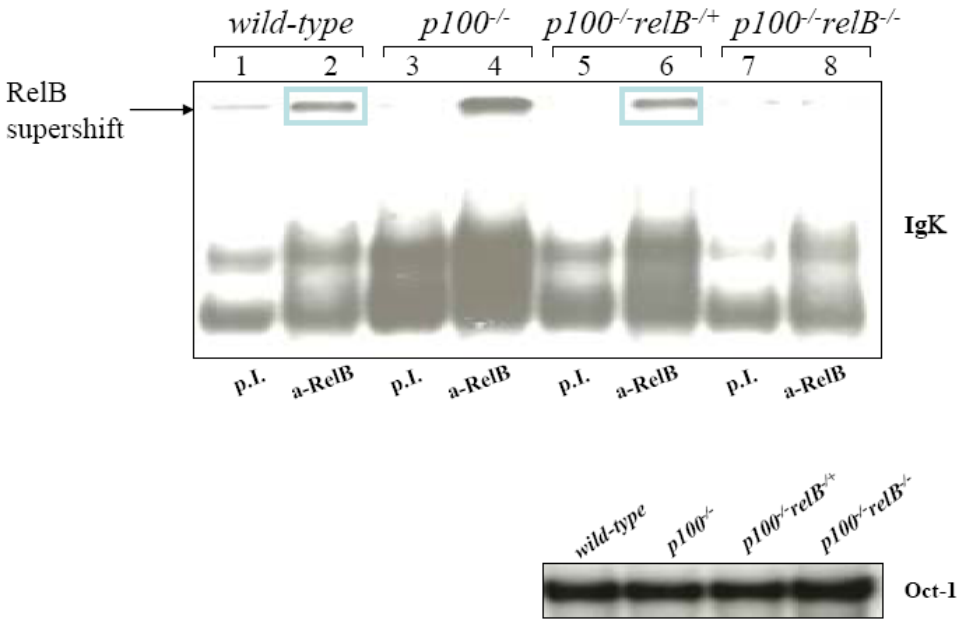

Figure 3.8: Electrophoretic mobility shift assay (EMSA). Thymocyte nuclear extracts from wild-type, *p100*$^{-/-}$, *p100*$^{-/-}$*relB*$^{-/+}$, and *p100*$^{-/-}$*relB*$^{-/-}$ mice were prepared and analyzed for κB DNA-binding activity by EMSA using Igκ probe. α-RelB: α-RelB mAb; p.i.: preimmune treatment. RelB supershift is indicated by arrow. Integrity of the extracts was analyzed by EMSA using Oct-1 probe. The blue-color rectangles indicate the supershifted RelB bands from either wild-type (left) or *p100*$^{-/-}$*relB*$^{-/+}$ (right) mice.

3.1.2.4 B-cell developmental defect in *p100*$^{-/-}$ mice can not be rescued by deletion of the *nfκb1* gene

Nuclear extracts of various lymphoid and non-lymphoid tissues from *p100*$^{-/-}$ mice exhibits a significant increase of κB DNA-binding activity mainly consisting p52/RelB heterodimers. To rule out the opportunity that the increased p50 complexes DNA-binding activity is another reason for the impaired B-cell development, the *nfκb1* gene was deleted in *p100*$^{-/-}$ mice and the B-cell development was analyzed by flow cytometry.

Neither *p100*$^{-/-}$*nfκb1*$^{-/-}$ nor *p100*$^{-/-}$*nfκb1*$^{-/+}$ mice could be distinguished from age-matched *p100*$^{-/-}$ mice: they were severely runted since 14–16-day old, approximately half to one third smaller than wild-type controls, and did not survive longer than 21 days after birth.

It is known that NF-κB1/p50 is not involved in the mainstream B-cell development [21].

Flow cytometric analysis showed that the percentages of both $B220^+CD19^+$ and $B220^+CD19^-$ cell populations were comparable between *nfκb1*$^{-/-}$ and wild-type mice (**Figure 3.9,** upper panels). However, $B220^+CD19^+$ cells were dramatically reduced in both *p100*$^{-/-}$*nfκb1*$^{-/+}$ and *p100*$^{-/-}$*nfκb1*$^{-/-}$ mice (**Figure 3.9,** lower panels), similar to that in *p100*$^{-/-}$ mice. Moreover, $B220^+CD19^-$ cells were reduced to some extent in these mice, compared to *p100*$^{-/-}$, *nfκb1*$^{-/-}$, and wild-type animals.

These data show that deleting either one allele or two alleles of the *nfκb1* gene in *p100*$^{-/-}$ mice could not rescue the B-cell developmental defects in *p100*$^{-/-}$ mice as indicated by the massive loss of $B220^+CD19^+$ cells in bone marrow. Thus, DNA-binding activity of p50 complexes does not contribute to the impaired B-cell development in *p100*$^{-/-}$ mice. In addition, due to the mild but discernable reduction of $B220^+CD19^-$ cells in *p100*$^{-/-}$*nfκb1*$^{-/+}$ and *p100*$^{-/-}$*nfκb1*$^{-/-}$ mice, the B-cell developmental defect in these animals could be even more severe and complex than that in *p100*$^{-/-}$ mice.

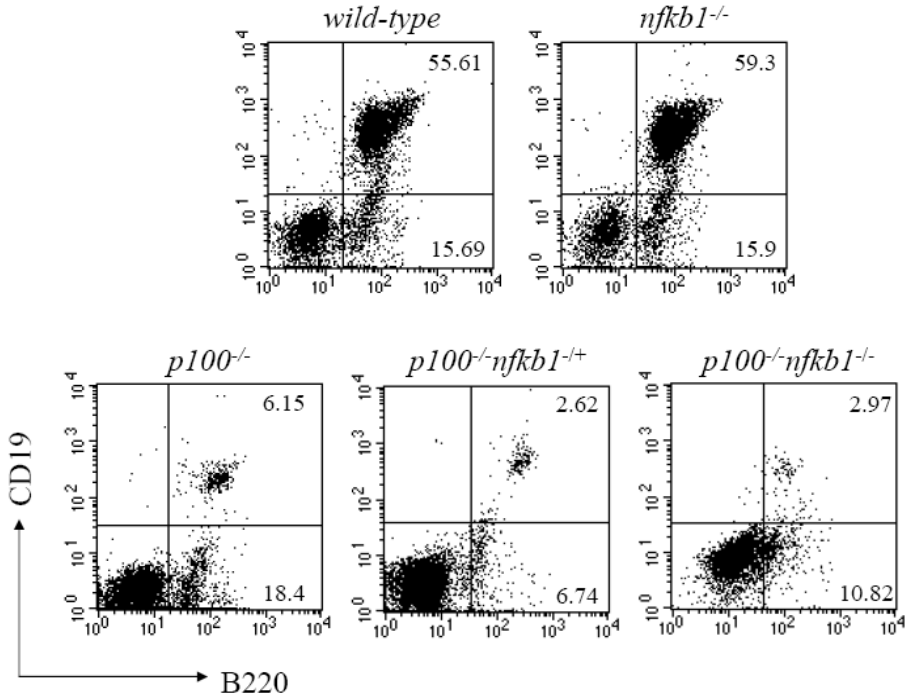

Figure 3.9: p50 does not contribute to B-cell developmental defect in *p100*$^{-/-}$ mice. Bone marrow cells were isolated from wild-type, *nfκb1*$^{-/-}$, *p100*$^{-/-}$, *p100*$^{-/-}$*nfκb1*$^{-/+}$, and *p100*$^{-/-}$*nfκb1*$^{-/-}$ mice. Lymphocytes were gated for flow cytometric analysis after staining with anti-B220 and anti-CD19 antibodies.

3.1.3 The expression of certain B-lineage commitment genes is affected by enhanced RelB DNA-binding activity in *p100*$^{-/-}$ mice

The transcription factor Pax5 is crucial in maintaining B-lymphocyte commitment. In *Pax5*$^{-/-}$ bone marrow, B220^{+}CD43^{+}CD19^{+} cells are absent [123]. In *p100*$^{-/-}$ mice, B lymphopoiesis is arrested at a similar stage (from Fr. A to Fr. B) as in *Pax5*$^{-/-}$ mice (**Figure 3.10 A**). Thus, one possibility is that p100 regulates the expression of Pax5.

To address this point, *Pax5* mRNA expression was analyzed using real-time PCR in the sorted B220^{+}CD19^{-} cell population from control and mutant mice. Cells were sorted using MACS depletion combined with positive selection methods and 95% purity was achieved in these experiments. Interestingly, almost no *Pax5* expression was detected in the mutant mice in contrast to wild-type controls (**Figure 3.10 B**).

Another two transcription factors E2A and EBF are also required for the proper development of early B progenitors and for the cooperative activation of the B-lymphoid gene expression program at the onset of B-cell development. In *E2A*$^{-/-}$ or *EBF*$^{-/-}$ bone marrow, B220^{+}CD43^{+}CD19^{-} cells are greatly reduced, suggesting that the developmental arrests in these mice take place at Fr. A1 to Fr. A2 stage (**Figure 3.10 A**). *E2A* and *EBF* mRNA expressions were also examined by real-time PCR. *E2A* expression was comparable to wild-type controls. *EBF* mRNA levels were 5-fold reduced in mutant mice (**Figure 3.10 B**). These results suggest that p100 regulates the expression of certain B-lineage transcription factors, such as Pax5 and EBF.

A downregulated expression pattern of B-lineage transcription factors Pax5 and EBF was found in *p100*$^{-/-}$ mice, explaining the phenotype in B-cell development. It is known from the study that, in *p100*$^{-/-}$ mice, B-cell development is arrested due to the constitutively increased RelB DNA-binding activity. When one allele of the *relB* gene is deleted in *p100*$^{-/-}$ mice, the elevated RelB DNA-binding activity recovers to wild-type levels, correlated with the rescued B-cell development. Interestingly, the expression levels of

Pax5 and *EBF* were also rescued to wild-type levels (data not shown) when one allele of the *relB* gene was deleted in $p100^{-/-}$ mice, indicating that the expression of *Pax5* and *EBF* was affected by the strength of RelB DNA-binding activity as well. Thus, the downregulation of *Pax5* and *EBF* in $p100^{-/-}$ mice is likely due to the enhanced RelB DNA-binding activity.

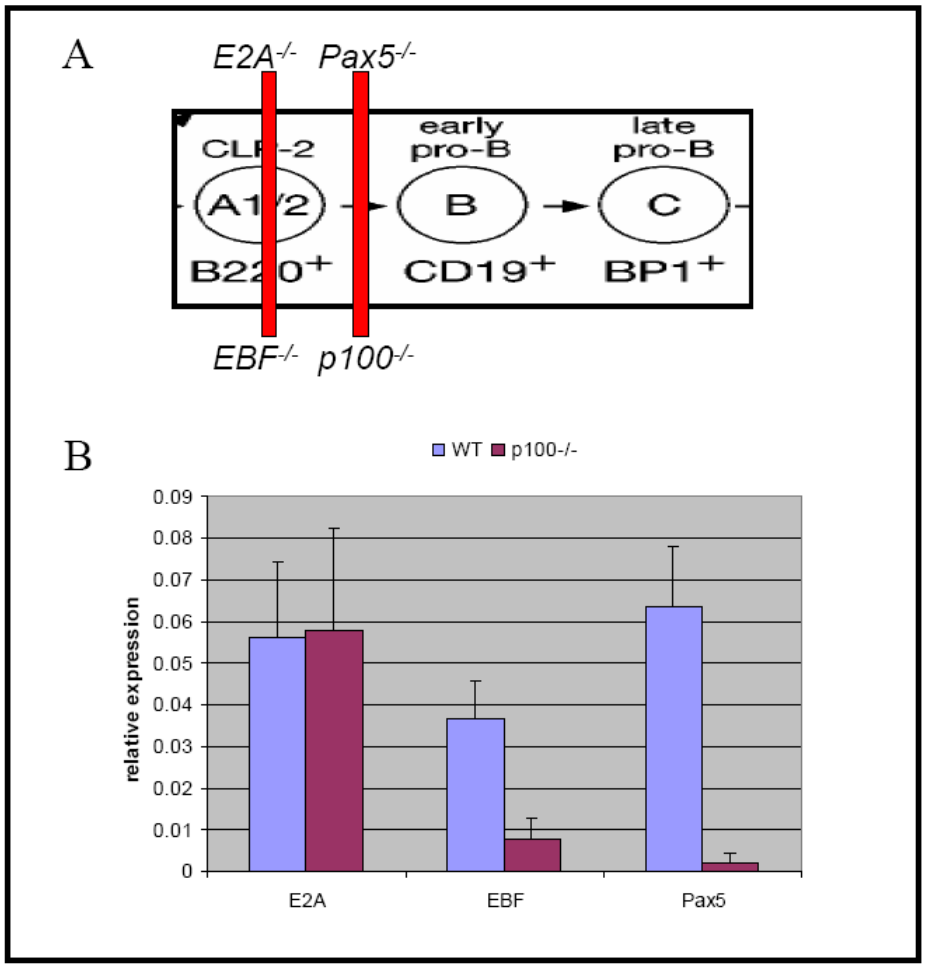

Figure 3.10: p100 regulation of the expression of B-lineage transcription factors. (A) Schematic figure of the developmental stages at which the B-lymphocyte differentiation was arrested in $E2A^{-/-}$, $EBF^{-/-}$, $Pax5^{-/-}$, and $p100^{-/-}$ mice. Vertical bars indicate the development blocks at different stages. **(B)** Real-time PCR of B-lineage transcription factors. $B220^{+}CD19^{-}$ cells were sorted from bone marrow of 3-week-old wild-type and $p100^{-/-}$ mice using MACS. Real-time PCR was performed to examine the expression of B-lineage transcription factors. Data represent two independent experiments.

B-cell associated genes such as *CD19*, *mb1* (*Igα*), and *BLNK* also showed the attenuated mRNA levels in sorted $B220^{+}CD19^{-}$ bone marrow cells from 3-week-old *p100*$^{-/-}$ mice. The expression of T- and myeloid-lineage specific genes, such as *Notch1*, *M-CSFR*, and *MPO* was comparable to wild-type controls (**Figure 3.11**), corresponding to the intact development of T cells and myeloid cells in *p100*$^{-/-}$ mice.

It is known that in B-cell development, Pax5 activates the B-cell associated genes. Moreover, Pax5 represses genes such as *M-CSFR* and *MPO* as well as *Notch1*, which are involved in the development of other lineages. This dual function of Pax5 leads to the consolidation of the B-lymphoid gene expression program. Thus, it is likely that the disturbed lineage-associated gene expression pattern observed in *p100*$^{-/-}$ mice is due to the marked reduction of *Pax5* expression [56].

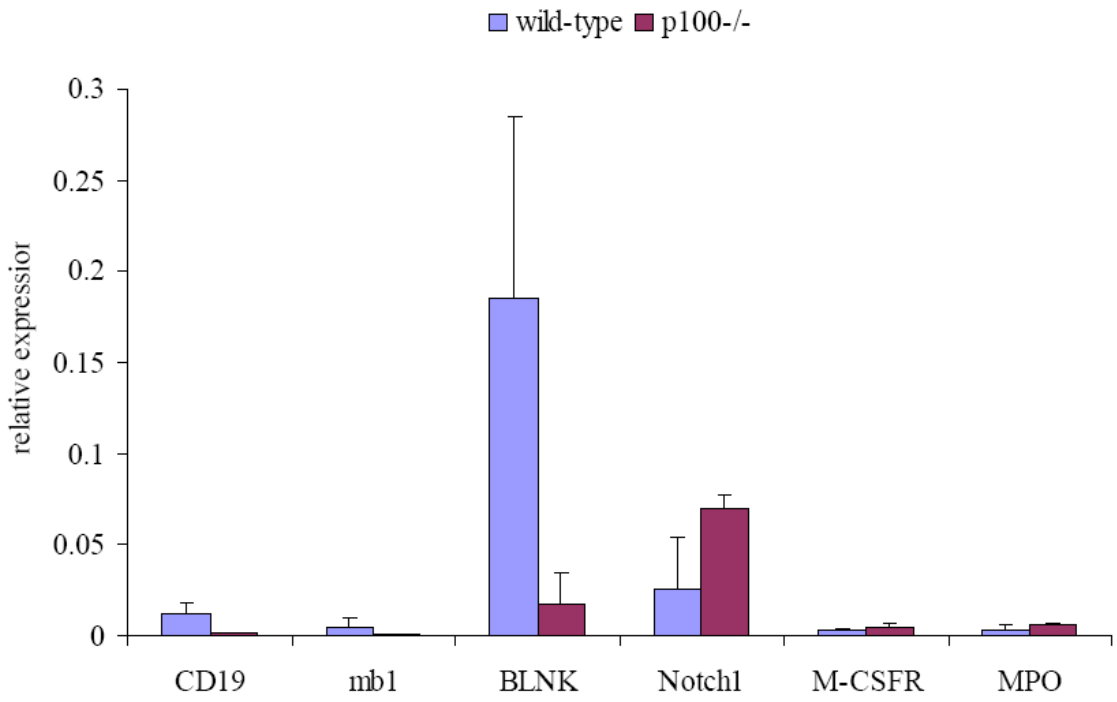

Figure 3.11: The expression of lineage-associated genes in mice lacking p100. $B220^{+}CD19^{-}$ cells were sorted from bone marrow of 3-week-old wild-type or *p100*$^{-/-}$ mice using MACS. Real-time PCR was performed to examine the mRNA expression of different lineage-associated genes. Data represent two independent experiments.

3.1.4 B-cell developmental defect in *p100*$^{-/-}$ mice is not due to increased number of myeloid cells

3.1.4.1 Myeloid hyperplasia in *p100*$^{-/-}$ mice

In addition to B-lymphocyte developmental abnormality in bone marrow which results in reduced number of B lymphocytes in the periphery of *p100*$^{-/-}$ mice, myeloid hyperplasia without clear evidence of infection was observed in bone marrow, spleen, peripheral blood, and other lymphoid organs of these mice (**Figure 3.12**). Mac-1 (CD11b) and Gr-1 were used as myeloid lineage markers for flow cytometric analysis.

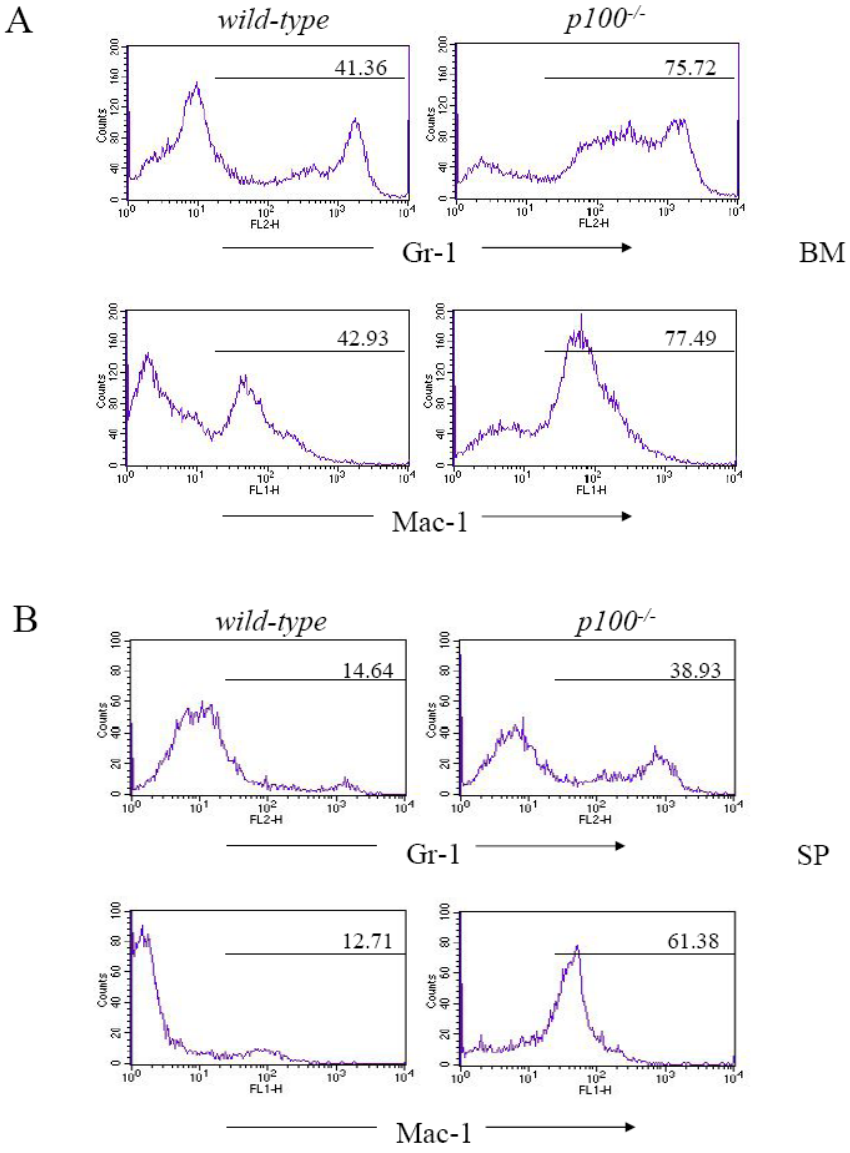

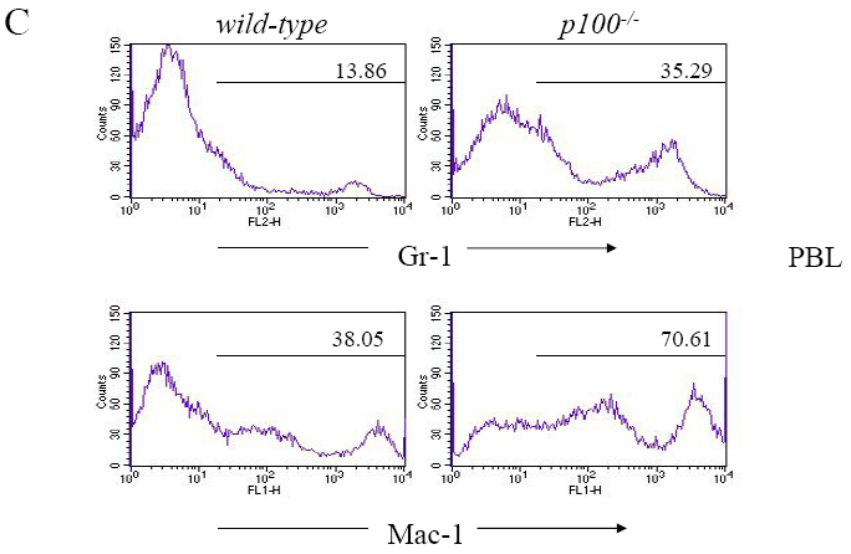

Figure 3.12: Increased number of myeloid cells in *p100*$^{-/-}$ mice. Single cell suspensions were prepared from **(A)** bone marrow (BM), **(B)** spleen (SP), and **(C)** peripheral blood (PBL)**.** Gr-1 and Mac-1 expressions were analyzed by flow cytometry in 3-week-old wild-type (left panels) and mutant mice (right panels).

3.1.4.2 Myeloid hyperplasia in *p100*$^{-/-}$ mice is not due to the increased myeloid precursors

The myeloid hyperplasia in *p100*$^{-/-}$ mice could be due to an increased frequency of myeloid precursor cells. To investigate this possibility, colony formation assays were performed using different FACS-sorted bone marrow cells (**Table 3-1**) from either wild-type or mutant chimeras (in collaboration with Dr. Terszowski, Ulm).

FACS-sorted cells	Cell surface markers
CMP^+	$Lin^-/Thy\text{-}1.1^-/IL\text{-}7R^-/c\text{-}Kit^{high}/Sca\text{-}1^-/CD34^+/Fc\gamma R^{low}$
GMP	$Lin^-/Thy\text{-}1.1^-/IL\text{-}7R^-/c\text{-}Kit^{high}/Sca\text{-}1^-/CD34^{high}/Fc\gamma R^{high}$

Table 3-1: The expression patterns of cell surface markers in different FACS-sorted bone marrow cell populations. CMP: common myeloid progenitors, **GMP**: granulocyte/macrophage progenitors.

In general, CMP^+ cells give rise to myeloid, erythroid, and megakaryocyte colonies including mixed colonies (Mix). GMP cells only give rise to colonies composed of macrophages and/or granulocytes.

The results of colony formation assays are summarized in **Table 3-2**. Numbers indicate the colonies obtained after plating different sorted bone marrow cell populations in methylcellulose supplemented with EPO (erythropoietin), TPO (thrombopoietin), IL-3, SCF, M-CSF, and GM-CSF.

CMP^+ cells either from wild-type or *p100*$^{-/-}$ chimeras generated erythrocytes (BFU-E), myeloid cells (CFU-GM), megakaryocytes (CFU-Meg), and mixed cell colonies (Mix). Moreover, similar numbers in CFU-GM, Mix, and CFU-GM&CFU-Meg colonies generated from CMP^+ cells were found in both wild-type and mutant animals (**Table 3.2**, shaded with blue color). GMP cells only generated myeloid cells (CFU-GM). Same numbers of CFU-GM colonies were obtained in both wild-type and mutant animals (**Table 3.2**, shaded with pink color).

***wild-type* chimeras**	BFU-E	CFU-GM	CFU-Meg	Mix	BFU-E CFU-GM	BFU-E CFU-Meg	CFU-GM CFU-Meg
CMP^+	10	87	2	1	3	1	2
	7	95	3	0	2	1	3
GMP	0	76	0	0	0	0	0
	0	79	0	0	0	0	0
***p100*$^{-/-}$ chimeras**							
CMP^+	6	105	1	1	9	15	4
	7	103	0	0	11	16	5
GMP	0	78	0	0	0	0	0
	0	81	0	0	0	0	0

Table 3-2: Colony formation assays. Individual FACS-sorted BM cell populations (CMP^+ and GMP) from wild-type and mutant chimeras were cultured in methylcellulose. The numbers from two independent experiments are presented in two rows (upper and lower) for every assay. **BFU-E**: erythroid burst-forming units; **CFU-GM**: colony forming unit-granulocyte macrophage; **CFU-Meg**: colony forming unit-megakaryocyte.

Taken together, there was no statistically significant difference in the myeloid-colony formation, indicating that the number of myeloid precursor cells in *p100*$^{-/-}$ chimeras bone marrow was comparable to that in wild-type chimeras. Thus, accumulation of myeloid cells observed in different lymphoid organs in mice lacking p100 is not due to an increased myeloid-precursor frequency.

3.1.4.3 B-cell developmental defect in *p100*$^{-/-}$ mice can not be rescued upon depletion of myeloid cells

The myeloid hyperplasia in *p100*$^{-/-}$ mice is evident as indicated by the above observations. It is possible that the defective B-cell development in *p100*$^{-/-}$ mice is caused by the massively increased myeloid cells. To examine this possibility, myeloid cells were depleted using anti-granulocyte monoclonal antibodies (mAb) RB6-8C5 in mutant animals. In this case, B-cell development in mice lacking p100 can be investigated without the influence of a large number of myeloid cells. RB6-8C5 mAb reacts with a common epitope on Ly-6G and Ly-6C, known as the myeloid differentiation antigen Gr-1 [124].

The *p100*$^{-/-}$ mice usually survive no more than 21 days, hampering the feasibility to perform a myeloid-cell depletion experiment. Therefore, bone marrow chimeras were generated (see **3.1.1.3**, **Figure 3.3)** and used for this experiment because they can survive longer.

p100$^{-/-}$→wt bone marrow chimeras received 150 μg RB6-8C5 mAb intraperitoneally (i.p.) and another 150 μg two days later, resulting in neutropenia for 3 to 4 days [125]. *p100*$^{-/-}$→wt chimeras without injection and wt→wt chimeras that received PBS i.p. were used as controls. Mac-1 and CD19 expression in peripheral blood was analyzed by flow cytometry every other day to monitor the fluctuation of myeloid and B-lymphoid cells after injections.

Only 9.54% Mac-1^{+} cells (**Figure 3.13 A**, right panel) in peripheral blood were detected in *p100*$^{-/-}$→wt chimeras three days after RB6-8C5 mAb injections (one day after the second injection). Mac-1^{+} cells in these animals were clearly reduced compared to those in *p100*$^{-/-}$→wt chimeras without injection (51.16%, **Figure 3.13 A**, middle panel), indicating successful myeloid cell depletion. However, depletion of myeloid cells did not lead to an increase of B lymphocytes in peripheral blood; only 23% CD19^{+} B cells were detected (**Figure 3.13 B**, right panel). This percentage was close to 17.64% observed in *p100*$^{-/-}$→wt chimeras without injection (**Figure 3.13 B**, middle panel) and was 3-fold

reduced compared to 71% $CD19^+$ B cells in wt→wt chimeras that received PBS injections (**Figure 3.13 B**, left panel). These phenomena lasted six days after injections. On the seventh day, the percentage of myeloid cells in *p100*$^{-/-}$→wt chimeras that received RB6-8C5 mAb injections went back to 65.45% (**Figure 3.13 A**, lower-right panel).

Despite the fluctuation in the number of PBL myeloid cells in *p100*$^{-/-}$→wt chimeras that received RB6-8C5 mAb injections, the number of PBL $CD19^+$ B-lymphoid cells of these animals stayed low and unchanged for seven days. These results become much clear when plotted on a line chart (**Figure 3.13 C**). In conclusion, it is unlikely that the defective B-cell development in mice lacking p100 is caused by increased number of myeloid cells. The reason for the increased myeloid cells in *p100*$^{-/-}$ mice is not clear; colony formation assay has excluded the possibility of the increased frequency of myeloid precursors.

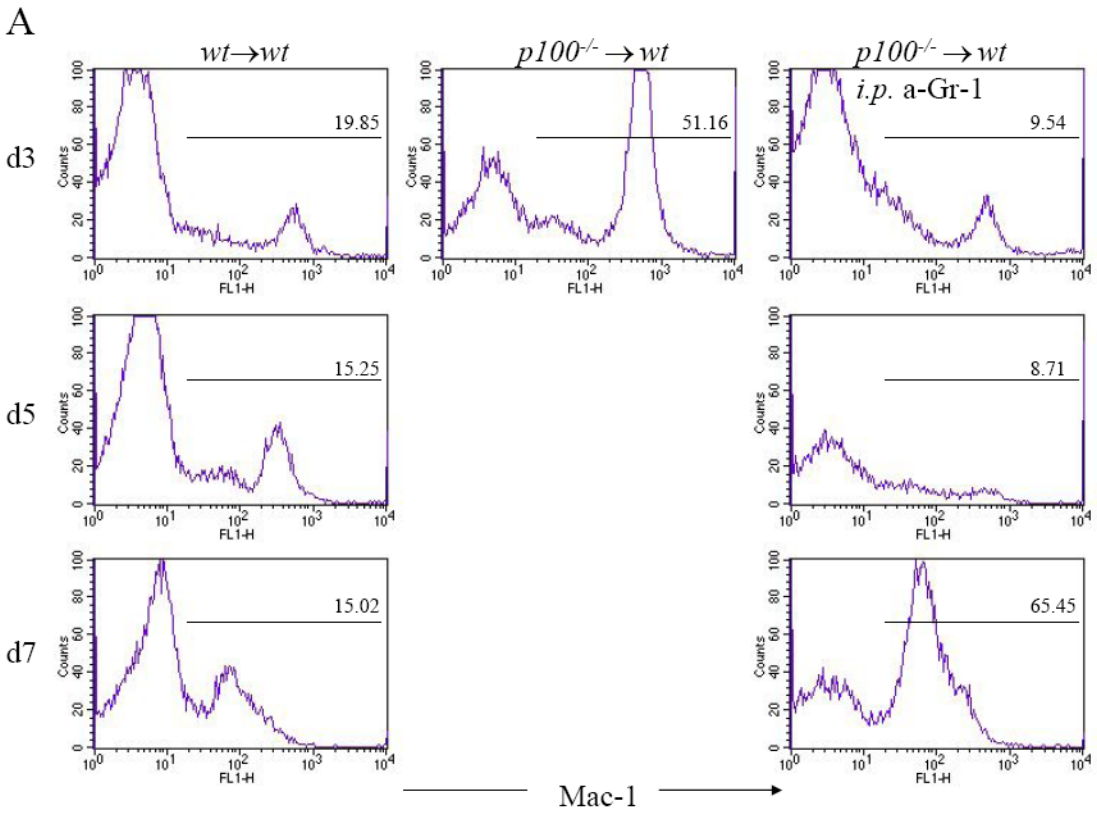

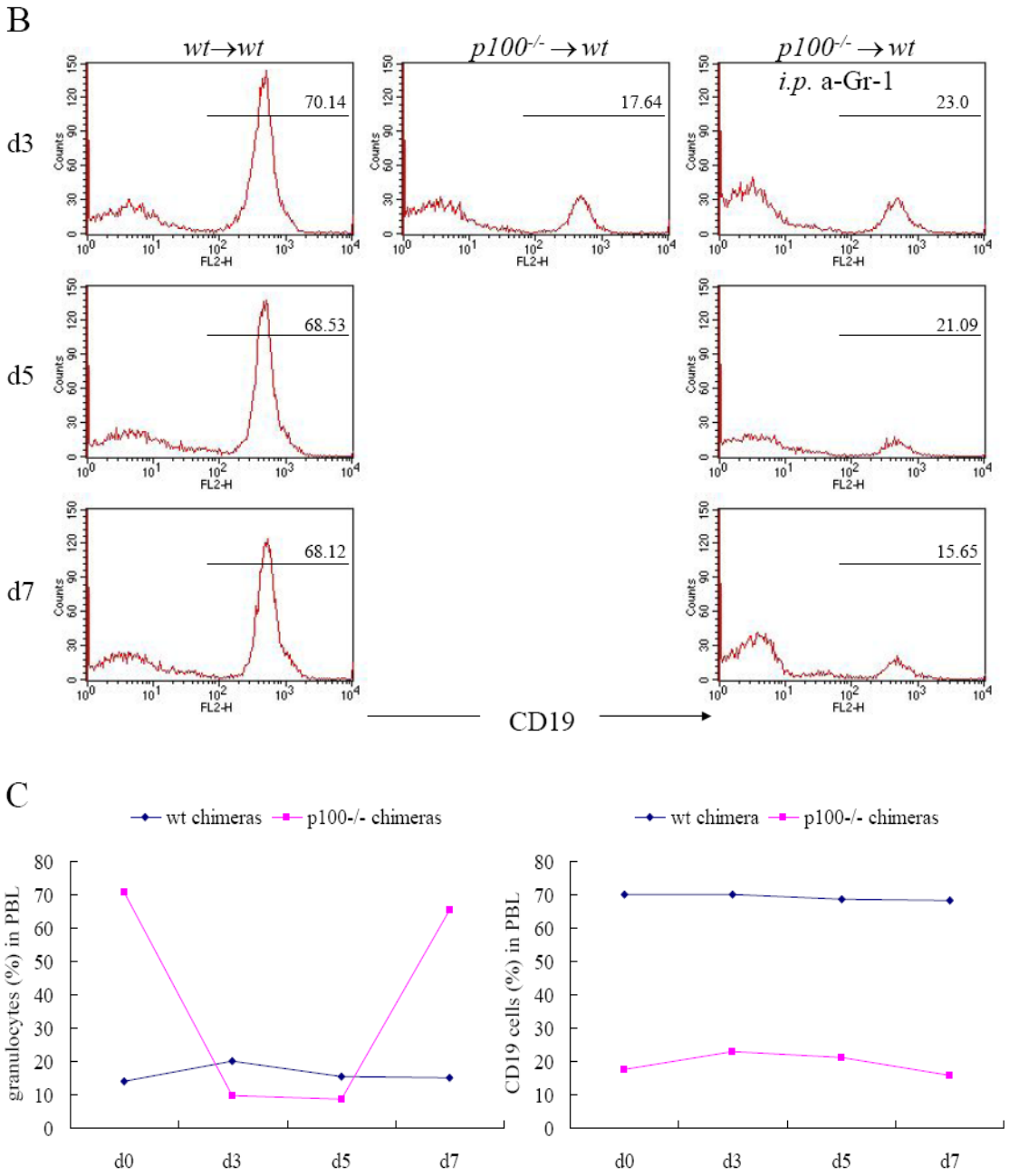

Figure 3.13: Analysis of the correlation between B-cell developmental defect and myeloid hyperplasia in mice lacking p100. Depletion of myeloid cells was preformed using anti-granulocyte monoclonal antibody RB6-8C5 injections i.p.. Peripheral blood was analyzed every other day after the antibodies injections. **(A)** Flow cytometric analysis after staining with Mac-1 antibody showed the fluctuation of myeloid cells from wt→wt that received PBS (left panels), *p100*$^{-/-}$→wt without injection (middle panels), and *p100*$^{-/-}$→wt chimeras that received RB6-8C5 antibody injections (right panels). **(B)** Flow cytometric analysis after staining with CD19 antibody**.** Lymphocytes were gated for this analysis. **(C)** Line charts for the fluctuation in myeloid cells and the percentage of CD19^{+} cells in PBL before and after injections. Blue lines indicate wt→wt that received PBS, pink line *p100*$^{-/-}$→wt chimeras that received RB6-8C5 injections.

3.1.5 The lympho-myeloid potential of *p100*$^{-/-}$ pro-B cells

3.1.5.1 *p100*$^{-/-}$ pro-B cells undergo transition to myeloid lineage

It has been shown that *Pax5*$^{-/-}$ pro-B cells can be cultured on the stromal cells *ex vivo* in the presence of IL-7. These cells can be induced to differentiate into various cell types including nature killer cells, dendritic cells, macrophages, osteoclasts, and granulocytes upon withdrawal of IL-7 and addition of appropriate cytokines [126]. A similar phenotype between *p100*$^{-/-}$ and *Pax5*$^{-/-}$ mice with respect to early B-cell development (see **Figure 3.10 A**) has been found in this study, raising the possibility that *p100*$^{-/-}$ pro-B cells may also have the lympho-myeloid potential similar to the plasticity of *Pax5*$^{-/-}$ pro-B cells in the differentiation into other lineages (see **Figure 1.6**).

To address this possibility, B220^{+}CD19^{-} bone marrow cells from 3-week-old wild-type and mutant mice were sorted using MACS to obtain a purity of ≥ 95%. These cells were then cultured on ST2 stromal cells in the presence of either IL-7 or M-CSF. After 10 days, the suspension cells were harvested and analyzed for CD19 and Mac-1 expression by flow cytometry.

In wild-type cultures, almost all B220^{+}CD19^{-} pro-B cells differentiated along B-cell lineage in the presence of IL-7 (94% CD19^{+} cells, **Figure 3.14**, upper-left panel) while nearly half of them lost B-lineage specific markers in the presence of M-CSF (63% CD19^{+} cells and 27% Mac-1^{+} cells, **Figure 3.14**, upper-right panel). After 10 days in IL-7 cultures, only 28% *p100*$^{-/-}$ pro-B cells differentiated into CD19^{+} cells while 60% pro-B cells lost their B-lymphocyte potential and differentiated into Mac-1^{+} cells (**Figure 3.14**, lower-left panel). When *p100*$^{-/-}$ pro-B cells were cultured in the presence of M-CSF, the percentage of cells, which underwent differentiation to myeloid cells, was not further enhanced (62%). However, the biphenotypic cells, expressing low levels of both CD19 and Mac-1 in this culture, were detected in greatly increased numbers (**Figure 3.14**, lower-right panel) and merely 7% CD19^{+} cells were found.

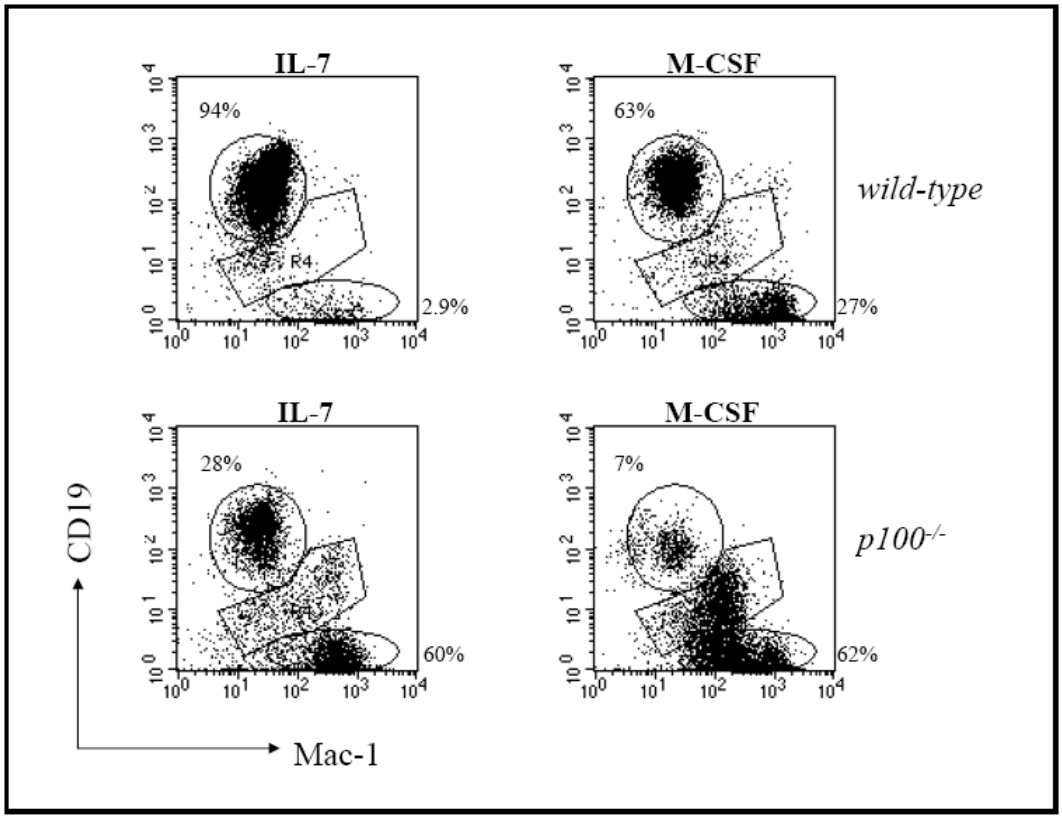

Figure 3.14: *p100*$^{-/-}$ pro-B cells transit to myeloid cells *ex vivo*. Sorted B220^{+}CD19^{-} cells from 3-week-old wild-type and mutant mice were cultured on ST2 stromal cells with IL-7 or M-CSF. Flow cytometric analysis was performed for CD19 and Mac-1 expression after 10 days of culture.

Taken together, *p100*$^{-/-}$ pro-B cells have a similar potential to *Pax5*$^{-/-}$ pro-B cells in terms of lympho-myeloid transdifferentiation. Interestingly, *p100*$^{-/-}$ pro-B cells can even transdifferentiate into myeloid cells in the culture of IL-7, which supports B-lymphocyte proliferation and differentiation. In addition, *p100*$^{-/-}$ pro-B cells do produce less CD19^{+} B lymphocytes than wild-type pro-B cells (28% vs. 94%) when they are cultured on the stromal cells *ex vivo*, further supporting that B-cell developmental defect in *p100*$^{-/-}$ mice is cell-intrinsic. It is assumed, then, that the evident myeloid hyperplasia without evidences of inflammation in different lymphoid organs of *p100*$^{-/-}$ mice is arise from the transdifferentiation of B-lineage progenitors to myeloid cells.

3.1.5.2 Transition of *p100*$^{-/-}$ pro-B cells to the myeloid lineage correlates with increased C/EBPα expression

p100$^{-/-}$ pro-B cells can transit to myeloid cells as indicated by the above observations. The molecular mechanism in this process is unknown. Recent report [91] shows that the transfection of C/EBPα can reprogram wild-type mature B cells to transdifferentiate into myeloid cells. This process is accompanied by the downregulation of Pax5 and intact endogenous PU.1 activity (see **1.2.1.5**). C/EBPα is expressed in myeloid progenitors and upregulated during granulocyte development. PU.1 belongs to the Ets transcription factors family and is expressed in hematopoietic stem cells and all differentiated cells except erythroblasts, megakaryocytes, and T cells. Low PU.1 expression favors B-cell development while high PU.1 level promotes macrophage differentiation.

To determine whether C/EBPα and/or PU.1 play a role in the process of transition of *p100*$^{-/-}$ pro-B cells to myeloid cells, mRNA levels in sorted B220^{+}CD19^{-} bone marrow cells were checked by real-time PCR. Surprisingly, the expression of *C/EBPα* mRNA levels was increased 5-fold, whereas *PU.1* expression remained unchanged (**Figure 3.15**). Thus, it is most likely that the plasticity of *p100*$^{-/-}$ pro-B cells in the differentiation to myeloid cells is due to the upregulation of C/EBPα expression.

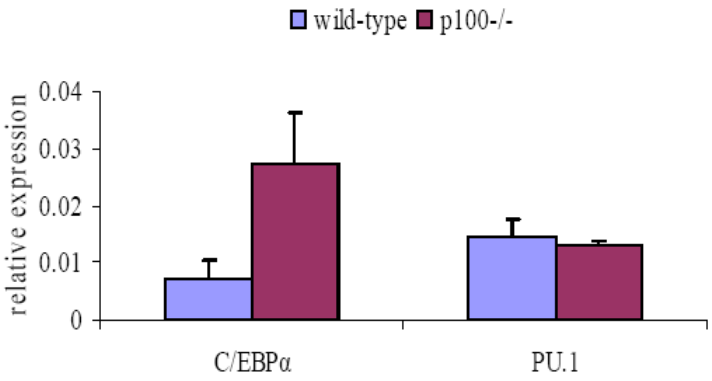

Figure 3.15: Increased expression of *C/EBPα* mRNA in *p100*$^{-/-}$ pro-B cells. B220^{+}CD19^{-} bone marrow cells were sorted from 3-week-old wild-type and *p100*$^{-/-}$ mice. Real-time PCR was performed using cDNA prepared from sorted B220^{+}CD19^{-} cells. Data represent two independent experiments.

3.1.6 Other B-cell subpopulations affected by p100 deficiency

After successful immunoglobulin gene rearrangement in bone marrow, immature B cells further migrate to spleen. Upon completing maturation from the T1 stage to the T2 stage, the majority of these cells enter the follicular subset, which constitutes the bulk of the peripheral B-cell pool and populates B-cell follicles in secondary lymphoid organs. Alternatively, some of these newly formed (NF) cells can be recruited to the far smaller MZ B or B1 B subset (see **Figure 1.4**).

3.1.6.1 Altered B-cell subpopulations in *p100*$^{-/-}$ spleen

The splenic IgM^{hi}IgD^{-} population includes T1 B cells (CD21^{-}CD23^{-}) and MZ B cells (CD21^{hi}CD23^{-}). T2 B cells are IgM^{hi}IgD^{hi} whereas FO B cells are IgM^{lo}IgD^{hi} (**Table 3-3)**.

	IMM	T1	T2	M	MZ
IgM	+	+++	+++	+	+++
IgD	−	−	+++	+++	−
CD21	−	−	+++	++	+++
CD23	−	−	++	++	−
Location	BM	BM, B, S	S	BM, B, S, LN	S

Table 3-3: Phenotypic description and tissue distribution of immature, T1, T2, mature (FO), and MZ B cells. Expression of the indicated cell surface markers is given as negative (-), low (+), intermediate (++), and high (+++). The location where the various cell types are found is also indicated. BM: bone marrow, B: blood, S: spleen, and LN: lymph nodes. IMM: immature. (Adapted from [127])

A reduction in IgM^{hi}IgD^{hi} (T2 B) and IgM^{hi}IgD^{-} (T1 B and MZ B) populations was observed in spleen from 3-week-old *p100*$^{-/-}$ mice (**Figure 3.16**). However, the percentage of mature recirculating FO B cells (IgM^{lo}IgD^{hi}) was comparable to that in wild-type mice.

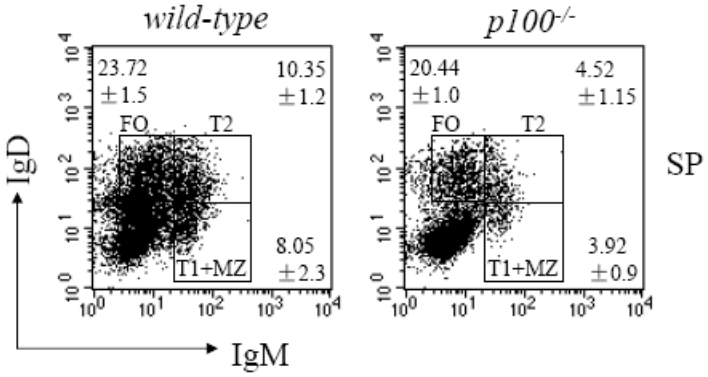

Figure 3.16: p100-deficiency alters T1, T2, MZ, and FO B-cell subsets. The expression of cell surface markers, IgM and IgD was examined to discriminate different B-cell subsets in spleen by flow cytometric analysis from 3-week-old wild-type (left panel) and *p100*$^{-/-}$ mice (right panel). Lymphocytes were gated for the analysis.

3.1.6.2 Accumulation of MZ B cells in *p100*$^{-/-}$ mice

MZ B cells are specifically located in the region outside of the marginal sinuses of lymphoid follicles in spleen and function as a first line of defense to blood-born pathogens. This specialized B-cell population is characterized by high surface expression of CD21/CD35 and negative expression CD23, whereas follicular B cells are CD21/CD35^{int}CD23^{int} (see **Table 3-3)**.

Flow cytometric analysis of splenocytes from 3-week-old *p100*$^{-/-}$ mice revealed a substantial increase of MZ B cells (*p100*$^{-/-}$, 7.04% vs. wild-type 1.72%) and a decrease of follicular B cells (**Figure 3.17 A** and **C**). In the CD23^{-} population, the increase of MZ B cells (CD21^{hi}IgM^{hi}) was also detected upon CD21 and IgM staining, 7.08% in *p100*$^{-/-}$ vs. 1.53% in wild-type mice. The percentage of the T1 B-cell population (CD21^{-}IgM^{hi}) was moderately decreased from 15.53% in wild-type to 11.07% in *p100*$^{-/-}$ mice (**Figure 3.17 B**, left panels). In the CD23^{+} population, a ~2-fold reduction in the T2 B-cell population (CD21^{hi}IgM^{hi}) was detected in *p100*$^{-/-}$ mice (**Figure 3.17 B**, right panels). This result is consistent with the previous observations when IgM and IgD were used as cell surface markers for detection of T2 B cells (see **Figure 3.16**).

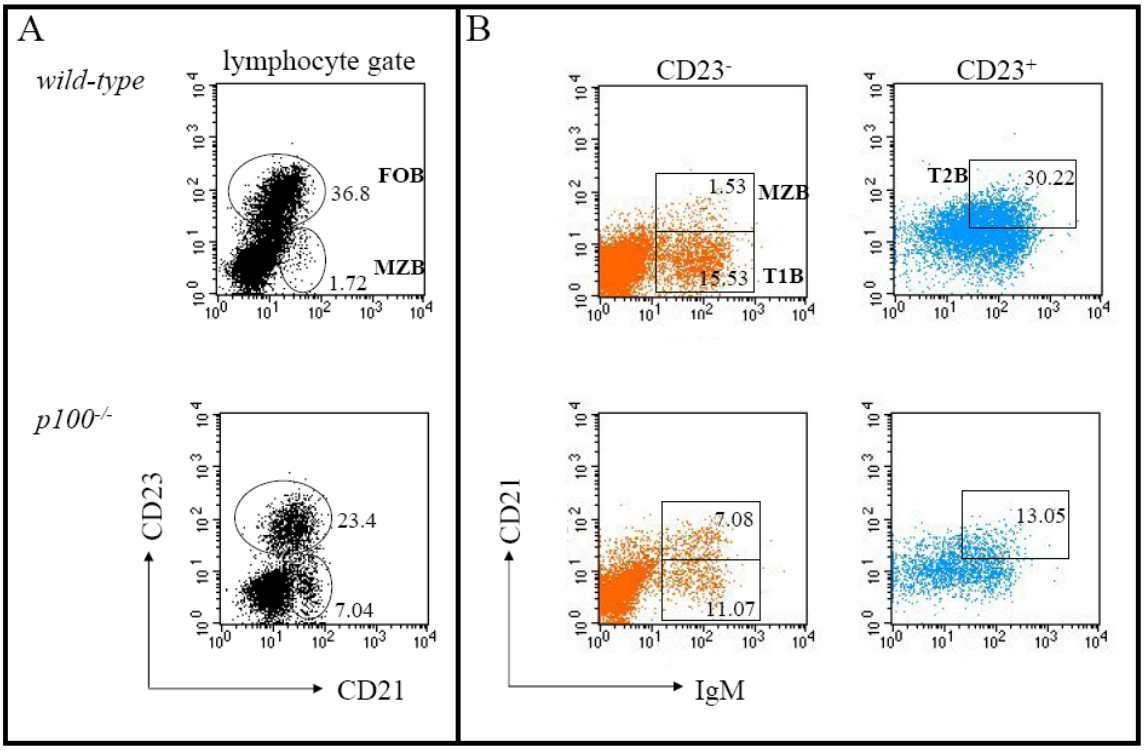

C

	T1	T2	FO	MZ
wild-type	15.53	30.22	36.8	1.53
p100$^{-/-}$	11.07	13.05	23.4	7.08

Figure 3.17: Increase of MZ B cells in *p100*$^{-/-}$ mice. (A) Flow cytometric analysis of splenocytes from 3-week-old wild-type (upper panels) and *p100*$^{-/-}$ mice (lower panels) stained with CD23 and CD21 antibodies. Lymphocytes were gated for the analysis. **(B)** Lymphocytes were gated as CD23^{-} (left panels) or CD23^{+} population (right panels) for further analysis of CD21 and IgM expression. **(C)** The percentage of T1, T2, FO, and MZ B-cell populations in wild-type and *p100*$^{-/-}$ mice.

Thus, there is an altered distribution of B cells in *p100*$^{-/-}$ spleen. The transitional compartment, which constitutes T1 B and T2 B cells, is decreased. However, the mature compartment, which constitutes MZ B and FO B cells, is enlarged and unaffected respectively. The reduction in T1 B and T2 B subsets actually leads to the 2–3-fold reduction of total B lymphocytes in spleen (see **Figure 3.1**).

3.1.6.3 Accumulation of MZ B cells in *p100*$^{-/-}$ mice is cell-intrinsic

The accumulation of marginal zone B cells in *p100*$^{-/-}$ spleen could result either from a B-cell autonomous defect or from a defect in the stromal microenvironment. To test this, competitive bone marrow reconstitution experiments were performed as previously described (see **3.1.1.3**). In brief, bone marrow cells from CD45.1^{+} wild-type and CD45.2^{+} *p100*$^{-/-}$ mice were mixed at equal proportions and injected into lethally irradiated CD45.1^{+} wild-type recipients. Six weeks after bone marrow transplantation, the development of MZ B cells was analyzed by flow cytometry for the expression of CD21 and CD23 together with CD45.1 or CD45.2 in spleen of chimeric mice.

A normal frequency of CD21^{hi}CD23^{-} MZ B cells (3.99%, **Figure 3.18**, left panel) was found in spleen of mixed chimeric mice (CD45.1^{+} wt & CD45.2^{+} *p100*$^{-/-}$→CD45.1^{+} wt). Interestingly, CD45.2^{+} *p100*$^{-/-}$ bone marrow cells had a priority to generate MZ B cells despite the co-existence of CD45.1^{+} wild-type bone marrow cells, 7.35% compared to 2.2% from CD45.1^{+} wild-type bone marrow cells (**Figure 3.18**, middle and right panels).

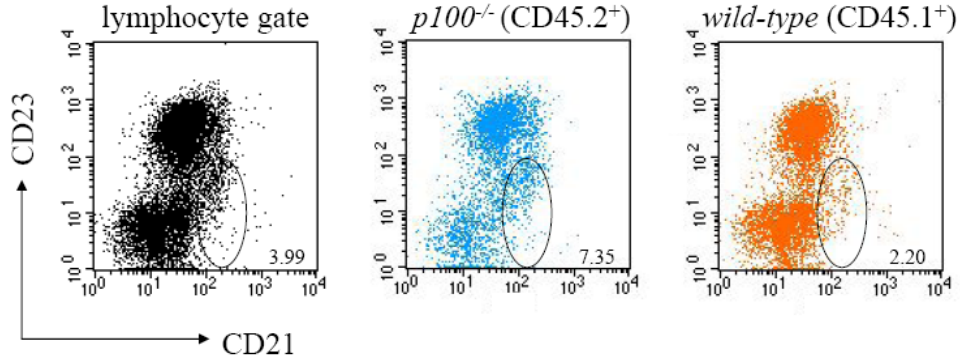

Figure 3.18: Analysis of marginal zone B-cell development in mixed bone marrow chimeric mice. Splenocytes were isolated from lethally irradiated mice that were reconstituted with bone marrow cells mixed at a 1:1 ratio. Flow cytometric analysis was performed after staining with anti-CD45.1 or anti-CD45.2 together with anti-CD21 and anti-CD23 antibodies.

Thus, *p100*$^{-/-}$ bone marrow cells are not able to undergo normal MZ B-cell development even with the support of wild-type bone marrow cells and stromal environment. p100 within B cells rather than in any other cell types is necessary for proper MZ B-cell development. Taken together, these data suggest that the MZ B-cell developmental defect in mice lacking p100 is a hematopoietic defect and is intrinsic to B cells.

3.1.6.4 Partial rescue of MZ B-cell accumulation by deleting one allele of the *relB*

It is demonstrated from above studies that deleting one allele of the *relB* gene in *p100*$^{-/-}$ mice, which reduced the increased RelB DNA-binding activity to wild-type levels, could rescue the phenotypes in *p100*$^{-/-}$ mice regarding to the early mainstream B-cell developmental defect (see **3.1.2**). It is likely that MZ B-cell development could also be affected by RelB DNA-binding activity.

Flow cytometric analysis of splenocytes from 3-week-old *p100*$^{-/-}$*relB*$^{-/+}$ mice revealed a moderate increase of CD21^{hi}CD23^{-} MZ B cells compared to that in wild-type mice (3.1% vs. 2.04%, **Figure 3.19 A**, upper and middle panels). The follicular B-cell compartment is unaffected. Almost no MZ B cells were found in 3-week-old *p100*$^{-/-}$*relB*$^{-/-}$ mice (0.2%, **Figure 3.19 A**, lower panel), which was similar to that in *relB*$^{-/-}$ mice [107].

In the CD23^{-} population, the increase of MZ B cells (CD21^{+}IgM^{+}) was much clear in *p100*$^{-/-}$*relB*$^{-/+}$, 4.38% vs. 1.67% in wild-type mice. This percentage of MZ B cells is lower than that in *p100*$^{-/-}$ (7.08%, **Figure 3.17 B)** but higher than that in wild-type mice. This increment in MZ B cells was absent when two alleles of the *relB* gene were deleted in *p100*$^{-/-}$ mice (**Figure 3.19 B** and **C**).

A constitutively increased RelB DNA-binding activity and an enlarged MZ B-cell compartment are detected in *p100*$^{-/-}$ mice lacking RelB inhibitor. When one allele of the *relB* is inactivated in *p100*$^{-/-}$ mice (*p100*$^{-/-}$*relB*$^{-/+}$), the RelB DNA-binding activity restores to wild-type levels (see **Figure 3.8**), correlated with the rescue in mainstream B-cell development. However, unlike the rescue in the mainstream B-cell development, only a partial rescue is found in the MZ B-cell development in *p100*$^{-/-}$*relB*$^{-/+}$ mice. When the *relB* gene is completely inactivated in *p100*$^{-/-}$ mice (*p100*$^{-/-}$*relB*$^{-/-}$), almost no MZ B cells are present. These observations suggest that the strength of the RelB activity also plays an important role in the generation of MZ B cells. High levels of the RelB activity (*p100*$^{-/-}$) favor MZ B-cell generation; the lack of the RelB activity (*p100*$^{-/-}$*relB*$^{-/-}$) abolishes MZ B-cell generation.

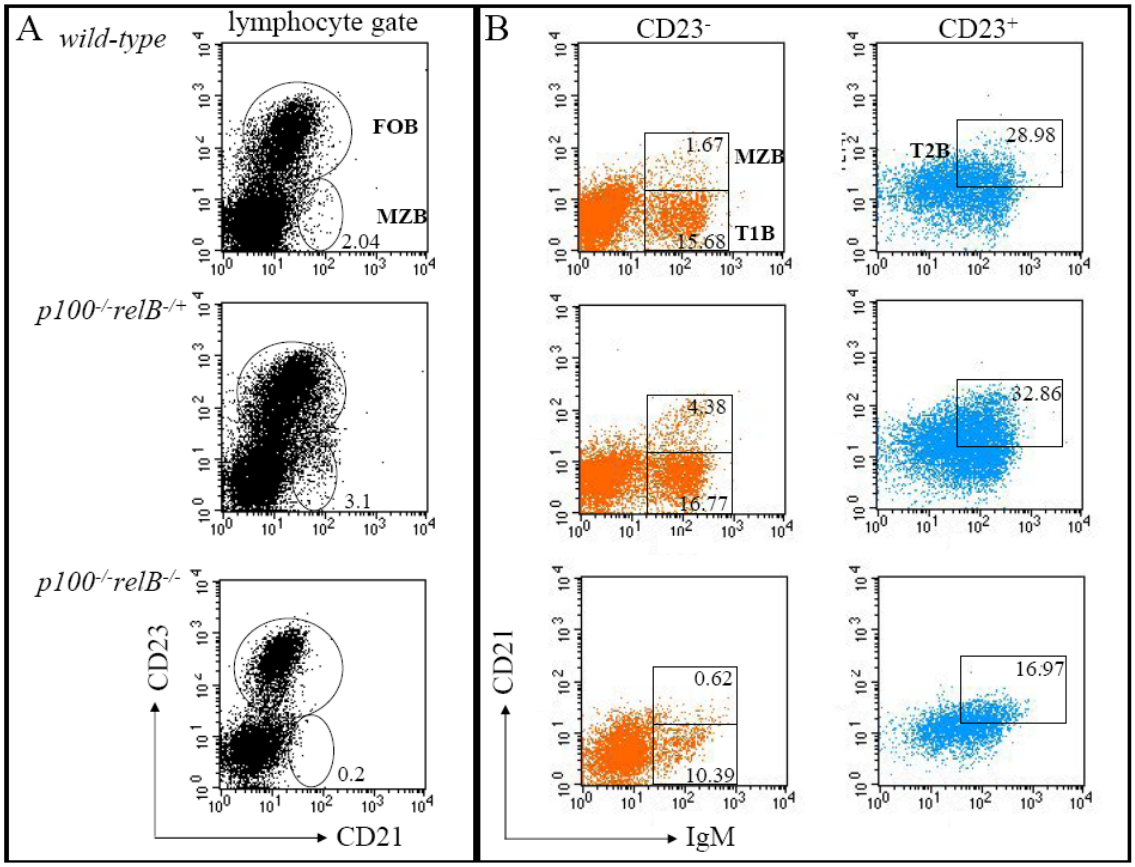

C

	T1	T2	MZ
wild-type	15.68	28.98	1.67
p100-/-relB-/+	16.77	32.86	4.38
p100-/-relB-/-	10.39	16.97	0.62

Figure 3.19: RelB activity affects the development of MZ B cells. (A) Flow cytometric analysis of splenocytes from 3-week-old wild-type, *p100*$^{-/-}$*relB*$^{-/+}$, and *p100*$^{-/-}$*relB*$^{-/-}$ mice for the expression of CD23 and CD21 expression. Lymphocytes were gated for the analysis. **(B)** Lymphocytes were gated as CD23^{-} population or CD23^{+} population when analyzed for the expression of CD21 and IgM. **(C)** The percentage of T1, T2, and MZ B-cell populations.

Collectively, in addition to that RelB functions mainly in the activation of mature B cells from previous studies, the work here demonstrates, for the first time, that the strength of RelB activity does affect the development of mainstream B-cell at early stage in bone marrow as well as the development of other B-cell subsets such as MZ B cells in a cell-intrinsic manner. Thus, p100, the potent inhibitor of RelB, functions crucially in B lymphopoiesis at different stages (see **Figure 4.1**).

3.2 Generation of mouse models to dissect the role of individual NF-κB pathways in secondary lymphoid organogenesis

The LTβR signaling pathway is involved in the development of secondary lymphoid organs such as lymph nodes (LNs) and Peyer's patches (PPs) as well as the lymphoid compartment in spleen. When triggered by membrane-bound $LT\alpha_1\beta_2$ heterotrimers, two NF-κB signaling pathways are activated in mouse fibroblast system [12-15]. The importance of alternative NF-κB signaling pathway, activating p52/RelB heterodimers in secondary lymphoid organogenesis, is illustrated by similar phenotypes in different mutant mice (see **Table 1-4**). The classical NF-κB signaling pathway, activating mainly p50/RelA heterodimers, contributes to secondary lymphoid organogenesis as well since mice deficiency in both RelA and TNFR-1 lack LNs and PPs.

However, the precise *in vivo* contribution of RelB and RelA downstream of LTβR signaling for secondary lymphoid organogenesis is unclear. The work here will focus on establishing an *in vivo* model system, in which the individual contribution of alternative (RelB) and classical (RelA) complexes downstream of LTβR signaling can be analyzed with a focus on secondary lymphoid organ development.

Toward this goal, one approach is to generate transgenic mouse lines, in which the activation of RelB or RelA complexes by LTβR can be selectively blocked. To achieve this, transgenic mouse lines that express the Cre recombinase under the control of LTβR regulatory elements will be generated. These mice will then be crossed with mice carrying conditional (floxed) *relB* or *relA* alleles to selectively block RelB or RelA in LTβR-expressing cells (**Figure 3.20**). This strategy will provide a significant mice model system for studying the individual contribution of each NF-κB pathway to LTβR-dependent processes on the organic level.

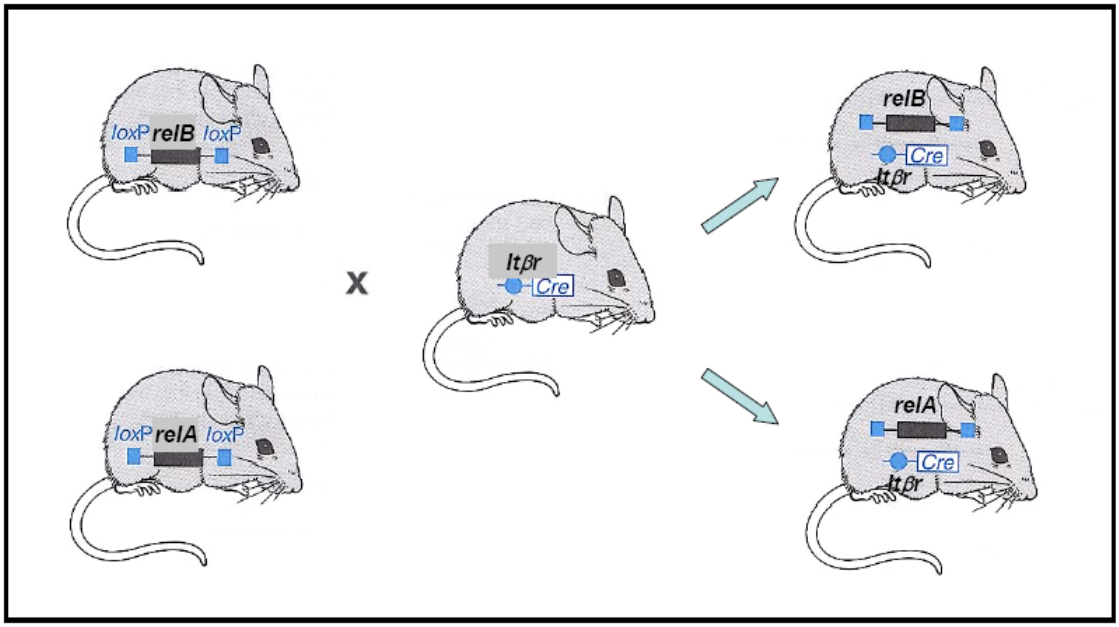

Figure 3.20: Schematic figure of the *relB* and *relA* gene targeting in LTβR-expressing cells. Mice with a floxed *relB* or *relA* allele will be generated by homologous recombination in murine embryonic stem (ES) cells and then crossed to mice in which the Cre recombinase is expressed under the control of the LTβR regulatory elements. In the resulting $relB^{ltbr\text{-}cre}$ and $relA^{ltbr\text{-}cre}$ mice, the expression of RelB or RelA will be disrupted specifically in LTβR-expressing cells.

In short, three mouse strains should be established for further analysis including mice harboring floxed *relB* ($relB^{flox/flox}$) or *relA* alleles ($relA^{flox/flox}$) and one mouse strain with Cre recombinase activity in LTβR-expressing cells. The $relA^{flox/flox}$ mice have already been generated in the lab of Dr. Roland Schmid (Munich) and are currently available in our lab. Thus, it is necessary to generate $relB^{flox/flox}$ mice and mice expressing Cre recombinase under the control of LTβR regulatory elements.

The principal procedures to generate knockout mice and to further generate tissue-specific (conditional) knockout mice are illustrated in **Figure 3.21**.

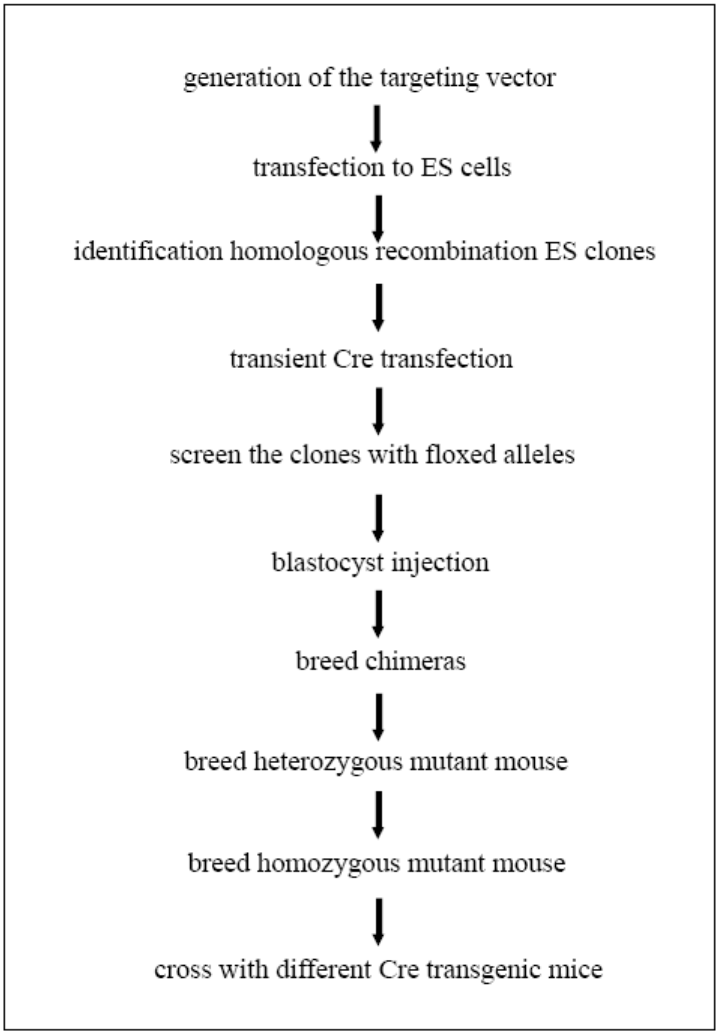

Figure 3.21: Summary of experimental procedures for generating tissue-specific knockout mice. A modified version of the gene of interest (targeting vector) is introduced into ES cells. Only a few rare ES cells will have their corresponding normal gene replaced by the modified gene through a homologous recombination (HR) event. These altered ES cells are then injected into a very early mouse embryo (blastocyst). These cells will be incorporated into the growing embryo. A mouse produced by such an embryo will contain some somatic cells that carry the modified gene. Some of these mice may have germline cells that contain the modified gene. When bred with a wild-type mouse, some of progenies may contain the modified gene in all of their cells. When homozygous mouse is crossed with *cre*-transgenic mouse, the target gene of interest will be specifically mutated in certain tissues.

3.2.1 Generation of *relB*$^{flox/flox}$ mice

3.2.1.1 Construction of the targeting vector pRelBXS11.2-LLTNL

Homologous sequences in the targeting vector were amplified by PCR using proofreading eLONGase enzyme mix (a mixture of *Taq* mixed and Pyrococcus species GB-D thermostable DNA polymerases, Invitrogen GmbH) from plasmid pRelB-XS11.2 [25], which contains *relB* genomic DNA, spanning intron III to exon VII. The homologous sequences of a length of 11.2 kb were divided into a 7.6 kb long arm (XB6.85 and BA773, **Figure 3.22 A**, panel 4)) and a 3.6 kb short arm (AS3.6, **Figure 3.22 A**, panel 1)).

The 4 kb long LTNL cassette, containing the *neo* and the thymidine kinase (HSV*tk*) selection marker genes, is flanked by the loxP sites. This combination pattern of the *neo* and the HSV*tk* genes allows negative selection using ganciclovir after transient Cre transfection in homologously recombined ES clones. However, only the positive selection using G418 can be performed after transfection of this targeting vector.

LTNL cassette was placed into intron IV of the *relB* gene. Oligodeoxynucleotides encoding a single loxP sequences were inserted into intron III of the *relB* gene (**Figure 3.22 A**, panel 3)). Exon IV will be flanked by two loxP sites in homolougous recombination allele (see **Figure 3.23 A)** and mutated in *relB*$^{ltbr\text{-}tg}$ mice. Exon IV encodes the beginning of the Rel homology domain (RHD) of RelB. In *relB*$^{-/-}$ mice, exon IV is replaced by PGK-*neo* cassette [25] . The presence of three loxP sites in the same orientation was confirmed by sequencing. The cloning procedures, leading to the final construction of the 18.2 kb targeting vector pRelBXS11.2-LLTNL, are described in detail in **Figure 3.22**.

A

1) PCR Cloning of AS3.6 into pLTNL

Forward Primer:
*Pac*I
AAAA TTAATTAA TCCAAAGTTACCATCAACCTC start of genomic seq. at 10936 (3´of *Asc*I)

Reverse Primer:

AATT CCATGG TTCTTCAGGGAGCCA start of genomic seq. at 14523 (5' of *Sal*I site)

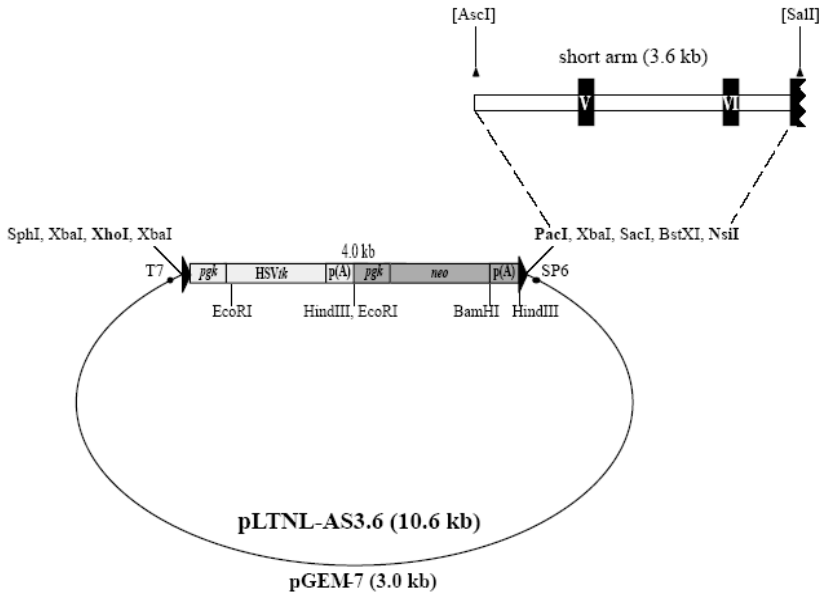

2) PCR Cloning of BA773 into pLTNL-AS3.6

Forward Primer:
*Xba*I *Bgl*II
AAAT TCTAGA TCTGCCTAGTTCCAAGCC start of genomic seq. at 10163 (*Bgl*II site)

Reverse Primer:
*Spe*I
AAAA ACTAGT GGCGCGCCTTTGGGATCCAGA start of genomic seq. at 10936 (*Asc*I site)

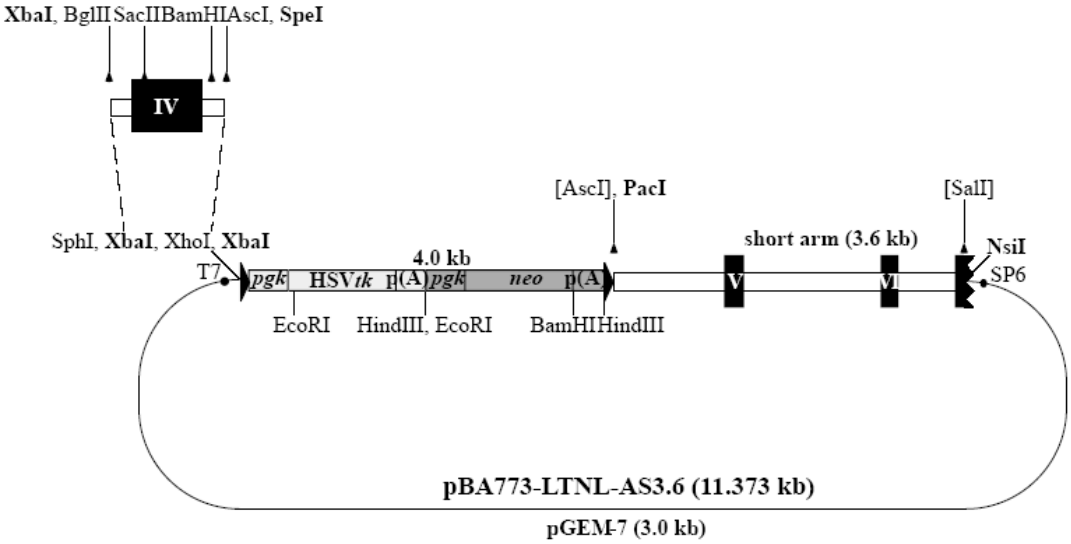

3) Oligo Cloning of loxP site into pBA773-LTNL-AS3.6

XbaI-HpaI-**loxP**-SpeI upper:

loxP

5'-Ⓟ-CTAGA GTTAAC ATAACTTCGTATA **ATGTATGC** TATACGAAGTTAT A

SpeI-**loxP**-HpaI-XbaI lower:

loxP

5'-Ⓟ-CTAGT ATAACTTCGTATA **GCATACAT** TATACGAAGTTAT GTTAAC T

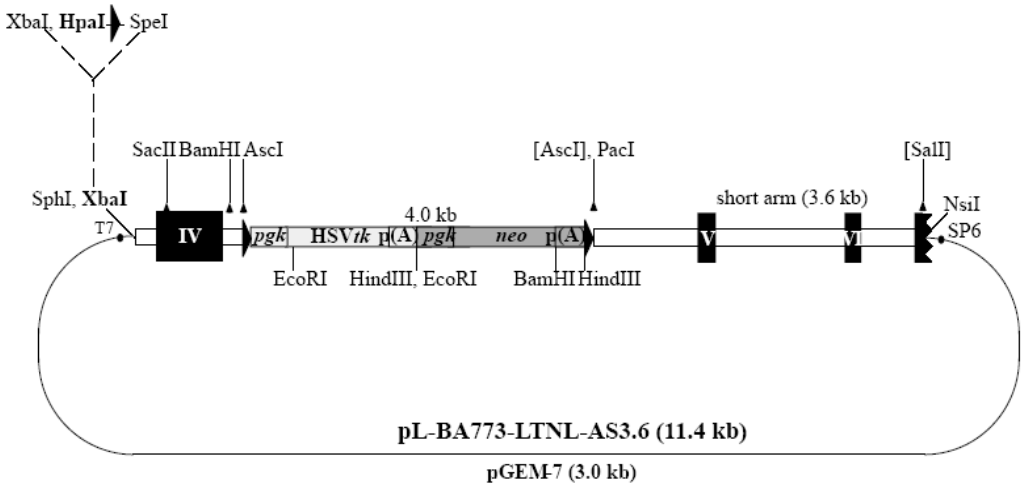

4) PCR Cloning of XB6.85 into pL-BA773-LTNL-AS3.6 generating pRelB-XS11.2-LLTNL

Forward Primer:

*Xba*I

5'-AAAA TCTAGA CCCTTGGTGAAGCAG **start of genomic seq. at 3315 (*Xba*I site)**

Reverse Primer:

*Hpa*I

5'-AAAA GTTAAC ACACAGAGATCCACTCTC **start of genomic seq. at 10160 (5' of *Bgl*II site)**

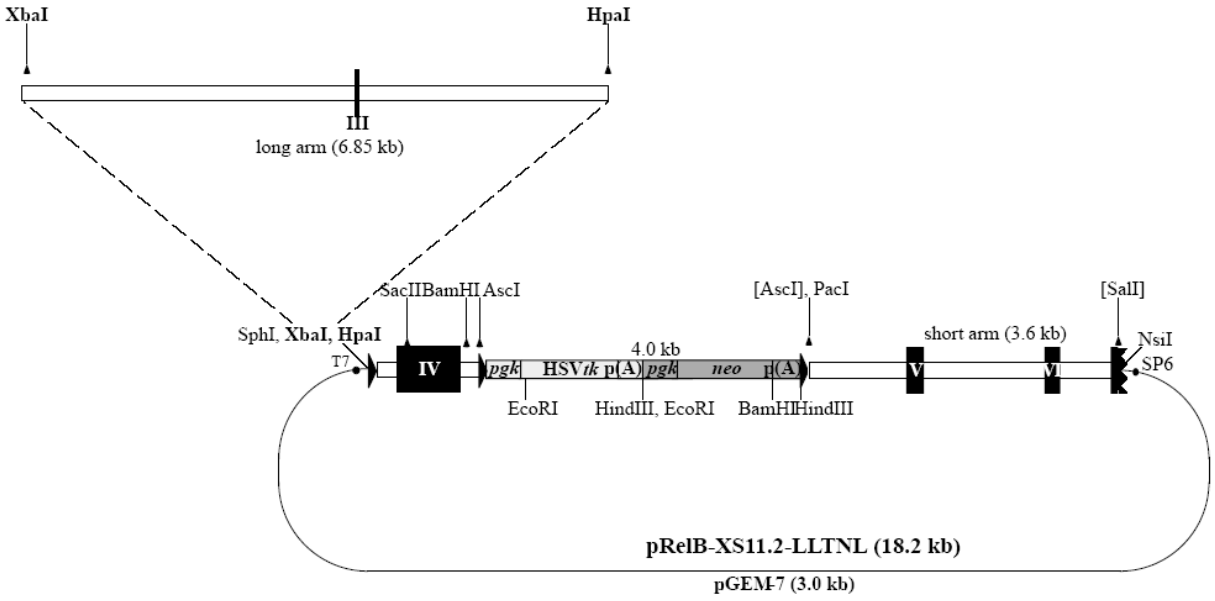

B

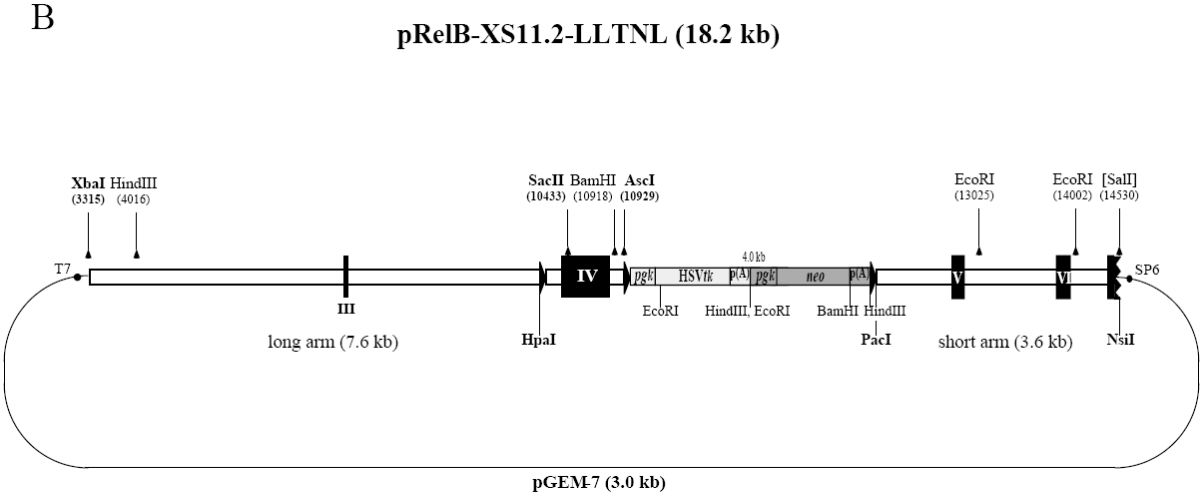

Figure 3.22: Generation of the targeting vector pRelBXS11.2-LLTNL. (A) The cloning procedures were separated into four steps as listed in panels 1) - 4). AS3.6 fragment was the short arm of the targeting vector. Long arm was composed of XB6.85 and BA773 fragment. The single loxP was located in intron III of the *relB* gene. **(B)** Schematic diagram of the 18.2 kb targeting vector pRelBXS11.2-LLTNL. Open boxes indicate *relB* genomic sequences; closed boxed indicate exons III-VII. *Xba*I was used for linearization of the targeting vector before electroporation.

3.2.1.2 Transfection of mouse embryonic stem cells with the targeting vector pRelBXS11.2-LLTNL and Southern blot screening

After linearization with *Xba*I, the targeting vector pRelBXS11.2-LLTNL (**Figure 3.23 A** and see **Figure 3.22 B)** was transfected into E14.1 (from Prof. Wang Z-Q, Lyon, France) embryonic stem (ES) cells by eletroporation. Cells were cultured in G418 selection media for 9-10 days before being picked (see **2.2.11.2.2**). Surviving colonies were expanded for freezing and for DNA preparation. The screening strategy is illustrated in schematic diagrams in **Figure 3.23 A**.

Homologous recombination of the targeting vector with wild-type genomic DNA introduces an additional 4 kb LTNL cassette into the genome. The SM592 probe [25] was located just outside of the targeting vector pRelBXS11.2-LLTNL. This probe discriminated a 7.9 kb *Hind*III DNA fragment, specific for the recombined allele, from a 14.8 kb DNA fragment, specific for the wild-type *relB* allele. A total of 550 G418-

resistant ES clones were picked. Among ~450 ES clones that were screened successfully by Southern blotting, no ES clone containing the desired homologous recombination (HR) event was found. All G418-resistant ES clones showed the 14.8 kb DNA fragment, specific for the wild-type *relB* allele (**Figure 3.23 B**).

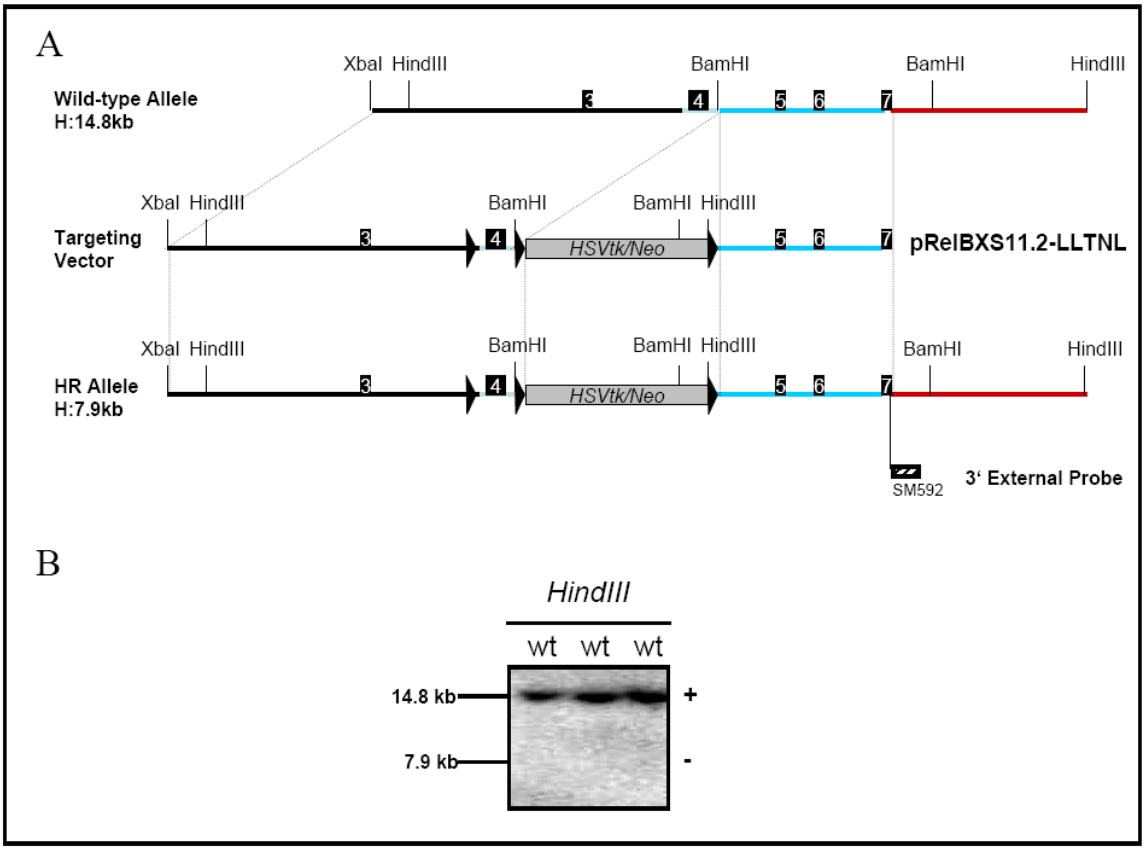

Figure 3.23: Gene targeting of the mouse *relB* gene using the targeting vector pLRelBXS11.2-LLTNL. (A) Schematic diagrams (from top to bottom) of the wild-type *relB* gene locus, the targeting vector, and the homologous recombination allele. Thick lines represent *relB* genomic sequences. Arrows represent the loxP sites and indicate orientation of the loxP sites as well. Closed boxes indicate exons III-VII of the mouse *relB* gene. Cleavage sites for relevant restriction endonucleases are indicated. The 3' external probe (SM592) used for Southern blot analysis are indicated by hatched box. The lengths of diagnostic restriction fragments used for Southern blotting are also indicated. **H**: *Hind*III. **(B)** Southern blot analysis of genomic DNA isolated from G418-resistant ES cell clones. After overnight digestion with *Hind*III, a 14.8 kb DNA fragment recognized by the probe SM592 indicated the wild-type alleles. The 7.9 kb DNA fragment indicative for the homologously recombined alleles was not detected.

3.2.1.3 Construction of the targeting vector pTVFlox-LRelBXS11.2 and screening for HR events

The targeting frequency of the vector pRelBXS11.2-LLTNL was extremely low as indicated by the above work. Only positive selection using G418 was able to be performed after transfection due to the presence of the *HSVtk* gene in the homologously recombined alleles. In order to increase the targeting frequency, a second targeting vector was generated based on 5.84 kb pTVFlox-0 plasmid (constructed by Dieter Riethmacher and Karin Gottschling). This plasmid constitutes the selection marker genes, the *neo* gene flanked by two loxP sites and the *HSVtk* gene, in a separate pattern (**Figure 3.24 A**, panel 1)). Using this plasmid as the backbone of the targeting vector allows a positive-negative double selection.

Homologous sequences of the *relB* gene and the location of the isolated loxP site were identical to those of the targeting vector pRelBXS11.2-LLTNL. In brief, the AS3.6 fragment was the short arm. The long arm was composed of XB6.85 and BA773 fragment. The single loxP site was located in intron III of the *relB* gene (**Figure 3.24 A**, panel 2)). The *HSVtk* gene was located at the end of the short arm AS3.6 (**Figure 3.24 A**, panel 1)) and served as the negative selection marker (using ganciclovir) against ES clones, which had randomly integrated the targeting vector.

The cloning procedures for the 17 kb targeting vector pTVFlox-LRelBXS11.2 is illustrated in **Figure 3.24 A** in detail. The homologous sequences (7.6 kb long arm and 3.6 kb short arm) and the three loxP sites were confirmed by sequencing before transfection to ES cells.

A

1) Cloning short arm into pTVFlox-0

Digested pRelBXS11.2 with *Asc*I and *Sal*I (destroyed *Sal*I site by blunting afterwards)

Inserted 3.6 kb *Asc*I[*Sal*I] fragment to pTVFlox-0 which was digested with *Asc*I and *Hpa*I

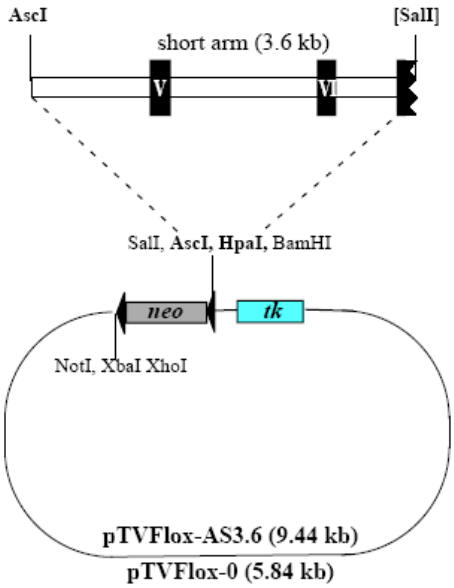

2) Cloning LBA773 into pTVFlox-AS3.6

Digested pLBA773-LTNL-AS3.6 with *Xba*I and *Asc*I (destroyed *Asc*I site by blunting afterwards, see **Figure 3.22**)

Inserted the 818 bp *Xba*I[*Asc*I] fragment to pTVFlox-AS3.6 which was digested with *Xba*I and *Xho*I (destroyed *Xho*I site by blunting afterwards)

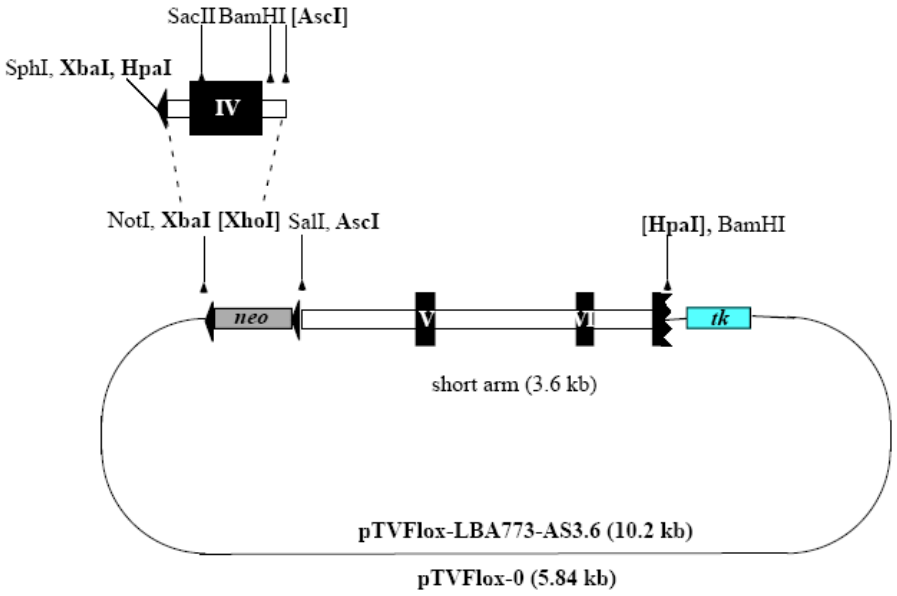

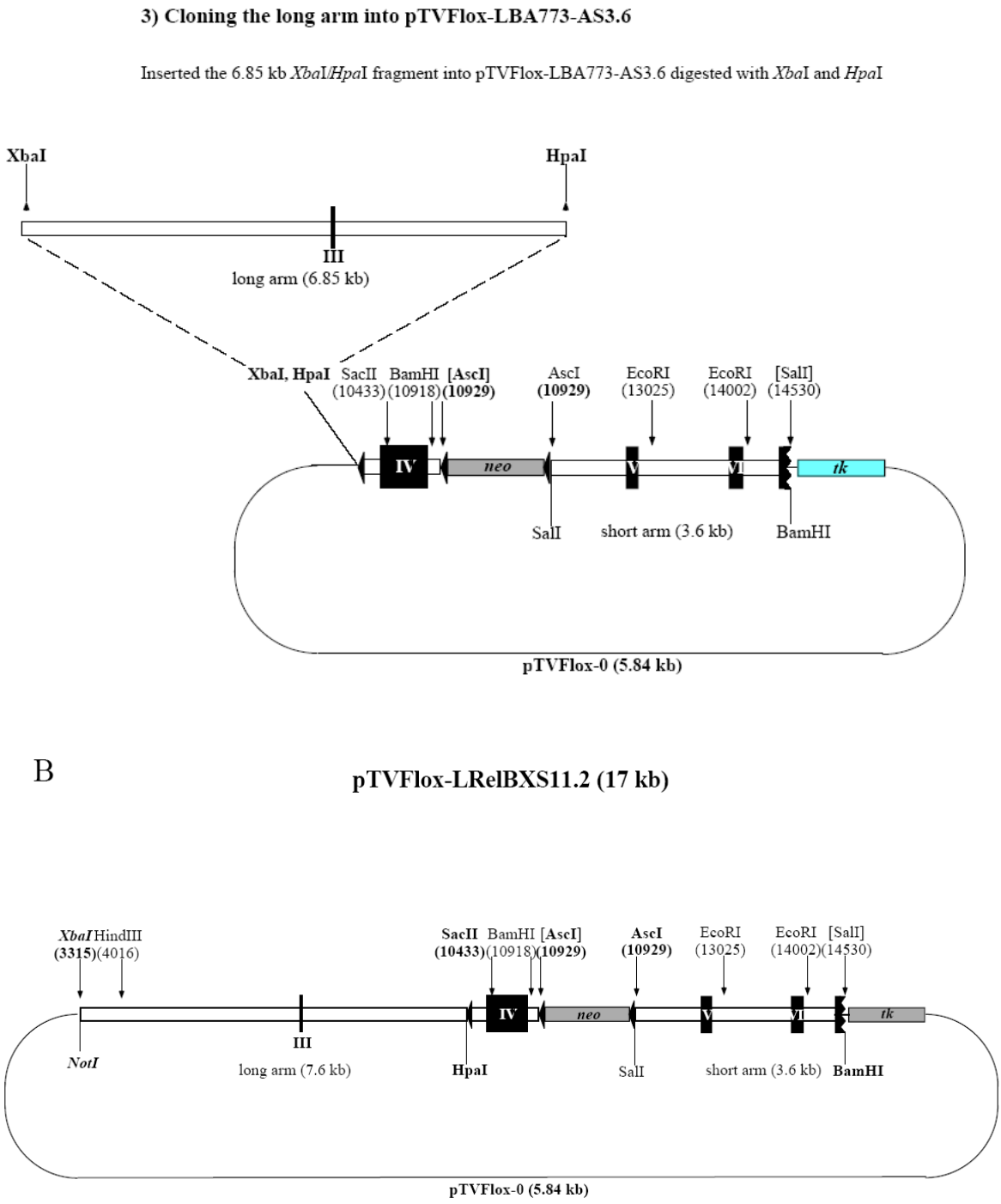

Figure 3.24: Generation of the targeting vector pTVFlox-LRelBXS11.2. (A) The cloning procedures were separated into three steps as listed in panels 1) - 3). AS3.6 fragment was the short arm of the targeting vector. The long arm was composed of XB6.85 and BA773 fragment. The *HSVtk* gene was located at the end of the short arm. **(B)** Schematic diagram of the 17 kb targeting vector. The isolated loxP site was located in intron III and the loxP-flanking *neo* gene was located in intron IV of the *relB* gene. The three loxP sites were in the same orientation. *Xba*I was used for linearization of the targeting vector before electroporation. Open boxes indicate *relB* genomic sequences and closed boxed exons III-VII of the mouse *relB* gene.

3.2.1.4 Transfection of the targeting vector pTVFlox-LRelBXS11.2 into ES cells and Southern blot screening

After linearization with *Xba*I, the targeting vector pTVFlox-LRelBXS11.2 (**Figure 3.25 A** and see **Figure 3.24 B)** were transfected into E14.1 ES cells by eletroporation. Positive-negative selection was performed after the transfection. With this strategy, ES clones with a randomly integrated targeting vector can be negatively selected, resulting in a 3–5-fold enrichment over G418 selection (positive) alone. Surviving colonies, which still manifest a good morphology, were picked carefully under microscope and cultured in 96-well plates before freezing at –80ºC.

A total of 450 double-resistant E14.1 ES cell clones were picked and screened successfully by Southern blotting. The screening strategy using the 3' external probe (SM592) is described in diagrams in **Figure 3.25 A**. Homologous recombination of the targeting vector pTVFlox-LRelBXS11.2 with wild-type genomic DNA introduced an additional 1.2 kb *neo* cassette into the genome. The SM592 probe distinguished a 6.14 kb *BamH*I DNA fragment, specific for the recombined allele, from a 4.86 kb DNA fragment [25], specific for the wild-type *relB* allele (**Figure 3.25 B**).

Two ES cell clones were found containing the desired homologous recombination event, resulting in a targeting frequency of 1 in 225 double-resistant ES cell clones.

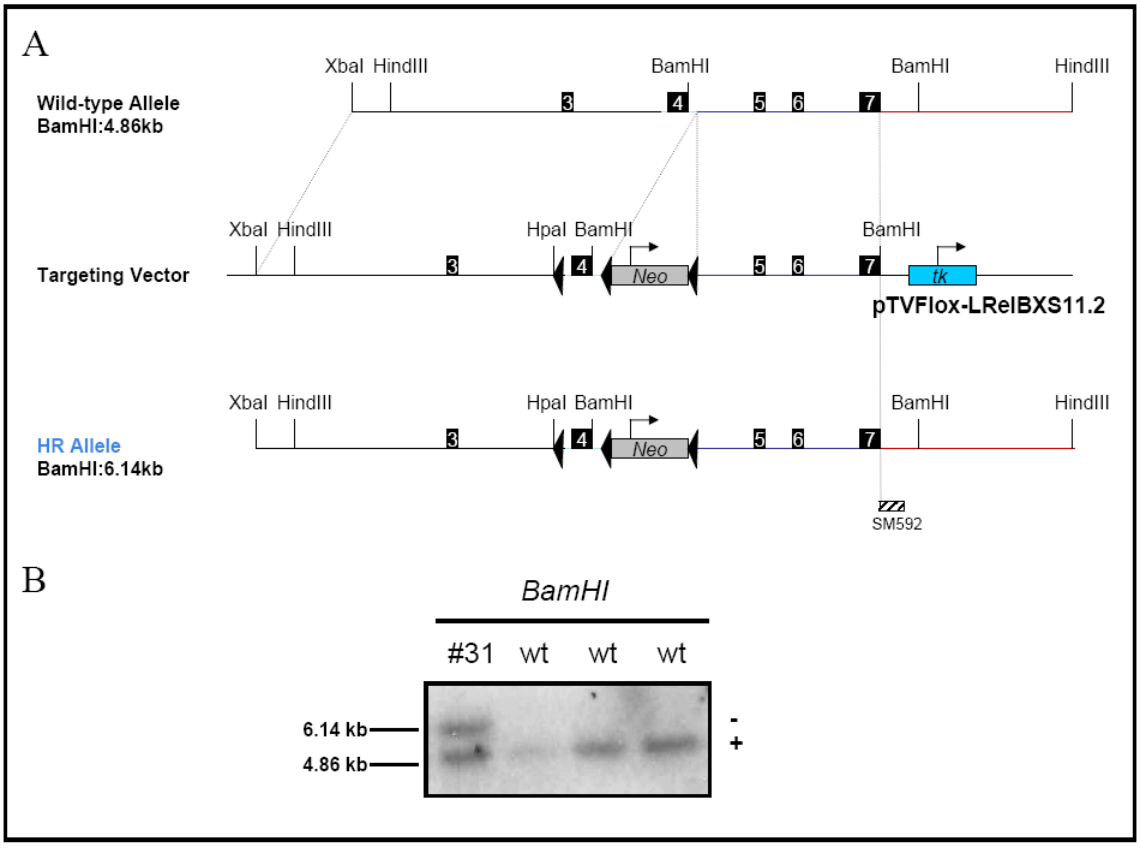

Figure 3.25: Gene targeting of the mouse *relB* gene using the targeting vector pTVFlox-LRelBXS11.2. (A) Schematic diagrams (from top to bottom) of the wild-type *relB* gene locus, the targeting vector, and the homologous recombination allele. Lines represent *relB* genomic sequences. Arrows represent the loxP sites and indicate orientation of the loxP sites as well. Closed boxes indicate exons III-VII of the mouse *relB* gene. Cleavage sites for relevant restriction endonucleases are indicated. The 3' external probe (SM592) used for Southern blot analysis are indicated by hatched box. The lengths of diagnostic restriction fragments used for Southern blotting are also indicated. **(B)** Southern blot analysis of genomic DNA isolated from double-resistant ES cell clones. After overnight digestion with *BamH*I, a 4.86 kb and a 6.14 kb DNA fragments, which could be recognized by the 3' probe (SM592), were generated from wild-type and homologously recombined alleles, respectively. The homologously recombined ES cell clone, termed as #31, is shown.

3.2.1.5 Cre-mediated recombination in the HR ES cells

In order to obtain ES cell clones containing the floxed alleles, a subsequent transient Cre transfection into the homologously recombined ES cell clones (see **Figure 1.12** and **Figure 3.21**) is necessary to be performed.

Twenty-five µg supercoiled pGK-Cre plasmid was transfected into the homologously recombined ES cell clone (#31) by electroporation. Cells were cultivated for three to four days before being picked. Upon Cre transfection, three individual recombination events among three loxP sites took place (see **Figure 1.12**). The aim of screening was to get the ES cell clones containing the floxed alleles (*relB*$^{flox/+}$ cells), in which recombination events occurred between the loxP sites flanking the *neo* cassette.

The Southern blot screening strategy is described in **Figure 3.26 A**. The recombination events, which happened between the loxP sites flanking the *neo* cassette, resulted in the exclusion of the 1.2 kb *neo* cassette from the HR allele. This event left one loxP site in intron IV of the *relB* gene which generated, together with the isolated loxP site in the intron III, the floxed version of the *relB* gene (type I, see **Figure 1.12**). The SM592 probe recognized a 4.86 kb *BamH*I DNA fragment, indicative of the floxed allele (**Figure 3.26 B)**. ES clones containing the floxed allele were further confirmed in Southern blots of *Hpa*I/*Hind*III-digested DNA hybridized with SM592. A 9.7 kb band indicated the floxed allele (data not shown). The wild-type alleles also gave rise to a 4.86 kb *BamH*I DNA fragment as shown in **Figure 3.26 B**. The Cre transient transfection was performed in HR cells. It was unlikely that the 4.86 kb *BamH*I DNA fragment came from wild-type ES cells. Nevertheless, to make sure that this fragment was contributed by the floxed allele (*relB*$^{flox/+}$ cells) rather than by the contamination of wild-type cells, a PCR-based screening strategy was generated as well. The PCR reaction amplified sequences spanning the isolated loxP site in intron III of the *relB* gene (see **2.1.4.2**), generating one 200 bp band from wild-type cells, but an additional 243 bp band from HR and *relB*$^{flox/+}$ cells (**Figure 3.26 B**).

Cells containing the deleted alleles, in which the recombination events happened between the outer loxP sites leading to the mutation of the *relB* gene, produced a 9.7 kb band by *BamH*I/*Hind*III digestion in Southern blotting (**Figure 3.26 A)**.

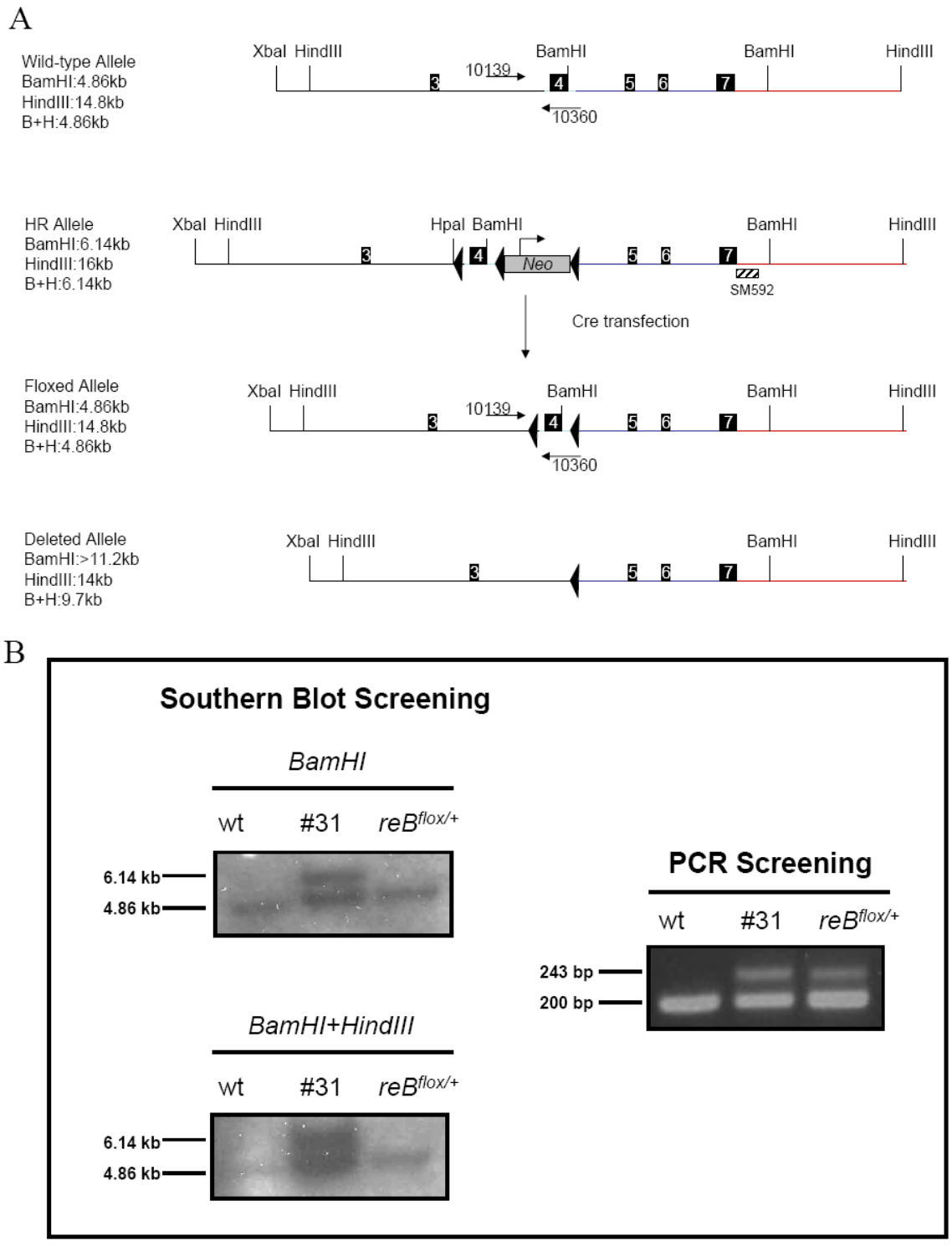

Figure 3.26: Transient Cre transfection into HR ES cell clones. (A) Schematic diagrams (from top to bottom) of the wild-type *relB* gene locus, the homologous recombination allele, the floxed allele, and the deleted allele. PCR amplification is indicated with arrows in diagrams of the wild-type and floxed allele. **(B)** The Southern blotting and the PCR results, the first lanes indicate the wild-type clone, the middle lane the homologously recombined clone, and the right lanes the floxed clone.

3.2.1.6 Blastocyst injections and breeding of chimeras

E14.1 ES cell clones, which were identified to carry the *relB*$^{flox/+}$ allele, were cultured and injected into blastocysts subsequently (see **Figure 3.12**) by Ms. Yvonne Peterson (ITG/FZK, Karlsruhe). The blastocysts (C57BL/6J; black coat color) and E14.1 ES cell line (129/Ola; agouti coat color) were from different mouse lines. Chimeric animals with a different coat color were expected to be generated upon the integration of embryonic stem cells. The degree of chimerism indicates how many ES cells contribute to the transgenic animals and can be estimated by the coat color. More than 20 chimeras with different degree of chimerism were generated; unfortunately, none of them transmitted to germline.

3.2.2 Generation of *cre*-transgenic mice that specifically express Cre in LTβR-positive cells

To establish mouse models in which the activation of RelB or RelA complexes by LTβR can be selectively blocked, transgenic mouse lines that express the Cre recombinase under the control of LTβR regulatory elements need to be generated (see **Figure 3.20**).

Cre transgenic mice can be generated either by pronucleus injection of randomly integrating transgene constructs or by targeted introduction of the *cre* recombinase gene. The former method is more convenient. However, the promoter region for transgenic expression must be available. Moreover, in order to identify a decent mouse strain, it is necessary to generate different founder lines. The number of these founder lines is unpredictable since the level and the pattern of transgene expression vary greatly, mainly depending on copy number and integration site. The gene targeting-based *cre* "knock-in" approach, which drives Cre expression by the endogenous gene regulation, is much more reliable but, certainly, more complicated and troublesome. In addition, the disadvantage of the gene-targeting *cre* knock-in is that they create a mutation in the endogenous gene, which may affect further applications.

3.2.2.1 Generation of *ltbr-cre* transgenic mice

The promoter of the mouse *ltbr* gene is defined. About one kb 5' flanking region of the mouse *ltbr* gene has been functionally analyzed. The -938 bp to -1 bp *ltbr* promoter construct shows a 35-fold higher luciferase activity in NIH 3T3 cells and a 15-fold higher activity in RAW 264.7 cells compared to control plasmids, confirming the functional promoter activity in both cell lines. The transcriptional start site of the mouse *ltbr* gene is located at -60 bp [128].

A 1.25 kb genomic DNA fragment, spanning from –938 bp to 5'-end of exon II (+318 bp) of the mouse *ltbr* gene, was amplified by PCR and subcloned into plasmid pBluescript SK(+). The first ATG codon of the *ltbr* gene was mutated by the site-directed mutagenesis method (Stratagene) in order to ensure sufficient transcription from the first ATG of *cre*. The 1.25 kb PCR products and the point mutation were confirmed by sequencing. Plasmid pGKcre^{NLS}bpA was used to isolate the *cre*-coding sequences including the nuclear localization (NLS) and the polyadenylation signal (bpA). The 1.2 kb *cre* cDNA fragment was then cloned into 3' of the *ltbr* promoter region (**Figure 3.27 B**). The 2.45 kb *Not*I fragment was isolated from the transgene construct with *Not*I digestion and eletroeluted from agarose gel for pronucleus injection.

Among 21 mice borne, 4 mice were found containing the *ltbr-cre* transgene by PCR genotyping (**Figure 3.27 C**). These four founder lines were further confirmed by Southern blot analysis of *Not*I-digested tail DNA using a 1.2 kb probe, hybridizing with the *cre*-coding sequences (**Figure 3.27 D**).

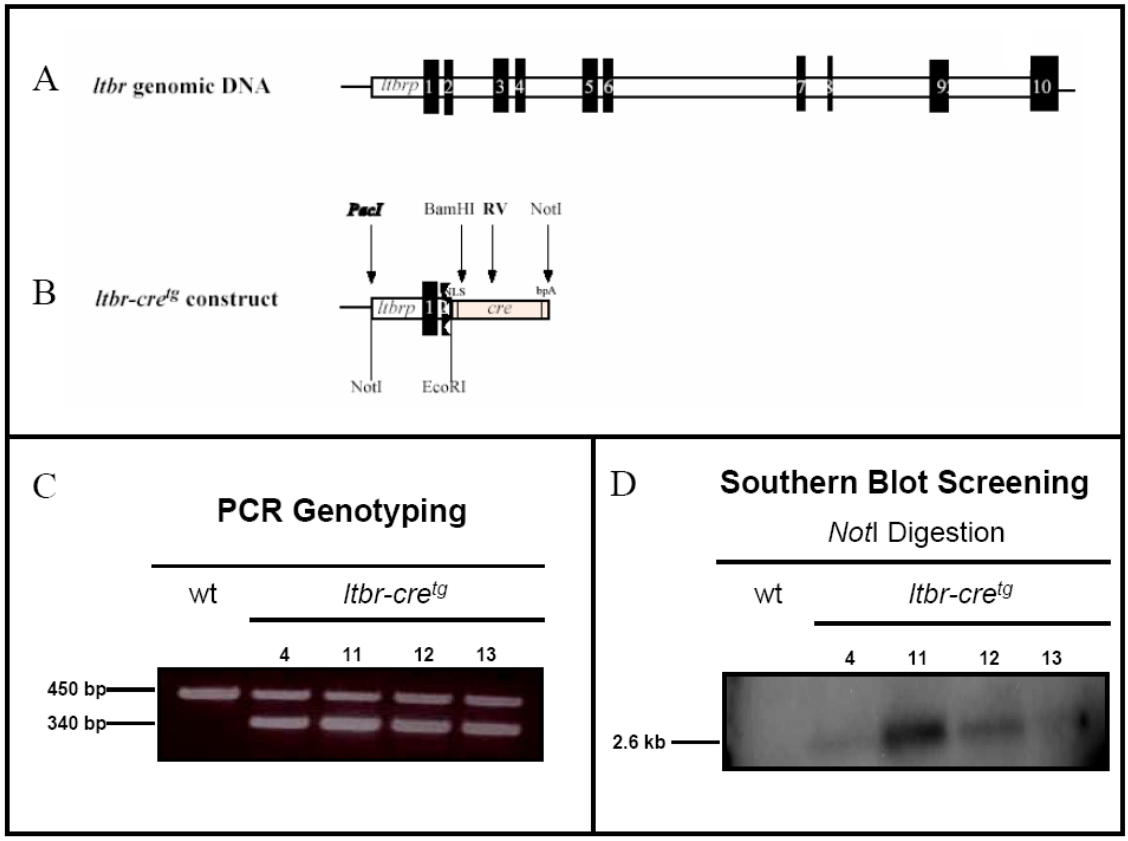

Figure 3.27: Generation of *ltbr-cre* transgenic mouse. (A) The mouse *ltbr* gene contains 10 exons spanning 6.9 kb and maps to mouse chromosome 6. Open boxes indicate *ltbr* genomic sequences. Closed boxes indicate exons I-X of the mouse *ltbr* gene. **(B)** The *ltbr-cre* transgene construct. The *cre*-coding sequences were coupled to the *ltbr* promoter region extending to 5'-end of exon II. The *ltbr* promoter drove *cre* transcription in LTβR-expressing cells in theory. Digestion sites for relevant restriction enzymes are indicated. **(C)** PCR analysis of tail DNA. In *ltbr-cre* transgenic mice, a 340 bp band was detected along with a 450 bp wild-type band. The details for PCR genotyping are described in **2.1.4.3**. **(D)** Southern blot analysis. Tail DNA from transgenic (line 4, 11, 12, and 13) and wild-type mice was digested overnight with *Not*I and hybridized with a 1.2 kb cre probe**.**

3.2.2.2 Characterization of *ltbr-cre* transgenic mouse lines

For identification of a *cre*-transgenic strain suitable for further experiments, it is necessary to produce a series of transgenic mice with the same construct and to compare the efficiency and specificity of the Cre-mediated recombination among these founders. To address the efficiency of the *ltbr* regulatory elements, which are supposed to drive the expression of Cre recombinase specifically in LTβR-expressing cells, the mRNA levels of *cre* and endogenous *ltbr* in various tissues from different transgenic founder lines were analyzed.

ltbr mRNA is detectable in developing sinus, sub maxillary gland, thymus, lung, stomach, gut, and muscle in an E16.5 mouse embryo. In the developing thymus, *ltbr* mRNA are detected in both cortical and medullar thymic regions. *ltbr* mRNA is expressed ubiquitously in adult mice and a high level of *ltbr* expression is found in liver, lung, and kidney by Northern blotting [129-131].

Similarly, a universal tissue distribution of *ltbr* mRNA was detected in wild-type and *ltbr-cre* transgenic mice by real-time PCR (data not shown and **Figure 3.28**). The highest *ltbr* expression was found in livers. The *ltbr* expression in lung and kidney is also higher than that in other tissues.

The *cre* expression pattern in the offspring from each transgenic line was analyzed by real-time PCR. *cre* mRNA was detected in several tissues as well, including thymus (TH), spleen (SP), mesenteric lymph node (LN), liver (LI), lung (LU), kidney (KI), skin (SK), stomach (ST), and intestine (IN, without PPs). In founder line 13, 12, and 11, the tissue expression pattern of *cre* mRNA was consistent with that of endogenous *ltbr* mRNA (**Figure 3.28**).

These observations suggest that the *ltbr* regulatory elements in certain *ltbr-cre* transgenic lines were functionally active and able to drive appropriate Cre expression specifically in LTβR-expressing cells. In addition, a similar expression level of *cre* mRNA, especially in

lymphoid organs such as thymus, spleen, and lymph node was observed in *ltbr-cre* transgenic line 12 and 13.

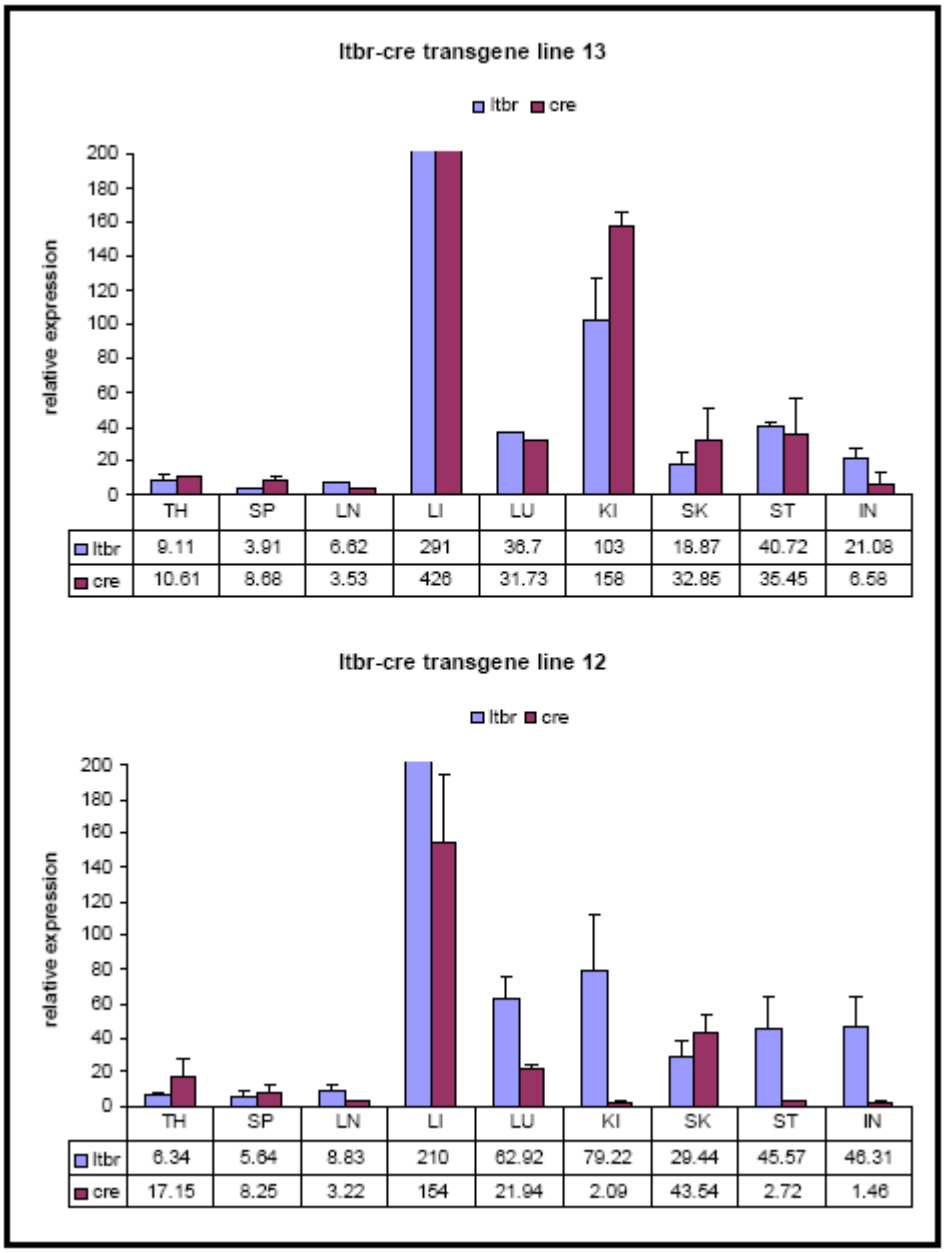

Figure 3.28: Tissue distribution of *cre* and endogenous *ltbr* mRNA in *ltbr-cre* transgenic lines by real-time RT-PCR. Numbers in tables below the bar charts indicate the relative mRNA expression levels in individual tissues. Data represent at least two offspring from each transgenic line. Line 13 and 12 were chosen to breed with reporter (R26R) mice.

The accurate assessment of a tissue-specific *cre* transgenic mouse is highly dependent on the availability of a reliable reporter mouse line. The R26R mouse line, in which the ROSA26 locus has been targeted with the floxed *neo* cassette and the *lacZ* gene, is widely used for monitoring the Cre expression [132]. Upon breeding the R26R mouse with a Cre-expressing transgenic mouse, Cre-mediated deletion of the floxed *neo* cassette activates the transcription of the *lacZ* gene. The *lacZ* expression can be detected by staining tissues for β-galactosidase (β-Gal) activity. A positive *lacZ* signal is only visible in cells expressing functional Cre protein.

Two founder lines (13 and 12), in which the *cre* mRNA expression largely reflected that of the endogenous *ltbr* expression, were selected to breed with a reporter mouse line (R26R) for further characterization. Breeding *ltbr-cre*^{tg} mice with R26R mice result in a restricted lacZ expression pattern, which can then be detected histo-chemically upon Xgal staining. Thus, the expression pattern of lacZ indicates the *ltbr* promoter activity and further reflects the *ltbr* expression pattern. A wide range of tissues from individual *ltbr-cre*^{tg}/R26R transgenic line was collected for this analysis.

3.2.2.3 Generation of *ltbr-cre* knock-in mice

As an alternative method to the conventional transgenic approach by pronucleus injection, Cre expression can be brought under the control of an endogenous promoter by homologous recombination in ES cells. Using this strategy, Cre expression becomes optimally regulated since all control elements of the targeted gene are present at their natural chromosomal position. Therefore, inappropriate transgene expression, which is often encountered with the conventional strategy especially when the promoter is not well characterized, can be avoided.

The *ltbr-cre* knock-in targeting vector pTVFlox-LTβR-Cre was constructed based on the plasmid pTVFlox-0. A 6.5 kb long arm was amplified from plasmid pLTβR by PCR using eLONGase enzyme mix and subsequently inserted into 3' of the floxed *neo* cassette in pTVFlox-0 plasmid. A 1.25 kb fragment (short arm), spanning from –938 bp to the 5'-

end of exon II (+318 bp) of the mouse *ltbr* gene, was amplified from plasmid pLTβR as well. The first ATG codon was mutated as described before. The 1.25 kb PCR products were confirmed by sequencing. The 1.2 kb *cre* coding region, including the NLS and a bpA, was isolated from plasmid pGKcre^{NLS}bpA (see **Figure 3.27**). Then, the 2.6 kb *Not*I fragment was inserted into 5' end of the floxed *neo* cassette. The *tk* gene was located at the end of long arm of the targeting vector (**Figure 3.29**).

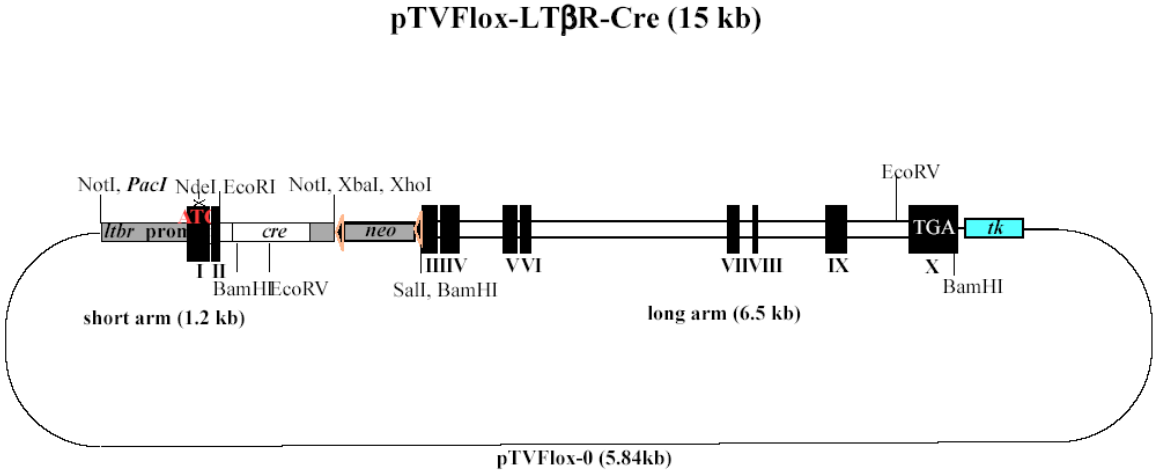

Figure 3.29: Schematic diagram of the *ltbr-cre* knock-in targeting vector pTVFlox-LTβR-Cre. The first ATG of the mouse *ltbr* gene was mutated so that the translation initiation codon of *cre* can be used. The *neo* gene flanked by the loxP sites was inserted downstream of *cre* coding sequences. The *tk* gene was located at the end of the 6.5 kb long arm. Open boxes represent *ltbr* genomic sequences. Arrows represent the loxP sites and indicate the orientation of the loxP sites as well. Closed boxes represent exons I-X of the mouse *ltbr* gene. Cleavage sites for relevant restriction endonucleases are indicated. *Pac*I can be used for linearization of the targeting vector before electroporation. The floxed *neo* gene will be deleted from the targeted locus upon the transient expression of Cre recombinase (see **Figure 3.30 A**).

The Southern blot strategies for screening the homologously recombined allele and the deleted allele upon transient Cre transfection in HR ES cells are described in detail in **Figure 3.30 A**. Procedures for cloning the 550 bp 5' external probe (RX550) are illustrated in **Figure 3.30 B**.

Due to the absence of germline transmission with pTVFlox-LRelBXS11.2 construct, the transfection of the *ltbr-cre* knock-in targeting vector pTVFlox-LTβR-Cre was postponed until promising ES cells are available.

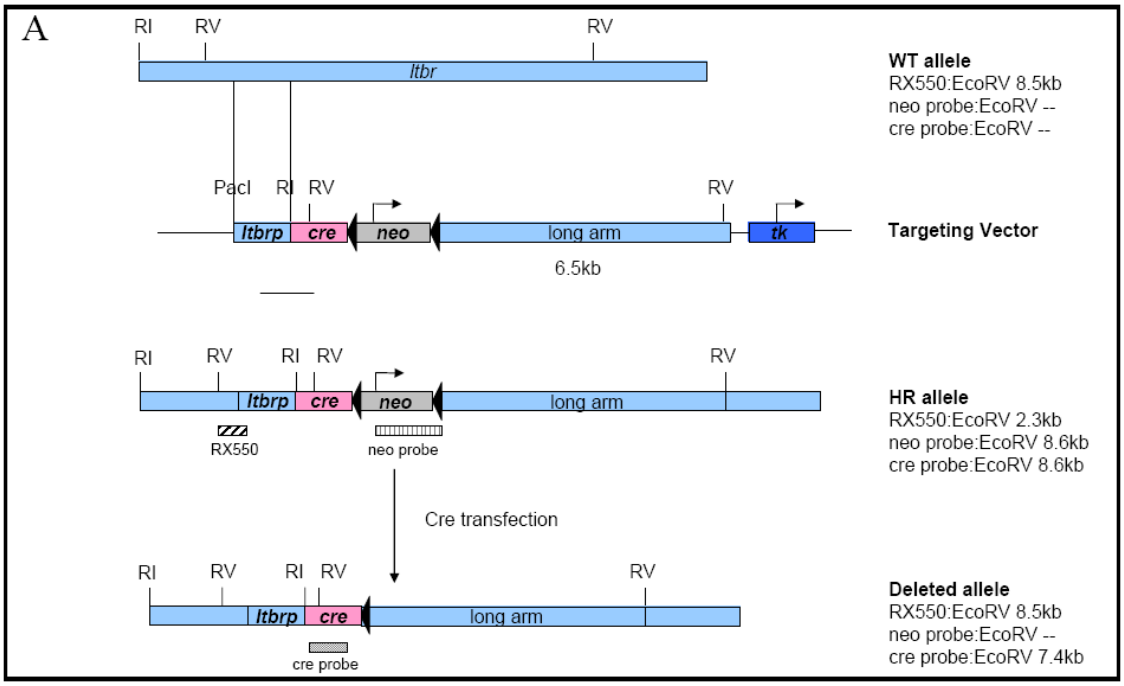

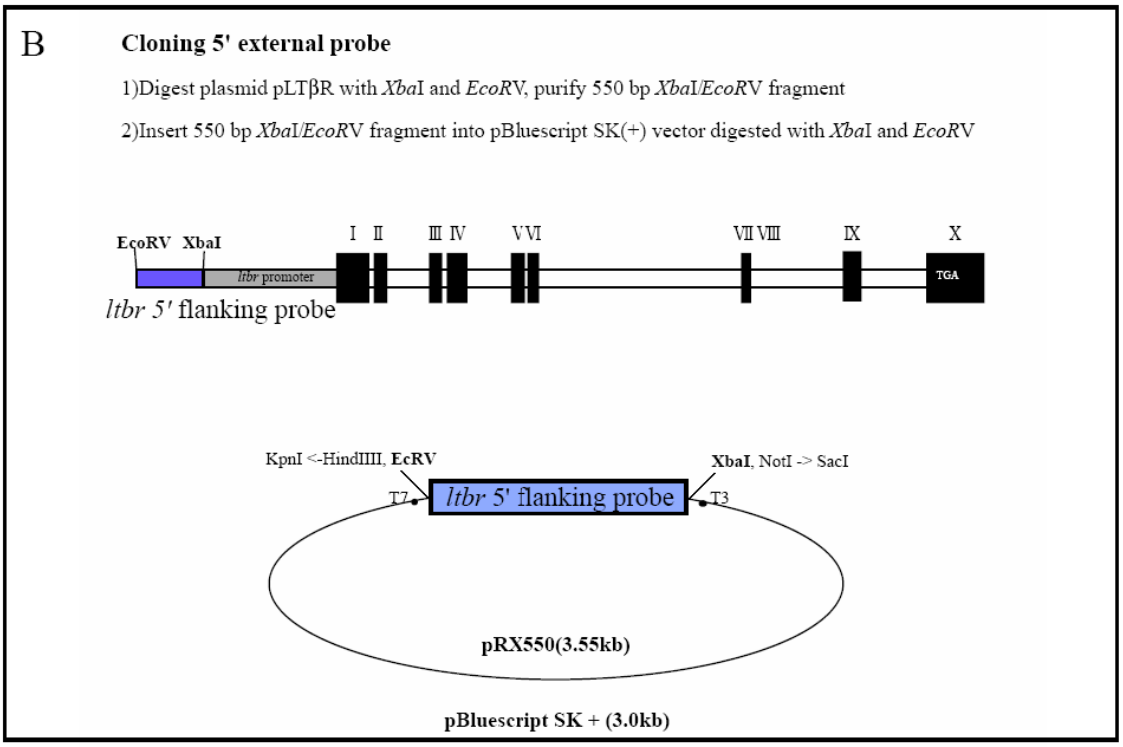

Figure 3.30: (A) Southern blot screening strategy for the targeting vector pTVFlox-LTβR-Cre. Schematic diagrams (from top to bottom) of the wild-type *ltbr* gene locus, the targeting vector, HR allele, and the deleted allele upon Cre transfection. The 5' external probe, Neo probe, and Cre probe for Southern blot hybridization are indicated by hatched boxes. *Eco*RV (RV) and *Eco*RI (RI) were used for digestion in Southern blot analysis. **(B) Cloning of the 5' external probe (RX550).**

4 Discussion

4.1 Role of Rel/NF-κB transcription factors in B lymphopoiesis

Rel/NF-κB transcription factors play a central role in the immune system. Members of this family are involved in many aspects of B-cell maturation and function. A patterned expression of Rel/NF-κB proteins in the process of B-cell differentiation was found from the analysis in individual B-cell lines and murine splenic B cells: mainly p50 and RelA (p65) in pre-B cells, a predominance of c-Rel and p50 in mature B cells, and expression of p52 and RelB in terminally differentiated cells [103]. This ordered pattern suggests the requirements for distinct Rel/NF-κB family members in different stage of B-cell maturation.

The role of NF-κB signaling pathway in B-cell development and function has been studied for nearly two decades. Mice lacking individual Rel/NF-κB family members manifest phenotypes restrictive to mature B-cell activation. Almost no clear abnormalities in the process of B-cell differentiation have been observed (see **Table 1-3**) likely due to functional redundancy among these transcription factors. Nevertheless, subtle perturbations in the generation of particular B-cell subsets are found. For example, *nfkb1*$^{-/-}$ mice have no MZ B cells and peritoneal B1 cells [98].

nfkb2$^{-/-}$ mice have a dramatic reduction in the absolute number of B cells in periphery such as spleen and lymph nodes. The number of *nfkb2*$^{-/-}$ B cells in bone marrow reduces ~50% between 8 and 12-week of age. Proliferation of *nfkb2*$^{-/-}$ B cells is moderately reduced in response to LPS, anti-IgD-dextran, and CD40. *nfkb2*$^{-/-}$ B cells display normal cell maturation to immunoglobulin secretion and class switching *in vitro* [22, 23]. The

MZ formation in *nfkb2*$^{-/-}$ mice is impaired. MZ B cells were partially reduced (data not shown).

relB, encoding one of Rel/NF-κB family members, has originally been identified as an immediate early gene. RelB is expressed in later stages of B-cell maturation and can bind to regulatory sites within the Ig heavy chain locus. *relB*$^{-/-}$ mice display a complex phenotype, including multifocal defects in immune responses, impaired natural killer T (NKT) cells [133] as well as myeloid dendritic cells (DC) differentiation, and defective secondary lymphoid organogenesis. RelB, like c-Rel, p50, and p52, plays a role in B-cell proliferation. B cells lacking RelB show a reduction in DNA synthesis in response to LPS, CD40, and membrane Ig-dependent activation. *relB*$^{-/-}$ B cells are normal in their ability to undergo maturation to IgM secretion and switch to the expression of IgG3, IgG1, IgG2b, IgG2a, IgE, and/or IgA [134]. In addition, RelB, similar to p50, is required for MZ B-cell development in a cell-autonomous manner [107].

Taken together, NF-κB2 (p100 and p52) and RelB is indeed involved in the activation of mature B cells and the development of certain B-cell subsets. However, the involvement of NF-κB2 and RelB in mainstream B-cell development, especially at early stage has not been well studied.

4.1.1 The involvement of alternative NF-κB activation pathway in mainstream B-cell development

The alternative NF-κB pathway activates p52/RelB heterodimers. Upon given signals such as BAFF in mature B cells [110], the C-terminal domain of the precursor p100 is proteolytically processed and degraded in a NIK-IKKα dependent manner (**Figure 1.2**). Consequently, p52/RelB heterodimers translocate to nucleus and bind to κB motifs in their target genes. Therefore, NF-κB2/p100 functions as a specific and potent inhibitor of RelB. Mice lacking p100 (still generating p52, see **Figure 1.3**), thus, provide a good system for investigating intensively the function of alternative NF-κB pathway (NF-κB2/p100 and RelB) with a special focus on mainstream B-cell development.

Strikingly, B-cell development was found being arrested almost completely at an early pro-B stage (Fr. A/B) in mice deficient of p100 (see **Figure 3.2)**. The reduced frequency of $B220^{+}CD19^{+}$ cells in *p100*$^{-/-}$ mice was unlikely owing to increased apoptosis since the percentage of Annexin-V positive cells among this population was similar to that in wild-type mice (data not shown). The impaired B-cell differentiation in bone marrow resulted in a reduction of peripheral B lymphocytes. Moreover, p100 was required in a cell-intrinsic manner within B-lineage precursors for appropriate B-cell development as indicated by competitive bone marrow transplantation experiments (see **Figure 3.3** and **3.4**).

RelB heterodimers bound constitutively to κB motifs in various lymphoid tissues when p100, the inhibitor of RelB was deleted (see **Figure 3.5**). Interestingly, the elevated RelB DNA-binding activity in *p100*$^{-/-}$ mice was recovered to wild-type levels when one allele of the *relB* gene was inactivated in these mice (*p100*$^{-/-}$*relB*$^{-/-}$ mice), correlated with the rescued B-cell development (see **Figure 3.6** and **3.8**). The study here, as first time, pinpoints that the strength of RelB DNA-binding activity functions crucially in B lymphopoiesis. High levels of RelB activity (*p100*$^{-/-}$) blocks B-cell development at an early stage; normal (medium) levels of RelB activity (*p100*$^{-/-}$*relB*$^{-/+}$) favor this process; absence of RelB activity (*p100*$^{-/-}$*relB*$^{-/-}$ and *relB*$^{-/-}$) affects B-cell activation and survival rather than mainstream B-cell development. Thus, the tightly regulated p100 processing in alternative NF-κB activation pathway in B-lineage precursors is an important event in B-cell development.

The involvement of the alternative NF-κB activation pathway in B-cell development is not well defined. This pathway does take place in peripheral B cells upon triggering of certain receptors such as BAFF-R and CD40. The p100 processing triggered by BAFF-R is initiated at the T1 stage, with the highest levels of p52 in T2 and mature B cells (see **Figure 1.9**) [110]. BAFF-deficient mice have a nearly complete block in B-cell differentiation at the T1 to T2 transitional stage in spleen, with subsequent loss of T2, FO, and MZ B cells [135, 136]. The T2 and MZ B-cell compartments are particularly enlarged in *BAFF*^{tg} mice, which are prone to autoimmune diseases [137, 138]. In *nfκb1*$^{-/-}$

nfκb2$^{-/-}$ double knockout mice, B-cell development is also blocked at the T1 stage in spleen due to the failure of receiving BAFF signaling (**Figure 4.1** and see **Figure 1.9**) [31].

The CD40-TRAF2 signaling evidences the involvement of the alternative NF-κB activation pathway in the generation of mature B cells as well [139]. TRAFs (TNFR-associated factors) belong to a family of adaptor proteins that transmits many signals delivered by TNFR. TRAF2 is essential for the CD40-mediated activation of the classical NF-κB pathway in primary B cells [140-143]. Recently, it is shown that TRAF2 actually functions as a multifunctional regulator of NF-κB activation. It mediates activation of the classical NF-κB pathway, but also acts as a negative regulator of the alternative NF-κB pathway. The constitutive p100 processing and increased p52/RelB DNA-binding activity are displayed in TRAF2-deficient B cells. B cells lacking TRAF2 possess a selective survival advantage, resulting in an accumulation preferentially in lymph nodes and marginal zone [142, 144]. This phenotype mirrors the observations in mice that overexpress BAFF.

Thus, constitutively activated alternative NF-κB pathway upon given signals, which results in increased p52/RelB DNA-binding activity, functions importantly in the generation of peripheral mature B cells. From the observations of this study, the importance of the alternative NF-κB activation pathway in the generation of bone marrow B-cell precursors is demonstrated *in vivo* (**Figure 4.1**).

On the other hand, the involvement of the classical NF-κB activation pathway in B-cell development has been suggested by distinct phenotypes in mice lacking different combination of NF-κB proteins. This pathway mainly activates p50/RelA heterodimers via IKK-mediated IκBα phosphorylation and subsequent ubiquitination and degradation. In chimeras engrafted with RelA-deficient fetal liver cells, a massive decrease of fetal liver-derived B220^{+} B-cell precursors in bone marrow and a moderate decrease of peripheral B lymphocytes are observed [145]. The almost absence of B220^{+} B-cell precursors in chimeras engrafted with *nfkb1*$^{-/-}$*relA*$^{-/-}$ fetal liver indicates that p50 and

RelA, not in a cell-autonomous manner, regulates the emergence of $B220^+$ B-lineage precursors (Fr. A1, **Figure 1.9**) [105]. RelA/c-Rel heterodimers, which is also activated in NF-κB classical pathway, do not affect the generation of B-lineage progenitors; rather, RelA and c-Rel serve redundant functions in regulating survival and differentiation of B lymphocytes at the transition from T2 to mature B cells in spleen [33].

Collectively, our knowledge about the function of alternative NF-κB activation signaling pathway in B cells is primarily restrict to the peripheral mature B cells. The observations in this study broaden our understanding of the function of alternative NF-κB pathway (NF-κB/p100 and RelB) in the context of early B-lymphocyte development. Moreover, individual NF-κB complexes do serve distinct roles at different checkpoints during B-cell maturation. While p50/RelA complexes (classical pathway) are known predominantly involving in the generation of $B220^+$ B-lineage progenitors (Fr. A1), p52/RelB complexes (alternative pathway), for the first time, are found playing an important role in the generation of $B220^+$ $CD19^+$ B cells (Fr. B) in bone marrow (**Figure 4.1**).

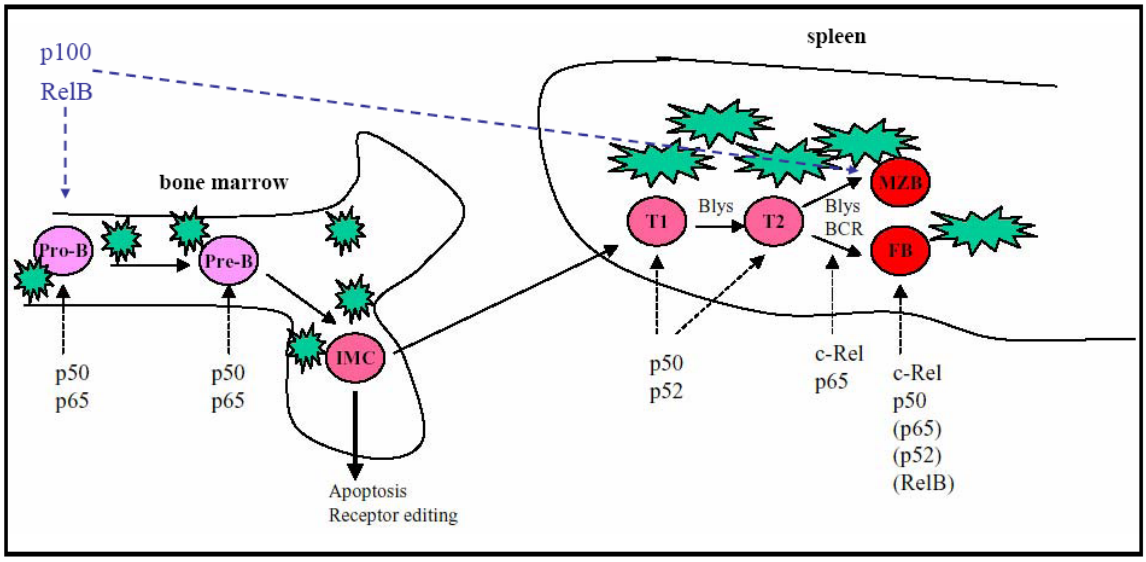

Figure 4.1: Model for the roles of Rel/NF-κB members in B-cell development. Individual Rel/NF-κB complexes do serve distinct roles at different checkpoints during B-cell maturation. The stages of B-cell development, in which the alternative Rel/NF-κB activation pathway (p100 and RelB) functions, are indicated by dashed lines in blue.

4.1.2 Enhanced RelB DNA-binding activity represses the expression of certain B-lineage commitment genes

The development and selection of B lymphocytes are complex processes that are initiated in embryo and proceed throughout life to provide organism an essential part of the immune system. A large number of different transcription factors have been linked to distinct stages in the life of B lymphocytes, such as differentiation in bone marrow, migration to peripheral organs, and antigen-induced activation.

Three transcription factors have been identified playing crucial roles at the onset of B-cell development by gene targeting: EBF, E2A, and Pax5. E2A and EBF act upstream of Pax5 in the genetic hierarchy of B-cell development and are equally expressed in *Pax5*$^{-/-}$ and wild-type pro-B cells. Mutation of Pax5 is considered to dissociate the initial activation of B-lineage-specific gene expression by E2A and EBF from the Pax5-dependent control of B-lineage commitment [56]. Inactivation of any of these three genes leads to a block in B lymphopoiesis before complete rearrangement of the immunoglobulin heavy chain gene (see **Figure 3.10**).

The findings in this study indicate that B-cell development is arrested at early pro-B stage (Fr. B) in the absence of p100 owing to the increased RelB activity. Interestingly, a downregulated expression of *EBF* and *Pax5* and an intact expression of *E2A* mRNA in *p100*$^{-/-}$ pro-B cells were found (see **Figure 3.10**). This disturbed expression pattern of B-lineage transcription factors was restored when one allele of the *relB* gene in *p100*$^{-/-}$ mice was deleted (*p100*$^{-/-}$*relB*$^{-/+}$), correlated with the rescued B-cell development in these mice. Taken together, p100 does regulate the transcription of *Pax5* and *EBF*, but not *E2A*. The impaired B-cell development in *p100*$^{-/-}$ mice is likely due to the reduced expression of B-lineage transcription factors EBF and Pax5, which is caused by the constitutively increased RelB activity. Thus, RelB behaves as a physiological repressor of Pax5 and EBF (**Figure 4.2**).

Low expression of EBF could functionally cooperate with the intact E2A, enabling B-lineage precursors differentiate through pre-pro-B stage. However, most of these pre-pro-B precursors fail to express CD19 and progress to the late stage since Pax5 activity is extremely low. CD19 expression is known to be an indicator of Pax5 activity [126, 146]. This may explain why the B-cell developmental defect observed in *p100*$^{-/-}$ mice is similar to that in *Pax5*$^{-/-}$ mice but not to that in *EBF*$^{-/-}$ or *E2A*$^{-/-}$ mice. The molecular mechanism by which RelB represses the expression of Pax5 and EBF is currently unknown and requires future investigation. A κB binding site was found in the EBF promoter region but not yet in the Pax5 promoter (date not show).

Interestingly, an arrested B lymphopoiesis, which is exactly same as *p100*$^{-/-}$ mice, has been observed in *il-7*$^{-/-}$ and *il-7rα*$^{-/-}$ mice [147, 148]. IL-7R is initially expressed on CLP but not on CMP or multipotent stem cells [149]. Signaling through IL-7R is necessary for both B- and T-lineage development [150]. Strikingly, it is shown that the ectopic expression of IL-7R in hematopoietic progenitors causes a severe block in B-cell differentiation at the early pro-B stage [151]. These developmentally arrested IL-7R^{+}B220^{+}CD19^{-} cells fail to express EBF and Pax5, suggesting that the transient downregulation of IL-7R expression in the process of B-cell differentiation is necessary for the induction of EBF and Pax5 expression and for the B-cell commitment. Very recent report show that *il-7*$^{-/-}$ CLPs express lower EBF and Pax5 than wild-type CLPs. Overexpression of EBF in *il-7*$^{-/-}$ cells is sufficient to restore the B-cell potential, indicating that IL-7 directs commitment of CLPs by regulating EBF expression [152].

The similarities between *p100*$^{-/-}$ and *il-7*$^{-/-}$ as well as *il-7rα*$^{-/-}$ mice in terms of B-cell development, together with the reduced expression of EBF and Pax5 in *p100*$^{-/-}$ mice suggests a correlation between p100 and IL-7 signaling. IL-7R was expressed in B220^{+}CD43^{+}CD19^{-} *p100*$^{-/-}$ pro-B cells. Moreover, transcription of both *IL-7* and *IL-7Rα* was intact (data not shown). Whether that p100 processing, leading to the constitutive p52/RelB nuclear translocation, is a downstream event of IL-7R signaling in B-cell precursors is currently unknown. Preliminary data suggested that IL-7 could induce p100 production and p100 processing in primary wild-type pro-B cells (data not shown).

Nevertheless, the above observations were not found in established B-cell lines, for example, BaF3 (pro-B-cell line) and 70Z/3 as well as WEHI 231 (pre-B-cell lines). Further studies are required to address that whether IL-7R signaling regulates p100 processing to p52, which further affects the expression of B-lineage transcription factors in B-cell precursors.

4.1.3 The lymphoid-myeloid potential of *p100*$^{-/-}$ pro-B cells

Classic model of hematopoietic differentiation state that stem cells become gradually restricted in their differentiation potential by a succession of symmetric and asymmetric divisions. Each intermediate progenitor has a distinct gene expression program, which is maintained by specific transcription factors. Once a cell commits to a particular lineage, it can no longer change its fate.

There are numerous reports demonstrate that the committed hematopoietic cells can be induced converting into other lineages [153]. A surprising degree of plasticity is discovered in *Pax5*$^{-/-}$ pro-B cells: on one hand, these cells exhibit characteristics of early pro-B cells (B220^{+}, c-Kit^{low}, CD43^{+}, and CD19^{-}). On the other hand, they have characteristics of pluripotent stem cells. They are able to undergo self-renewal on stromal cells in IL-7 cultures, home to bone marrow after transplantation, and differentiate into other cell types *in vitro* and *in vivo* (see **Figure 1.6**) [126, 154]. More strikingly, recent work shows that enforced expression of C/EBPα or C/EBPβ in differentiated B cells results in their rapid and efficient reprogramming into myeloid cells. C/EBPs induce these processes by inhibiting Pax5, leading to the downregulation of its target CD19, and synergizing with endogenous PU.1, leading to the upregulation of Mac-1 and other myeloid markers [91]. The myeloid specific gene *M-CSFR* is regulated by three transcription factors including C/EBP, PU.1, and AML1. They interact with critical regions of the M-CSFR promoter. AML1 is involved in several common leukemia-related chromosome translocations. A physical interaction between C/EBP and AML1 is revealed by *in vitro* binding analysis [155] .

The similarity between *p100*$^{-/-}$ and *Pax5*$^{-/-}$ mice in terms of early B-cell development raises the possibility that *p100*$^{-/-}$ pro-B cells may also have the lymphoid-myeloid potential similar to *Pax5*$^{-/-}$ pro-B cells (see **Figure 1.6**). This assumption was confirmed by the observation that *p100*$^{-/-}$ pro-B cells could differentiate into Mac-1^{+} cells even in the IL-7 cultures which supports B-lymphocyte proliferation and differentiation. The significantly increased expression of *C/EBPα* in *p100*$^{-/-}$ pro-B cells was a possible reason for the transition potential of *p100*$^{-/-}$ pro-B cells.

In summary, it is likely that elevated RelB activity in B-lineage progenitors due to the lack of p100 inhibitor, on one hand, suppresses the expression of B-lineage transcription factors EBF and Pax5, switching off the B-lineage differentiation program, on the other hand, induces the expression of C/EBPα, switching on the reprogramming machinery of *p100*$^{-/-}$ pro-B cells. Alternatively, the reduced Pax5 expression could be a sequential event in the process of *p100*$^{-/-}$ pro-B cells transdifferentiation to myeloid cells, which is driven by the increased *C/EBPα* activity (**Figure 4.2**). To unravel the molecular mechanism by which RelB represses the expression of Pax5 as well as EBF and induces the expression of C/EBPα in B-cell progenitors will be very interesting and constructive. The severe myeloid hyperplasia observed in *p100*$^{-/-}$ mice (see **Figure 3.12**) is then assumed rising from the converting of *p100*$^{-/-}$ pro-B cells to myeloid cells. The potential of *p100*$^{-/-}$ pro-B cells in differentiation to other cell types, for example, osteroclasts, T-lymphocytes will also be studied in the near future.

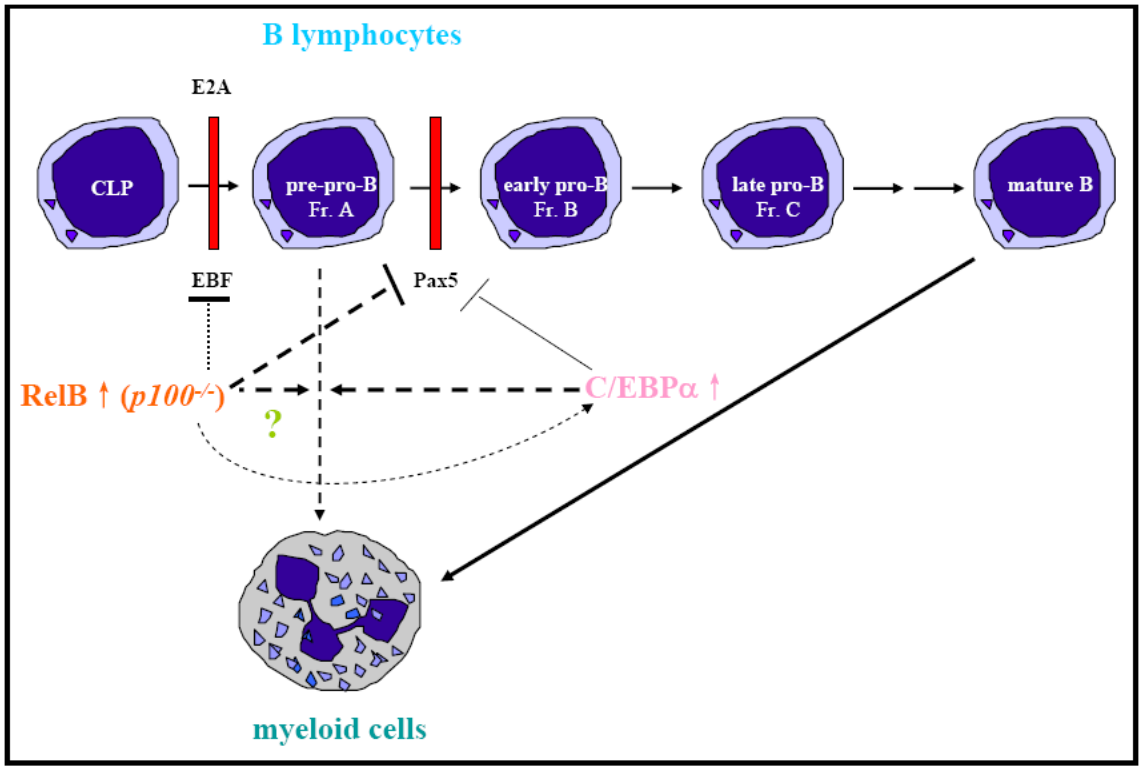

Figure 4.2: Model for B-lineage development and B-lineage versus myeloid-lineage conversion. Vertical bars in red indicate the B-cell development blocks at different stages. Straight arrows and T-shaped bars indicate activation and inhibition, respectively. Dashed lines indicate uncertainty.

4.1.4 Other B-cell subsets affected in *p100*$^{-/-}$ mice

MZ B cells function as a first line of defense, along with B1 B cells, against blood-borne pathogens. This B-cell subset helps to bridge the temporal gap between an innate immune response and a primary, T-cell dependent, adaptive antibody response. The generation and/or retention of MZ B cells is still largely unknown although recent studies using mutant mouse models underscore a direct or indirect involvement of certain signaling pathways (see **Table 1-2**). There are two major driving forces for normal MZ B-cell development [99, 156]. One determinant is the specificity of B-cell receptor (BCR), which allows a developing B cell to choose between FO and MZ B-cell fate. Another important factor is Notch signaling [157, 158]. B cells differentiate into MZ B-cell lineage when they receive additional signals from Notch2.

Weak BCR signaling favors the generation of MZ B cells, whereas strong signal favors that of FO B cells. NF-κB1/p50 is required in a cell-autonomous manner for the generation of MZ B cells. The loss of either RelA or c-Rel leads to a less severe reduction in MZ B-cell numbers. RelB, in terms of p52/RelB heterodimers in stromal cells downstream of LTβR, contributes to MZ microarchitecture formation. RelB is required for MZ B-cell development in a cell-autonomous manner. It is possible, therefore, that p50/RelB heterodimers are required downstream of weak signals delivered by BCR for the normal MZ B-cell development and survival [99].

An accumulation of MZ B-cell subset in a cell-intrinsic manner in *p100*$^{-/-}$ spleen was found in this study; in spite of a reduction in the number of transitional B cells (see **Figure 3.17**). The origin of MZ B cells is not well understood. It is generally believed that T2 B-cell population includes presumed MZ B-cell precursors, which further differentiate into MZ B cells [48, 94, 159]. It is unlikely, however, that the increment of splenic MZ B cells in *p100*$^{-/-}$ mice is differentiated from T2 B cells due to the reduction of T1 and T2 B-cell populations in these animals. The increased RelB function in the form of p50/RelB heterodimers in *p100*$^{-/-}$ B cells may play a role downstream of weak BCR signaling in the generation of MZ B cells. Unlike mainstream B-cell development, the impaired MZ B-cell development was only partially rescued when one allele of the *relB* gene was deleted in *p100*$^{-/-}$ mice. The p50 activity in theses mice may support the generation of MZ B cells.

Mammals have four Notch receptors encoded by four different genes (*Notch1–4*) [160, 161]. In early embryonic development, Notch is crucial for generation of hematopoietic stem cells. During hematopoiesis and immune development, Notch is critical for T/B lineage decision and for generation of splenic MZ B cells. The function of Notch receptor in the T/B-cell lineage decision is Notch1 specific [162, 163]. Notch2 is the predominant Notch receptor in B cells, with widespread expression throughout B-cell development and in peripheral B-cell subsets [158, 164]. Notch2 signaling plays a positive and essential role in the development of MZ B cells and B1 B cells [164-166]. B cell-specific deletion of Notch2 leads to a dramatic loss of MZ B cells. In addition, B cell-specific

deletion of MINT-1, an inhibitor of Notch signaling [167], leads to an increase in MZ B cells [168]. Thus, Notch2 activity determines the fate of MZ B cells. The loss-and-gain RelB activity on the generation of MZ B cells mirrors that of Nothch2. No MZ B cells developed in *p100*$^{-/-}$*relB*$^{-/-}$ and *relB*$^{-/-}$ mice (see **Figure 3.19**). An increased number of MZ B cells were observed in mice lacking the specific inhibitor of RelB, p100 (see **Figure 3.17**). However, the unaffected expression pattern of *Notch2* and *MINT* in *p100*$^{-/-}$ splenic B cells suggests that the increase of MZ B cells in *p100*$^{-/-}$ mice was independent of Notch2 signaling (data not show).

It has been hypothesized that bottlenecks in B-cell development (defective development of mainstream B cells) leads to increased MZ B cells. These observations have been found in *il-7*$^{-/-}$, *il-7rα*$^{-/-}$, and immunoglobulin λ-chain 5 (*λ5*)$^{-/-}$ mice [169, 170], in which the development of mainstream B cells is blocked, along with the enlarged MZ B-cell compartment. In *p100*$^{-/-}$ mice, the similar phenotype, in terms of generating mainstream B cells and MZ B cells, is in line with the 'bottleneck hypothesis".

Taken together, the findings in this study give a better insight into the specific role of alternative NF-κB activation pathway (NF-κB2/p100 and RelB) with respect to B-lymphocyte development. Each NF-κB activation pathway functions distinctively and critically in the development and the activation of B cells. p50/RelA (classical pathway), known from previous studies, is mainly involved in the generation of B220^{+} B-lineage progenitors (Fr. A1). From this study, it is demonstrated that p52/RelB activity (alternative pathway) regulates the emergence of B220^{+} CD19^{+} B cells (Fr. B) in bone marrow and the generation of MZ B cells in spleen (**Figure 4.1**). The elevated RelB activity in B-lineage progenitors due to the lack of p100 inhibitor suppresses the expression of B-lineage transcription factors EBF and Pax5, switching off the B-lineage differentiation program. The increased RelB function determines the fate of B lymphocytes versus myeloid cells likely attribute to the induction of C/EBPα expression (**Figure 4.2**). In conclusion, the tightly regulated p100 processing in alternative NF-κB activation pathway in B-lineage precursors is an important event in B-cell development and B-lymphoid/myeloid-lineage decision.

4.2 Generation of mouse models to investigate the role of Rel/NF-κB signaling pathways in secondary lymphoid organogenesis

The secondary lymphoid organs include spleen, lymph nodes, and organized lymphoid tissues associated with mucosal surfaces such as Peyer's patches. The development of secondary lymphoid organs requires the proper function of certain molecules within a defined timeframe during ontogeny. The activation of NF-κB pathway through LTβR has been demonstrated functioning crucially in this process.

The activation of LTβR in stromal cells by LTα1β2 on hematopoietic cells induces the classical as well as the alternative NF-κB signaling pathway [120]. The activation of p50/RelA heterodimers in the classical pathway depends on IKKβ–IKKγ subunits-mediated degradation of IκBα. In contrast, the activation of p52/RelB heterodimers through the alternative pathway requires NIK-IKKα dependent p100 processing.

The expression of p52 and RelB is restricted to specific regions of lymphoid organs, consistent with the constitutive basal p52/RelB DNA-binding activity in these tissues [171]. RelB-deficient mice display an impaired lymphoid organogenesis including lack of LNs and PPs as well as disorganized spleen microarchitectures [17, 107], suggesting that RelB complex functions importantly in the generation and the maintenance of intact structure of these organs. A similar phenotype is observed in *nfκb2*$^{-/-}$ mice [22, 23] but not in *nfκb1*$^{-/-}$ mice [21]. The role of RelA in secondary lymphoid organogenesis is less understood due to the embryonic lethality of *relA*$^{-/-}$ mice. In *relA*$^{-/-}$*tnfr1*$^{-/-}$ mice, the early lethality is rescued. These mice manifest a defective lymphoid organ development. However, TNFR1 itself contributes to the formation and the maintenance of these organs [172-174], which makes it difficult to discriminate a clear contribution of RelA. Induction of the classical p50/RelA NF-κB activity contributes, but rather involves in later developmental stages, such as proper cellular and structural organization of B-cell follicles. The phenotypes with respect to secondary lymphoid organogenesis in mice

lacking individual Rel/NF-κB family members, upstream kinases, and receptors are illustrated in detail in **Table 1-4**.

LTβR activates both NF-κB signaling pathways in mouse fibroblasts *in vitro*. It is still unclear that which NF-κB activity contributes to which part of secondary lymphoid organogenesis. There is also no direct proof that whether RelB and/or RelA does function downstream of LTβR signaling *in vivo*, regulating the development of secondary lymphoid organs. It is difficult to draw a conclusion that all lymphoid organ developmental defects in mice lack of RelB or RelA are due to the impaired LTβR signaling since other receptors are involved in this process as well. Thus, it would be very interesting to specifically dissect the individual contribution of each NF-κB pathway downstream of LTβR signaling *in vivo*. Towards this goal, one approach is to generate mouse modes in which LTβR-mediated activation of RelB and/or RelA can be selectively inactivated (see **Figure 3.20**). Therefore, *relB*$^{flox/flox}$ and *relA*$^{flox/flox}$ mice need to be generated and further crossed with transgenic mice expressing Cre recombinase under the control of the *ltbr* promoter (*ltbr-cre*^{tg} mice). Since *relB*$^{flox/flox}$ mice and *ltbr-cre*^{tg} mice are currently not available, the focus of this project is to generate these two mouse lines.

4.2.1 Generation *relB*$^{flox/flox}$ mice

A strategy for generating a spatially conditional mutation is to modify the target gene by homologous recombination in ES cells so that it can be flanked by the loxP sites. Mice containing such a modified gene (floxed mice) are then crossed with mice expressing Cre in the desired target tissue, and Cre-mediated excision results in tissue-specific gene ablation (see **Figure 1.11**).

4.2.1.1 Targeting efficiency

To generate *relB*$^{flox/flox}$ mice, two targeting vectors were constructed in this study. No homologous recombination ES cell clone was found after transfection of the targeting vector pRelBXS11.2-LLTNL. This construct constitutes a 4 kb LTNL cassette containing

combined pattern of the *neo* and the *HSVtk* gene. The advantage of this vector is that a negative selection can be performed using ganciclovir to enrich the frequency of floxed ES cell clones after transient Cre transfection into homologously recombined ES clones. However, only positive selection using G418 is able to be performed after transfecting the targeting vector into wild-type ES cells due to the presence of the *HSVtk* gene in the homologously recombined alleles. There are two major factors principally, which can influence the targeting frequency. First, the choice of a vector can significantly affect the targeting frequency. Secondly, the homologous sequences in the vector, specifically the length and the degree of polymorphic variation between the vector and the chromosome. The homologous sequences of the targeting vector were confirmed by sequencing, excluding the possibility of large mutations during PCR amplification. In order to increase the targeting frequency, a second targeting vector was generated based on a 5.84 kb pTVFlox-0 plasmid. This plasmid constitutes the separate selection marker genes the *neo* gene flanked by two loxP sites and the *HSVtk* gene (**Figure 3.24 A**, panel 1)). Using this plasmid as the backbone of the targeting vector allows a positive-negative double selection. The positive selection marker gene, *neo*, is primarily used to enrich for the rare stably transfected ES cell clones, obtain at a frequency of about one in 10^4 cells by electroporation. The enrichment by negative selection is usually in the range of 3–10-fold resulting in 1/10-1/40 of the homologous recombination ES clones as compared to random integrants. The positive ES cell clones, combined homologously with the targeting vector pTVFlox-LRelBXS11.2, were found and followed the transient Cre transfection. The ES cells identified carrying $relB^{flox/+}$ alleles were injected into blastocysts. More than 20 chimeras with different degree of chimerism were generated; unfortunately, none of them transmitted to germline.

4.2.1.2 Germ-line transmission

E14.1 ES cells are derived form 129/Ola mouse strain. E14.1 ES cells (from Prof. Wang Z-Q, Lyon, France) exhibited a good record of germline transmission (100% of chimeric males) in a test breeding, which confirmed the presence of a certain fraction of germline competent cells within the injected ES cells. However, when E14.1 ES cells were

transfected, none of the targeted ES cells contributed to germline. Half ES clones (20 clones injected) gave rise to a satisfactory degree of coat-color chimerism, though. The exact reason for the discrepancy is not clear. Using 129/Ola mouse-derived Knut I ES cell line (from Dr. Hubert Schorle, Bohn) which is established recently, the gene targeting experiment towards generating *relB*$^{flox/flox}$ mice is ongoing.

4.2.2 Generation of *ltbr-cre*^{tg} mice by pronucleus injection

To specifically delete RelB or RelA in LTβR-expressing cells, it is necessary to generate transgenic mice that express the Cre recombinase under the control of LTβR regulatory elements.

Four independent founder lines, in which Cre expression was driven by a 1.25 kb fragment of the mouse LTβR promoter, were generated by pronucleus injection. The tissue distribution of *cre* expression, which was driven by the *ltbr* promoter, was analyzed in offspring from individual founder lines by real-time PCR. Two founder lines, in which the *cre* expression pattern largely reflected the endogenous *ltbr* expression pattern, were further crossed with a reporter mouse line (R26R) for the specific characterization. Crossing R26R mice with *ltbr-cre* transgenic mice allows monitoring the Cre expression pattern by *lacZ* staining. Thus, the expression pattern of lacZ indicated the *ltbr* promoter activity and further reflected the *ltbr* expression pattern. Mice with reliable and faithful tissue specificity will be established as a transgenic line. A wide range of tissues from different *ltbr-cre*^{tg}/R26R transgenic line was collected for future analysis. The generation of *ltbr-cre*^{tg} mice will be very helpful to characterize the LTβR-positive cell types, which are not well defined currently in developing and adult mice.

To avoid position and copy number effects influencing the expression pattern of *ltbr-cre* transgenic mice, alternatively, a knock-in mouse line, in which the LTβR coding region can be replaced by a Cre cDNA via homologous recombination, is to be generated. The corresponding targeting vector pTVFlox-LTβR-Cre was constructed (see **Figure 3.29**) and will be transfected into ES cells in the near future.

Once *relB*$^{flox/flox}$ mice are generated, they will be bred with *ltbr-cre*^{tg} mice to get *relB*$^{ltbr\text{-}cre}$ mice. The phenotypes in *relB*$^{ltbr\text{-}cre}$ and *relA*$^{ltbr\text{-}cre}$ mice will then be compared in terms of secondary lymphoid organogenesis. With this mouse model system, the distinct role of classical (RelA complex) and alternative (RelB complex) NF-κB activation pathway downstream of LTβR signaling in lymphoid organogenesis can be characterized *in vivo*. This will broaden our current understanding of NF-κB function in secondary lymphoid organ development. The *relB*$^{flox/flox}$ mice can also be crossed with individual Cre transgenic mice controlled by different promoters, for example, CD19-Cre, lck-Cre, LysM-Cre [175], K5/K14-Cre, Colalpha1(I)-Cre or OG2-Cre [176], CD11b-Cre [177], and Ctsk-Cre mice [178], to dissect the particular function of RelB in B cells, T cells, myeloid cells, keratinocytes, osteoblasts, and osteoclasts without the influence of losing RelB function in other cell types. Analyzing mice with tissue-specific inactivation of RelB will be helpful to understand the severe and complex phenotype of *relB*$^{-/-}$ mice.

4.3 Outlook

The future work is focus on:

1. To unravel the molecular mechanism by which the elevated RelB activity represses the expression of *Pax5* and *EBF*, switching off the B-lineage differentiation program, meanwhile, induces the expression of *C/EBPα* in B-cell progenitors, switching on the reprogramming machinery of *p100*$^{-/-}$ pro-B cells.
2. To investigate that whether p100 processing, leading to the constitutive p52/RelB nuclear translocation, is a downstream event of IL-7R signaling in B-cell precursors.
3. To complete the generation of *relB*$^{flox/flox}$ mice, which will be further crossed with *ltbr-cre*^{tg} mice. The phenotype analysis in *relB*$^{ltbr\text{-}cre}$ and *relA*$^{ltbr\text{-}cre}$ mice will be helpful to understand the distinct role of classical and alternative NF-κB activation pathway downstream of LTβR signaling with respect to lymphoid organogenesis *in vivo.*

5 REFERENCES

1. Sen, R. and D. Baltimore, Inducibility of kappa immunoglobulin enhancer-binding protein Nf-kappa B by a posttranslational mechanism. Cell, 1986. 47(6): p. 921-928.
2. Ghosh, S., M.J. May, and E.B. Kopp, NF-kappa B and Rel proteins: evolutionarily conserved mediators of immune responses. Annu Rev Immunol., 1998. 16: p. 225-260.
3. Greten, F.R. and M. Karin, The IKK/NF-kappaB activation pathway-a target for prevention and treatment of cancer. Cancer Lett., 2004. 206(2): p. 193-199.
4. Dobrzanski, P., R.P. Ryseck, and R. Bravo, Differential interactions of Rel-NF-kappa B complexes with I kappa B alpha determine pools of constitutive and inducible NF-kappa B activity. Embo J, 1994. 13(19): p. 4608-16.
5. Ryseck, R.P., et al., RelB, a new Rel family transcription activator that can interact with p50-NF-kappa B. Mol Cell Biol, 1992. 12(2): p. 674-84.
6. Hayden, M.S. and S. Ghosh, Signaling to NF-kappaB. Genes Dev, 2004. 18(18): p. 2195-2124.
7. Karin, M. and Y. Ben-Neriah, Phosphorylation meets ubiquitination: the control of NF-[kappa]B activity. Annu Rev Immunol, 2000. 18: p. 621-63.
8. Rothwarf, D.M. and M. Karin, The NF-kappa B activation pathway: a paradigm in information transfer from membrane to nucleus. Sci STKE, 1999. 1999(5): p. RE1.
9. Chen, G., P. Cao, and D.V. Goeddel, TNF-induced recruitment and activation of the IKK complex require Cdc37 and Hsp90. Mol Cell., 2002. 9(2): p. 401-410.
10. Senftleben, U., et al., Activation by IKKalpha of a second, evolutionary conserved, NF-kappa B signaling pathway. Science, 2001. 293(5534): p. 1495-1499.
11. Xiao, G., et al., Retroviral oncoprotein Tax induces processing of NF-kappaB2/p100 in T cells: evidence for the involvement of IKKalpha. EMBO J., 2001. 20(23): p. 6805-6815.
12. Dejardin, E., et al., The lymphotoxin-beta receptor induces different patterns of gene expression via two NF-kappaB pathways. Immunity., 2002. 17(4): p. 525-535.
13. Weih, F. and J. Caamano, Regulation of secondary lymphoid organ development by the nuclear factor-kappaB signal transduction pathway. Immunol Rev, 2003. 195: p. 91-105.
14. Senftleben, U., et al., Activation by IKKalpha of a second, evolutionary conserved, NF-kappa B signaling pathway. Science, 2001. 293(5534): p. 1495-9.
15. Yin, L., et al., Defective lymphotoxin-beta receptor-induced NF-kappaB transcriptional activity in NIK-deficient mice. Science, 2001. 291(5511): p. 2162-5.
16. Claudio, E., et al., BAFF-induced NEMO-independent processing of NF-kappa B2 in maturing B cells. Nat Immunol., 2002. 3(10): p. 958-965.
17. Yilmaz, Z.B., et al., RelB is required for Peyer's patch development: differential regulation of p52-RelB by lymphotoxin and TNF. EMBO J., 2003. 22(1): p. 121-130.

18. Coope, H.J., et al., CD40 regulates the processing of NF-kappaB2 p100 to p52. EMBO J., 2002. 21(20): p. 5375-5385.
19. Mordmuller, B., et al., Lymphotoxin and lipopolysaccharide induce NF-kappaB-p52 generation by a co-translational mechanism. EMBO Rep, 2003. 4(1): p. 82-87.
20. Attar, R.M., et al., Genetic approaches to study Rel/NF-kappa B/I kappa B function in mice. Semin Cancer Biol., 1997. 8(2): p. 93-101.
21. Sha, W.C., et al., Targeted disruption of the p50 subunit of NF-kappa B leads to multifocal defects in immune responses. Cell, 1995. 80(2): p. 321-30.
22. Caamano, J.H., et al., Nuclear factor (NF)-kappa B2 (p100/p52) is required for normal splenic microarchitecture and B cell-mediated immune responses. J Exp Med, 1998. 187(2): p. 185-96.
23. Franzoso, G., et al., Mice deficient in nuclear factor (NF)-kappa B/p52 present with defects in humoral responses, germinal center reactions, and splenic microarchitecture. J Exp Med, 1998. 187(2): p. 147-59.
24. Beg, A.A., et al., Embryonic lethality and liver degeneration in mice lacking the RelA component of NF-kappa B. Nature, 1995. 376(6536): p. 167-70.
25. Weih, F., et al., Multiorgan inflammation and hematopoietic abnormalities in mice with a targeted disruption of RelB, a member of the NF-kappa B/Rel family. Cell, 1995. 80(2): p. 331-40.
26. Weih, F., et al., Both multiorgan inflammation and myeloid hyperplasia in RelB-deficient mice are T cell dependent. J Immunol, 1996. 157(9): p. 3974-9.
27. Burkly, L., et al., Expression of relB is required for the development of thymic medulla and dendritic cells. Nature, 1995. 373(6514): p. 531-6.
28. Grumont, R.J., I.J. Rourke, and S. Gerondakis, Rel-dependent induction of A1 transcription is required to protect B cells from antigen receptor ligation-induced apoptosis. Genes Dev, 1999. 13(4): p. 400-11.
29. Grigoriadis, G., et al., The Rel subunit of NF-kappaB-like transcription factors is a positive and negative regulator of macrophage gene expression: distinct roles for Rel in different macrophage populations. Embo J, 1996. 15(24): p. 7099-107.
30. Kontgen, F., et al., Mice lacking the c-rel proto-oncogene exhibit defects in lymphocyte proliferation, humoral immunity, and interleukin-2 expression. Genes Dev, 1995. 9(16): p. 1965-77.
31. Franzoso, G., Requirement for NF-kB in osteoclast and B-cell development. Genes Dev, 1997. 11: p. 3482–3496.
32. Rosenfeld, M.E., et al., Prevention of hepatic apoptosis and embryonic lethality in RelA/TNFR-1 double knockout mice. Am J Pathol, 2000. 156(3): p. 997-1007.
33. Grossmann, M., et al., The combined absence of the transcription factors Rel and RelA leads to multiple hemopoietic cell defects. Proc Natl Acad Sci U S A, 1999. 96(21): p. 11848-53.
34. Horwitz, B.H., M.L. Scott, and S.R. Cherry, Failure of lymphopoiesis after adoptive transfer of NF-kB-deficient fetal liver cells. Immunity, 1997. 6: p. 765–772.
35. Weih, F., et al., p50-NF-kappaB complexes partially compensate for the absence of RelB: severely increased pathology in p50(-/-)relB(-/-) double-knockout mice. J Exp Med, 1997. 185(7): p. 1359-70.
36. Ishikawa, H., et al., Gastric hyperplasia and increased proliferative responses of lymphocytes in mice lacking the COOH-terminal ankyrin domain of NF-kappaB2. J Exp Med, 1997. 186(7): p. 999-1014.
37. Osmond, D.G., B cell development in the bone marrow. Semin Immunol, 1990. 2(3): p. 173-80.
38. Osmond, D.G., Population dynamics of bone marrow B lymphocytes. Immunol Rev, 1986. 93: p. 103-124.

39. Alt, F.W., et al., Activity of multiple light chain genes in murine myeloma cells producing a single, functional light chain. Cell, 1980. 21(1): p. 1-12.
40. Lu, L. and D.G. Osmond, Apoptosis during B lymphopoiesis in mouse bone marrow. J Immunol, 1997. 158: p. 5136-5145.
41. Goodnow, C.C., Transgenic mice and analysis of B-cell tolerance. Annu Rev Immunol, 1992. 12: p. 489-518.
42. Nemazee, D., Clonal deletion of autospecific B lymphocytes. Immunol Rev, 1991. 122: p. 117-132.
43. Gay, D., et al., Receptor editing: an approach by autoreactive B cells to escape tolerance. J Exp Med, 1993. 177: p. 999-1008.
44. Radic, M.Z., et al., B lymphocytes may escape tolerance by revising their antigen receptors. J Exp Med, 1993. 177: p. 1165-1173.
45. Tiegs, S.L., D.M. Russell, and D. Nemazee, Receptor editing in self-reactive bone marrow B cells. J Exp Med, 1993. 177: p. 1009-1020.
46. Loder, F., B cell development in the spleen takes place in discrete steps and is determined by the quality of B cell receptorderived signals. J Exp Med, 1999. 1190: p. 75-89.
47. Martin, F. and J.F. Kearney, B-cell subsets and the mature preimmune repertoire. Marginal zone and B1 B cells as part of a 'natural immune memory'. Immunol Rev, 2000. 175: p. 70-79.
48. Martin, F. and J.F. Kearney, Marginal-zone B cells. Nat Rev Immunol, 2002. 2(5): p. 323-35.
49. Kondo, M., I.L. Weissman, and K. Akashi, Identification of clonogenic common lymphoid progenitors in mouse bone marrow. Cell, 1997. 91: p. 661-672.
50. Hardy, R.R. and K. Hayakawa, A developmental switch in B lymphopoiesis. Proc Natl Acad Sci U S A, 1991. 88(24): p. 11550-4.
51. Hardy, R.R., et al., Resolution and characterization of pro-B and pre-pro-B cell stages in normal mouse bone marrow. J Exp Med, 1991. 173(5): p. 1213-25.
52. Li, Y.S., et al., Identification of the earliest B lineage stage in mouse bone marrow. Immunity, 1996. 5(6): p. 527-35.
53. Carvalho, T.L., et al., Arrested B lymphopoiesis and persistence of activated B cells in adult interleukin 7(-/)- mice. J Exp Med, 2001. 194(8): p. 1141-50.
54. Jung, D. and F.W. Alt, Unraveling V(D)J recombination; insights into gene regulation. Cell, 2004. 116: p. 229-311.
55. Schatz, D.G., M.A. Oettinger, and M.S. Schlissel, V(D)J recombination: molecular biology and regulation. Annual Review of Immunology,, 1992. 10: p. 359-383.
56. Busslinger, M., Transcriptional control of early B cell development. Annu Rev Immunol, 2004. 22: p. 55-79.
57. Klemsz, M., et al., The macrophage and B cell-specific transcription factor PU.1 is related to the ets oncogene. Cell, 1990. 61: p. 113-124.
58. McKercher, S.R., et al., Targeted disruption of the PU.1 gene results in multiple hematopoietic abnormalities. EMBO J, 1996. 15: p. 5647-5658.
59. Scott, E., et al., Requirement of transcription actor PU.1 in the development of multiple hematopoietic lineages. Science, 1994. 265: p. 1573-1577.
60. DeKoter, R.P., J.C. Walsh, and H. Singh, PU.1 regulates both cytokine-dependent proliferation and differentiation of granulocyte/macrophage progenitors. EMBO J, 1998. 17: p. 4456-4468.
61. DeKoter, R.P. and H. Singh, Regulation of B lymphocyte and macrophage development by graded expression of PU.1. Science, 2000. 288: p. 1439-1441.
62. DeKoter, R.P., H.-J. Lee, and H. Singh, PU.1 regulates expression of the interleukin-7 receptor in lymphoid progenitors. Immunity, 2002. 16: p. 297-309.

63. Murre, C., P.S. McCaw, and D. Baltimore, A new DNA binding and dimerization motif in immunoglobulin enhancer binding, daughterless, MyoD and myc proteins. Cell, 1989. 56: p. 777-783.
64. Murre, C., et al., Structure and function of helix-loop-helix proteins. Biochim Biophys Acta, 1994. 1218(129-135).
65. Bain, G., et al., Both E12 and E47 allow commitment to the B cell lineage. Immunity, 1997. 6: p. 145-154.
66. Shen, C.-P. and T. Kadesch, B-cell-Specific DNA binding by an E47 homodimer. Mol Cell Biol, 1995. 15: p. 4518-4524.
67. Bain, G., et al., E2A deficiency leads to abnormalities in alphabeta T-cell development and to rapid development of T-cell lymphomas. Mol Cell Biol, 1997. 17(4782-4791).
68. Zhuang, Y., P. Cheng, and H. Weintraub, B-lymphocyte development is regulated by the combined dosage of three basic helix-loop-helix genes, E2A, E2-2, and HEB. Mol Cell Bio., 1996. 16(6): p. 2898-2905.
69. Bain, G. and C. Murre, The role of E-proteins in B- and T-lymphocyte development. Semin Immunol, 1998. 10: p. 143-153.
70. Hagman, J., et al., Cloning and functional characterization of early B-cell factor, a regulator of lymphocyte-specific gene expression. Genes Dev, 1993. 7: p. 760-773.
71. Travis, A., et al., Purification of early- B-cell factor and characterization of its DNA-binding specificity. Mol Cell Biol, 1993. 13: p. 3392-3400.
72. Wang, S.S., R.Y.L. Tsai, and R.R. Reed, The characterization of the Olf-1/EBF-like HLH transcription factor family: implications in olfactory gene regulation and neuronal development. J Neurosci, 1997. 17: p. 4149-4158.
73. Hagman, J., et al., EBF contains a novel zinc coordination motif and multiple dimerization and transcriptional activation domains. EMBO J, 1995. 15: p. 2907-2916.
74. Lin, H. and R. Grosschedl, Failure of B-cell differentiation in mice lacking the transcription factor EBF. Nature, 1995. 376: p. 263–267.
75. Bain, G., et al., E2A proteins are required for proper B cell development and initiation of immunoglobulin gene rearrangements. Cell, 1994. 79: p. 885-892.
76. O'Riordan, M. and R. Grosschedl, Coordinate regulation of B cell differentiation by the transcription factors EBF and E2A. Immunity, 1999. 11: p. 21-31.
77. Sigvardsson, M., M. O'Riordan, and R. Grosschedl, EBF and E47 collaborate to induce expression of the endogenous immunoglobulin surrogate light chain genes. Immunity, 1997. 7: p. 25-36.
78. Romanow, W.J., et al., E2A and EBF act in synergy with the V(D)J recombinase to generate a diverse immunoglobulin repertoire in nonlymphoid cells. Mol Cel, 2000. 5: p. 343-353.
79. Schebesta, M., B. Heavey, and M. Busslinger, Transcriptional control of B-cell development. Curr Opin Immunol, 2002. 14(2): p. 216-23.
80. Urbanek, P., et al., Complete block of early B cell differentiation and altered patterning of the posterior midbrain in mice lacking Pax-5/BSAP. Cell, 1994. 79: p. 901-913.
81. Nutt, S.L., et al., Essential functions of Pax5 (BSAP) in pro-B cell development: difference between fetal and adult B lymphopoiesis and reduced V-to-DJ recombination at the IgH locus. Genes Dev, 1997. 11: p. 476–91.
82. Nutt, S.L., et al., Identification of BSAP (Pax-5) target genes in early B-cell development by loss- and gain-of-function experiments. EMBO J, 1998. 17: p. 2319-2333.
83. Nutt, S.L., et al., Commitment to the B lymphoid lineage depends on the transcription factor Pax5. Nature, 1999. 401: p. 556–562.

84. Rolink, A.G., et al., Long-term in vivo reconstitution of T-cell development by Pax5-deficient B-cell progenitors. Nature, 1999. 401: p. 603–606.
85. Schaniel, C., et al., Extensive in vivo self-renewal, long-term reconstitution capacity, and hematopoietic multipotency of Pax5 deficient precursor B-cell clones. Blood, 2002. 99: p. 2760–2766.
86. Heavey, B., et al., Myeloid lineage switch of Pax5 mutant but not wild-type B cell progenitors by C/EBPalpha and GATA factors. Embo J, 2003. 22(15): p. 3887-97.
87. Landschulz, W.H., P.F. Johnson, and S.L. McKnight, The DNA binding domain of the rat liver nuclear protein C/EBP is bipartite. Science, 1989. 243(4899): p. 1681-8.
88. Scott, L.M., et al., A novel temporal expression pattern of three C/EBP family members in differentiating myelomonocytic cells. Blood, 1992. 80(7): p. 1725-35.
89. Radomska, H.S., et al., CCAAT/enhancer binding protein alpha is a regulatory switch sufficient for induction of granulocytic development from bipotential myeloid progenitors. Mol Cell Biol, 1998. 18(7): p. 4301-14.
90. Zhang, D.E., et al., Absence of granulocyte colony-stimulating factor signaling and neutrophil development in CCAAT enhancer binding protein alpha-deficient mice. Proc Natl Acad Sci U S A, 1997. 94(2): p. 569-74.
91. Xie, H., et al., Stepwise reprogramming of B cells into macrophages. Cell, 2004. 117(5): p. 663-76.
92. Cooper, C.L., et al., Limited expression of C/EBP family proteins during B lymphocyte development. Negative regulator Ig/EBP predominates early and activator NF-IL-6 is induced later. J Immunol, 1994. 153(11): p. 5049-58.
93. Souabni, A., et al., Pax5 promotes B lymphopoiesis and blocks T cell development by repressing Notch1. Immunity, 2002. 17: p. 781–793.
94. Lopes-Carvalho, T. and J.F. Kearney, Development and selection of marginal zone B cells. Immunol Rev, 2004. 197: p. 192-205.
95. Lu, T.T. and J.G. Cyster, Integrin-mediated long-term B cell retention in the splenic marginal zone. Science, 2002. 297(5580): p. 409-12.
96. Kumararatne, D.S. and I.C. MacLennan, The origin of marginal-zone cells. Adv Exp Med Biol, 1982. 149: p. 83-90.
97. Guinamard, R., et al., Absence of marginal zone B cells in Pyk-2-deficient mice defines their role in the humoral response. Nat Immunol, 2000. 1(1): p. 31-6.
98. Cariappa, A., et al., Nuclear factor kappa B is required for the development of marginal zone B lymphocytes. J Exp Med, 2000. 192(8): p. 1175-82.
99. Pillai, S., A. Cariappa, and S.T. Moran, Marginal zone B cells. Annu Rev Immunol, 2005. 23: p. 161-96.
100. Weih, F., D. Carrasco, and R. Bravo, Constitutive and inducible Rel/NF-kappa B activities in mouse thymus and spleen. Oncogene, 1994. 9(11): p. 3289-3297.
101. Liou, H.C., et al., Sequential induction of NF-kappa B/Rel family proteins during B-cell terminal differentiation. Mol Cell Biol, 1994. 14(8): p. 5349-59.
102. Grumont, R.J. and S. Gerondakis, The subunit composition of NF-kB complexes changes during B-cell development. Cell Growth Differ, 1994. 5: p. 1321–1331.
103. Liou, H.C., et al., Sequential induction of NF-kappa B/Rel family proteins during B-cell terminal differentiation. Mol Cell Biol, 1994. 14(8): p. 5349-5359.
104. Gerondakis, S., et al., The regulation and roles of Rel/NF-kappa B transcription factors during lymphocyte activation. Curr Opin Immunol, 1998. 10(3): p. 353-9.
105. Horwitz, B.H., et al., The p65 subunit of NF-kappa B is redundant with p50 during B cell proliferative responses, and is required for germline CH transcription and class switching to IgG3. J Immunol, 1999. 162(4): p. 1941-6.
106. Snapper, C.M., et al., B cells lacking RelB are defective in proliferative responses, but undergo normal B cell maturation to Ig secretion and Ig class switching. J Exp Med, 1996. 184(4): p. 1537-41.

107. Weih, D.S., Z.B. Yilmaz, and F. Weih, Essential role of RelB in germinal center and marginal zone formation and proper expression of homing chemokines. J Immunol, 2001. 167(4): p. 1909-19.
108. Gilmore, T.D., et al., The c-Rel transcription factor and B-cell proliferation: a deal with the devil. Oncogene, 2004. 23(13): p. 2275-86.
109. Tumang, J.R., et al., c-Rel is essential for B lymphocyte survival and cell cycle progression. Eur J Immunol, 1998. 28(12): p. 4299-312.
110. Claudio, E., et al., BAFF-induced NEMO-independent processing of NF-kappa B2 in maturing B cells. Nat Immunol, 2002. 3(10): p. 958-65.
111. Grossmann, M., et al., The anti-apoptotic activities of Rel and RelA required during B-cell maturation involve the regulation of Bcl-2 expression. Embo J, 2000. 19(23): p. 6351-60.
112. Gugasyan, R., et al., Rel/NF-kappaB transcription factors: key mediators of B-cell activation. Immunol Rev, 2000. 176: p. 134-40.
113. Mebius, R.E., Organogenesis of lymphoid tissues. Nat Rev Immunol, 2003. 3(4): p. 292-303.
114. Rennert, P.D., et al., Surface lymphotoxin alpha/beta complex is required for the development of peripheral lymphoid organs. J Exp Med, 1996. 184(5): p. 1999-2006.
115. Matsumoto, M., et al., Involvement of distinct cellular compartments in the abnormal lymphoid organogenesis in lymphotoxin-alpha-deficient mice and alymphoplasia (aly) mice defined by the chimeric analysis. J Immunol, 1999. 163(3): p. 1584-91.
116. Shinkura, R., et al., Alymphoplasia is caused by a point mutation in the mouse gene encoding Nf-kappa b-inducing kinase. Nat Genet, 1999. 22(1): p. 74-7.
117. Koike, R., et al., The splenic marginal zone is absent in alymphoplastic aly mutant mice. Eur J Immunol, 1996. 26(3): p. 669-75.
118. Paxian, S., et al., Abnormal organogenesis of Peyer's patches in mice deficient for NF-kappaB1, NF-kappaB2, and Bcl-3. Gastroenterology, 2002. 122(7): p. 1853-68.
119. Matsushima, A., et al., Essential role of nuclear factor (NF)-kappaB-inducing kinase and inhibitor of kappaB (IkappaB) kinase alpha in NF-kappaB activation through lymphotoxin beta receptor, but not through tumor necrosis factor receptor I. J Exp Med, 2001. 193(5): p. 631-6.
120. Dejardin, E., et al., The lymphotoxin-beta receptor induces different patterns of gene expression via two NF-kappaB pathways. Immunity, 2002. 17(4): p. 525-35.
121. Sauer, B., Inducible gene targeting in mice using the Cre/lox system. Methods, 1998. 14(4): p. 381-92.
122. Lewandoski, M., Conditional control of gene expression in the mouse. Nat Rev Genet, 2001. 2(10): p. 743-55.
123. Urbanek, P., et al., Complete block of early B cell differentiation and altered patterning of the posterior midbrain in mice lacking Pax5/BSAP. Cell, 1994. 79(5): p. 901-12.
124. Hestdal, K., et al., Characterization and regulation of RB6-8C5 antigen expression on murine bone marrow cells. J Immunol, 1991. 147(1): p. 22-8.
125. Conlan, J.W. and R.J. North, Neutrophils are essential for early anti-Listeria defense in the liver, but not in the spleen or peritoneal cavity, as revealed by a granulocyte-depleting monoclonal antibody. J Exp Med, 1994. 179(1): p. 259-68.
126. Nutt, S.L., et al., Commitment to the B-lymphoid lineage depends on the transcription factor Pax5. Nature, 1999. 401(6753): p. 556-62.
127. Loder, F., et al., B cell development in the spleen takes place in discrete steps and is determined by the quality of B cell receptor-derived signals. J Exp Med, 1999. 190(1): p. 75-89.

128. Muller, P., D.N. Mannel, and T. Hehlgans, Functional characterization of the mouse lymphotoxin-beta receptor promoter. Eur Cytokine Netw, 2001. 12(2): p. 325-30.
129. Force, W.R., et al., Mouse lymphotoxin-beta receptor. Molecular genetics, ligand binding, and expression. J Immunol, 1995. 155(11): p. 5280-8.
130. Nakamura, T., et al., The murine lymphotoxin-beta receptor cDNA: isolation by the signal sequence trap and chromosomal mapping. Genomics, 1995. 30(2): p. 312-9.
131. Browning, J.L. and L.E. French, Visualization of lymphotoxin-beta and lymphotoxin-beta receptor expression in mouse embryos. J Immunol, 2002. 168(10): p. 5079-87.
132. Soriano, P., Generalized lacZ expression with the ROSA26 Cre reporter strain. Nat Genet, 1999. 21(1): p. 70-1.
133. Sivakumar, V., et al., Differential requirement for Rel/nuclear factor kappa B family members in natural killer T cell development. J Exp Med, 2003. 197(12): p. 1613-21.
134. Weih, F., S.A. Lira, and R. Bravo, Overexpression of RelB in transgenic mice does not affect I kappa B alpha levels: differential regulation of RelA and RelB by the inhibitor protein. Oncogene, 1996. 12(2): p. 445-9.
135. Schiemann, B., et al., An essential role for BAFF in the normal development of B cells through a BCMA-independent pathway. Science, 2001. 293(5537): p. 2111-4.
136. Kayagaki, N., et al., BAFF/BLyS receptor 3 binds the B cell survival factor BAFF ligand through a discrete surface loop and promotes processing of NF-kappaB2. Immunity, 2002. 17(4): p. 515-24.
137. Batten, M., et al., BAFF mediates survival of peripheral immature B lymphocytes. J Exp Med, 2000. 192(10): p. 1453-66.
138. Mackay, F., et al., Mice transgenic for BAFF develop lymphocytic disorders along with autoimmune manifestations. J Exp Med, 1999. 190(11): p. 1697-710.
139. Bishop, G.A., The multifaceted roles of TRAFs in the regulation of B-cell function. Nat Rev Immunol, 2004. 4(10): p. 775-86.
140. Bishop, G.A., B.S. Hostager, and K.D. Brown, Mechanisms of TNF receptor-associated factor (TRAF) regulation in B lymphocytes. J Leukoc Biol, 2002. 72(1): p. 19-23.
141. Nguyen, L.T., et al., TRAF2 deficiency results in hyperactivity of certain TNFR1 signals and impairment of CD40-mediated responses. Immunity, 1999. 11(3): p. 379-89.
142. Munroe, M.E. and G.A. Bishop, Role of tumor necrosis factor (TNF) receptor-associated factor 2 (TRAF2) in distinct and overlapping CD40 and TNF receptor 2/CD120b-mediated B lymphocyte activation. J Biol Chem, 2004. 279(51): p. 53222-31.
143. Yeh, W.C., et al., Early lethality, functional NF-kappaB activation, and increased sensitivity to TNF-induced cell death in TRAF2-deficient mice. Immunity, 1997. 7(5): p. 715-25.
144. Grech, A.P., et al., TRAF2 differentially regulates the canonical and noncanonical pathways of NF-kappaB activation in mature B cells. Immunity, 2004. 21(5): p. 629-42.
145. Horwitz, B.H., et al., Failure of lymphopoiesis after adoptive transfer of NF-kappaB-deficient fetal liver cells. Immunity, 1997. 6(6): p. 765-72.
146. Hardy, R.R., B-cell commitment: deciding on the players. Curr Opin Immunol, 2003. 15(2): p. 158-65.
147. Miller, J.P., et al., The earliest step in B lineage differentiation from common lymphoid progenitors is critically dependent upon interleukin 7. J Exp Med, 2002. 196(5): p. 705-11.

148. Monroe, J.G. and D. Allman, Keeping track of pro-B cells: a new model for the effects of IL-7 during B cell development. Eur J Immunol, 2004. 34(10): p. 2642-6.
149. Allman, D. and J.P. Miller, Common lymphoid progenitors, early B-lineage precursors, and IL-7: characterizing the trophic and instructive signals underlying early B cell development. Immunol Res, 2003. 27(2-3): p. 131-40.
150. Akashi, K., et al., Lymphoid development from hematopoietic stem cells. Int J Hematol, 1999. 69(4): p. 217-26.
151. Purohit, S.J., et al., Determination of lymphoid cell fate is dependent on the expression status of the IL-7 receptor. Embo J, 2003. 22(20): p. 5511-21.
152. Dias, S., et al., Interleukin-7 is necessary to maintain the B cell potential in common lymphoid progenitors. J Exp Med, 2005. 201(6): p. 971-9.
153. Graf, T., Differentiation plasticity of hematopoietic cells. Blood, 2002. 99(9): p. 3089-101.
154. Rolink, A.G., et al., Fidelity and infidelity in commitment to B-lymphocyte lineage development. Immunol Rev, 2000. 175: p. 104-11.
155. Zhang, D.E., et al., CCAAT enhancer-binding protein (C/EBP) and AML1 (CBF alpha2) synergistically activate the macrophage colony-stimulating factor receptor promoter. Mol Cell Biol, 1996. 16(3): p. 1231-40.
156. Martin, F. and J.F. Kearney, CD21high IgMhigh splenic B cells enriched in the marginal zone: distinct phenotypes and functions. Curr Top Microbiol Immunol, 1999. 246: p. 45-50; discussion 51-2.
157. He, Y. and W.S. Pear, Notch signalling in B cells. Semin Cell Dev Biol, 2003. 14(2): p. 135-42.
158. Tanigaki, K., et al., Regulation of B cell development by Notch/RBP-J signaling. Semin Immunol, 2003. 15(2): p. 113-9.
159. Viau, M. and M. Zouali, B-lymphocytes, innate immunity, and autoimmunity. Clin Immunol, 2005. 114(1): p. 17-26.
160. Maillard, I., S.H. Adler, and W.S. Pear, Notch and the immune system. Immunity, 2003. 19(6): p. 781-91.
161. Maillard, I., T. Fang, and W.S. Pear, Regulation of lymphoid development, differentiation, and function by the notch pathway. Annu Rev Immunol, 2005. 23: p. 945-74.
162. Han, H., et al., Inducible gene knockout of transcription factor recombination signal binding protein-J reveals its essential role in T versus B lineage decision. Int Immunol, 2002. 14(6): p. 637-45.
163. Tanigaki, K., et al., Regulation of alphabeta/gammadelta T cell lineage commitment and peripheral T cell responses by Notch/RBP-J signaling. Immunity, 2004. 20(5): p. 611-22.
164. Saito, T., et al., Notch2 is preferentially expressed in mature B cells and indispensable for marginal zone B lineage development. Immunity, 2003. 18(5): p. 675-85.
165. Witt, C.M., et al., Notch2 haploinsufficiency results in diminished B1 B cells and a severe reduction in marginal zone B cells. J Immunol, 2003. 171(6): p. 2783-8.
166. Tanigaki, K., et al., Notch-RBP-J signaling is involved in cell fate determination of marginal zone B cells. Nat Immunol, 2002. 3(5): p. 443-50.
167. Li, J., et al., The C terminus of MINT forms homodimers and abrogates MINT-mediated transcriptional repression. Biochim Biophys Acta, 2005. 1729(1): p. 50-6.
168. Kuroda, K., et al., Regulation of marginal zone B cell development by MINT, a suppressor of Notch/RBP-J signaling pathway. Immunity, 2003. 18(2): p. 301-12.
169. Shimizu, T., et al., VpreB1/VpreB2/lambda 5 triple-deficient mice show impaired B cell development but functional allelic exclusion of the IgH locus. J Immunol, 2002. 168(12): p. 6286-93.

170. Brauninger, A., et al., Regulation of immunoglobulin light chain gene rearrangements during early B cell development in the human. Eur J Immunol, 2001. 31(12): p. 3631-7.
171. Weih, F., D. Carrasco, and R. Bravo, Constitutive and inducible Rel/NF-kappa B activities in mouse thymus and spleen. Oncogene, 1994. 9(11): p. 3289-97.
172. Attar, R.M., et al., Genetic approaches to study Rel/NF-kappa B/I kappa B function in mice. Semin Cancer Biol, 1997. 8(2): p. 93-101.
173. Ettinger, R., et al., Effects of tumor necrosis factor and lymphotoxin on peripheral lymphoid tissue development. Int Immunol, 1998. 10(6): p. 727-41.
174. Pasparakis, M., et al., Peyer's patch organogenesis is intact yet formation of B lymphocyte follicles is defective in peripheral lymphoid organs of mice deficient for tumor necrosis factor and its 55-kDa receptor. Proc Natl Acad Sci U S A, 1997. 94(12): p. 6319-23.
175. Clausen, B.E., et al., Conditional gene targeting in macrophages and granulocytes using LysMcre mice. Transgenic Res, 1999. 8(4): p. 265-77.
176. Castro, C.H., et al., Development of mice with osteoblast-specific connexin43 gene deletion. Cell Commun Adhes, 2003. 10(4-6): p. 445-50.
177. Ferron, M. and J. Vacher, Targeted expression of Cre recombinase in macrophages and osteoclasts in transgenic mice. Genesis, 2005. 41(3): p. 138-45.
178. Chiu, W.S., et al., Transgenic mice that express Cre recombinase in osteoclasts. Genesis, 2004. 39(3): p. 178-85.

Acknowledgments

I am honored to pay my sincere thanks and heartiest obligations to my supervisor Prof. Dr. Falk Weih. His proper supervision, experience, time devotion, and keen interest enabled me to accumulate this work.

I am grateful to Prof. Dr. Peter Herrlich for his trust and inspiration.

I pay my special thanks to Dr. Helen Morrison for correcting my thesis.

Thanks also go to Esther Kamphausen for translating the "summary" of this dissertation into German.

I pay my enormous thanks to Dr. Sivakumar Vallabhapurapu, Dr. Buket Yilmaz, and Debra Weih for their kind help and valuable advice. Many thanks go to Yvonne Peterson, Elke Meier, and Simone Tänzer for their various help and enriching my experience in Germany.

I acknowledge all the animal staff in ITG, Karlsruhe and IMB, Jena.

I will never forget Dr. Ping Zhu and Andrea Jacob for introducing me gene targeting and embryonic stem cell culture.

I am deeply indebted to my sister and my boyfriend for their substantial support, continuous encouragement, and company. Last but not the least; I thank my grandma and my parents for their understanding.

Publications and Scientific Posters

Publications:

Orian-Rousseau V, Mink S, Mengwasser J, Hogenesch H, **Guo F,** Thies WG, Hofmann M, Herrlich P, Ponta H. Genes upregulated in a metastasizing human colon carcinoma cell lines. Int J Cancer, 2005 Feb 20; 113(5): 699-705.

Scientific Posters:

1st „Spring School on Immunology“ of the German Society of Immunology. February 2005, Ettal, Bavaria/Germany

CURRICULUM VITAE

Feng Guo
Institute of Molecular Biotechnology
Beutenbergstr.11, Jena D-07745, Germany
Tel: +49 3641 656051
fguo@imb-jena.de

EDUCATION:

- 2002-2005 **Ph.D.** (Feb, 2002 onwards)
  Department of Immunology, Institute of Molecular Biotechnology, Jena, Germany
- 1998-2001 **M.S.**
  Institute of Hematology, Medical School, Suzhou University, Suzhou, Jiangsu, P.R.China
- 1990-1995 **M.D.**
  Medical School, Suzhou University, Suzhou, Jiangsu, P.R.China.

PROFESSIONAL EXPERIENCE:

- 2002-2005 **Ph.D. student**, Friedrich-Schiller-Universität Jena, Department of Immunology, Institute of Molecular Biotechnology, Jena, Germany (Moved from University of Karlsruhe, Institute of Genetics in Forschungszentrum Karlsruhe in September, 2004 along with Prof. Dr.Weih). Study on NF-κB function in B-cell development and lymphoid organogenesis.
- 1998-2001 **Master student**, Institute of Hematology, Medical School, Suzhou University, Suzhou, Jiangsu, P.R.China. Study on the effects of HMG-CoA reductase inhibitors on leukemia cell lines aiming to broad chemotherapeutic agents targeting to the drug-resistant leukemia.
- 1995-2001 **Resident & Teach Assistant**, Department of Clinical Hematology, Suzhou University's First Affiliated Hospital, Suzhou, Jiangsu, P.R.China. Diagnosed and treated common hematological diseases.

- 1990-1995 **Medical Student**, Medical School, Suzhou University, Suzhou, Jiangsu, P.R.China. Studied basic and clinical medicine. I was an intern in the teaching hospital and completed rotations in all clinical divisions during my final year in medical school.

PUBLICATIONS:

1. Orian-Rousseau V, Mink S, Mengwasser J, Hogenesch H, **Guo F,** Thies WG, Hofmann M, Herrlich P, Ponta H. Genes upregulated in a metastasizing human colon carcinoma cell lines. *Int J Cancer*, 2005 Feb 20; 113(5): 699-705
2. Yang XW, **Guo F,** Wang W. Electroporation-mediated gene transduction and expression of class 1 aldehyde dehydrogenase (ALDH1) and multidrug resistance gene (MDR1). *Ai Zheng,* 2002 Feb; 21(2):138-41
3. Yang XW, Wang W, Fu JX, Cen JN, **Guo F,** Xia XM, Chen ZX. Aldehyde-dehydrogenase gene-transduced hematopoietic cell line K562 overcomes the cytoxicity of cyclophosphamide in vitro. *Chinese Journal of Experimental Hematology*, 2002 Jun; 10(3): 205-8
4. **Guo F**, Cen JN, Chen ZX. In vitro effect of lovastatin on NB4 promyelocytic leukemia cells. *Chinese Journal of Hematology*, 2001 Nov; 22(11): 584-8
5. **Guo F,** Cen JN, Chen ZX. Effects of lovastatin on leukaemia cells HL-60, KG-1, and K562 in vitro. *Chinese Journal of Cancer,* 2001 Aug; 20(8): 816
6. **Guo F**. Lovastatin and Leukemia. *Foreign Medicine of Hematology and Transfusion*. 2000 Aug; 27 (4):15-19 (Review)

Selbständigkeitserklärung

Ich erkläre, dass ich die vorliegende Arbeit selbständig und nur unter Verwendung der angegebenen Hilfsmittel und Literatur angefertigt habe.

Jena, den 10.06.2005

Feng Guo

Erklärung zur Bewerbung

Hiermit erkläre ich, dass ich mich mit der vorliegenden Arbeit an keiner anderen Hochschule um den akademischen Grad Doctor rerum naturalium beworben habe und dass ich weder früher noch gegenwärtig die Eröffnung eines Verfahrens zum Erwerb des o.g. akademischen Grades an einer anderen Hochschule beantragt habe.

Jena, den 10.06.2005

Feng Guo